Acoustic Observations of Zooplankton Distribution in Saanich Inlet,
an Intermittently Anoxic Fjord

By

Ian Alexander Beveridge
B.Sc., Simon Fraser University, 1994

A Thesis Submitted in Partial Fulfillment of the
Requirements of the Degree of

MASTER OF SCIENCE

in the Department of Biology

Acoustic Observations of Zooplankton Distribution in Saanich Inlet,
an Intermittently Anoxic Fjord

By

Ian Alexander Beveridge
B.Sc., Simon Fraser University, 1994

SUPERVISORY COMMITTEE

Dr. Verena Tunnicliffe (Department of Biology)
Supervisor

Dr. John Dower (Department of Biology)
Departmental Member

Dr. Richard Dewey (School of Earth and Ocean Sciences)
Outside Member

Supervisory Committee

Dr. Verena Tunnicliffe (Department of Biology)
Supervisor

Dr. John Dower (Department of Biology)
Departmental Member

Dr. Richard Dewey (School of Earth and Ocean Sciences)
Outside Member

ABSTRACT

A biological front at the mouth of Saanich Inlet results in higher rates of primary productivity at the inlet mouth relative to the head, creating a gradient that could influence zooplankton distribution. A shallow sill (75m) at the inlet mouth restricts circulation below sill depth, isolating the deep basin for much of the year. Anoxia develops in the isolated basin and the depth of the anoxic layer changes during the year. During the day, pelagic zooplankton form a deep scattering layer. Between April 2005 and March 2006, I conducted monthly 200kHz acoustic surveys between the mouth and head of Saanich Inlet to test the hypothesis that zooplankton density was greater near the mouth relative to the head. I was also interested in how changing anoxic layer depth affected the distribution of the deep scattering layer. I found that zooplankton density followed a headward gradient in the spring and summer, with the highest densities near the mouth. Zooplankton density was higher near the mouth or the mid-inlet relative to the head in 75% of transects. I did not observe a zooplankton density gradient during the winter. Zooplankton distribution was affected by dissolved oxygen concentration. Deep scattering layer depth was significantly correlated with the depth of the anoxic layer and vertical compression of the deep scattering layer increased as the anoxic layer moved upwards. When the depth of the anoxic layer was less than 90 meters, zooplankton were nearly absent.

Vertical migration of the deep scattering layer to surface waters at night has been well documented, but zooplankton migration patterns in the shallow waters of Saanich Inlet have not been described. I used 200kHz acoustic data collected by the VENUS observatory (96m) and an autonomous acoustic system deployed at a shallow site (62m) in Patricia Bay to study zooplankton migration patterns. Horizontal movement of the deep scattering layer over shallow depths following vertical migration was infrequent. Over 41 days of observation at the shallow site, I only observed deep scattering layer zooplankton on 12 days. At the shallow site, night-time volume backscatter was dominated by the emergence of benthic zooplankton. The movement of these scatterers into the water column at night resulted in a 14-fold increase in volume backscatter over daytime values. I observed this emergence pattern at both sites, which represents an important component of benthic-pelagic coupling in Saanich Inlet. In contrast to the deep scattering layer, which migrated to the surface each night, emergent zooplankton remained within 30-40 meters of the seafloor and did not ascend into surface waters.

TABLE OF CONTENTS

SUPERVISORY COMMITTEE ..... **ii**

ABSTRACT ..... **iii**

TABLE OF CONTENTS ..... **v**

LIST OF TABLES ..... **viii**

LIST OF FIGURES ..... **ix**

ACKNOWLEDGEMENTS ..... **xi**

CHAPTER 1 ..... **1**

1.1 ZOOPLANKTON DISTRIBUTION 1
1.2 ZOOPLANKTON BEHAVIOUR 2
1.3 ACOUSTIC SAMPLING 3
1.4 SAANICH INLET 6
1.4.1 Physical and Chemical Characteristics *8*
1.4.2 Biological Characteristics *9*
1.4.3 Species *10*
1.5 OBJECTIVES 12

CHAPTER 2 ..... **15**

2.1 INTRODUCTION 15
2.2 METHODS 17
2.2.1 Data Collection *17*
2.2.1.1 Acoustic Data 17
2.2.1.2 Position Data 19
2.2.1.3 Environmental Data 19
2.2.2 Data Processing *20*
2.2.2.1 Merging Acoustic and GPS Files 20
2.2.2.2 Internal Instrument Noise 21
2.2.2.3 Digital Counts to Volume Backscattering Strength (S_v) Conversion 24
2.2.2.4 Removing Fish School Echoes 24
2.2.2.5 Site Selection 26
2.2.3 Analysis *27*
2.2.3.1 Environmental Variables 27
2.2.3.2 Zooplankton Distribution 28
2.3 RESULTS 31
2.3.1 Chemical and Physical Characteristics *31*
2.3.1.1 Dissolved Oxygen 31
2.3.1.2 Temperature 39
2.3.1.3 Density 45
2.3.1.4 Chlorophyll Fluorescence 48
2.3.1.5 Wind and Currents 48
2.3.2 Zooplankton Distribution *48*
2.3.2.1 Site Comparison 55
2.3.2.2 Environmental Correlations 65
2.4 DISCUSSION 68

2.4.1 Physical and Chemical Characteristics *68*
2.4.1.1 Dissolved Oxygen 68
2.4.1.2 Temperature and Density 70
2.4.2 Zooplankton Distribution: Patricia Bay to Squally Reach *71*
2.4.2.1 Food Availability 71
2.4.2.2 Wind and Currents 73
2.4.2.3 Temperature and Density 73
2.4.2.4 Dissolved Oxygen 73
2.4.3 Zooplankton Distribution Within the Water Column *75*
2.4.3.1 Zooplankton Layer Depth 75
2.4.3.2 Zooplankton Layer Thickness 78
2.4.4 Conclusions *79*

CHAPTER 3 ..... **81**

3.1 INTRODUCTION 81
3.1.1 Zooplankton Migration Behaviour *81*
3.1.2 Patricia Bay *83*
3.1.3 Objectives *83*
3.2 METHODS 85
3.2.1 Data Collection *85*
3.2.1.1 Deep Site: VENUS Observatory 85
3.2.1.2 Shallow Site 87
3.2.2 Data Analysis *87*
3.2.2.1 Processing 87
3.2.2.2 Near-Surface Zooplankton 88
3.2.2.3 Zooplankton Density 88
3.2.2.4 Vertical Migration Timing 88
3.2.2.5 Vertical Migration Depth 92
3.2.2.6 Fish School Identification 92
3.3 RESULTS 92
3.3.1 Day-night Distribution *92*
3.3.2 Vertical Migration Depth *98*
3.3.3 Near-surface Zooplankton *98*
3.3.4 Vertical Migration Timing *98*
3.3.5 Planktivore Distribution *104*
3.4 DISCUSSION 107
3.4.1 Zooplankton Distribution *107*
3.4.2 Zooplankton Vertical Migration Timing and Depth *110*
3.4.3 Horizontal Migration/Advection *113*
3.4.4 Planktivore Distribution *115*
3.4.5 Conclusions *117*

CHAPTER 4 ..... **119**

4.1 PELAGIC ZOOPLANKTON DISTRIBUTION 119
4.2 BENTHIC ZOOPLANKTON 124
4.3 FUTURE RESEARCH 125

APPENDIX 1 ..... **127**

A1.1 INTRODUCTION 127
A1.2 SOUND 128
A1.3 SOUND MEASUREMENT 130

A1.4 SOUND TRANSMISSION 131
A1.4.1 Far-Field *132*
A1.5 BEAM PATTERN AND WIDTH 132
A1.6 PROPAGATION LOSSES 134
A1.6.1 Beam Spreading *134*
A1.6.2 Absorption *134*
A1.7 SOUND SPEED 135
A1.8 ACOUSTIC SCATTERING 136
A1.9 SONAR EQUATION 137

REFERENCES 139

LIST OF TABLES

Table 1.1. Zooplankton, fish, and other species captured within the deep scattering layer in Saanich Inlet (Bary et al. 1962; Bary 1966). 11

Table 2.1. Data collection date and time (PST) for mid-inlet transect data between April 2005 and March 2006. 19

Table 2.2. Location of Saanich Inlet CTD stations. 20

Table 2.3. Zooplankton captured or observed in the deep scattering layer during net tows or during ROPOS ROV operations in Saanich Inlet between November 2004 and February 2007.. 26

Table 2.4. P-values from paired t-tests for comparisons of environmental variables between the Patricia Bay and Squally Reach sites. 35

Table 2.5. P-values from paired t-tests for comparisons of scattering layer characteristics between the Patricia Bay and Squally Reach sites. 59

Table 2.6. Page test for ordered alternatives (α=0.05) for a zooplankton density gradient between Patricia Bay and Squally Reach. 60

Table 2.7. Pearson product-moment correlations between zooplankton scattering layer characteristics and environmental variables. 64

Table 3.1. Zooplankton arrival and departure times for the zooplankton layer, defined as scattering within 20m of the surface, at the shallow site in Patricia Bay. 100

Table 3.2. Spatial and temporal distribution of fish schools at the deep and shallow sample sites in Patricia Bay. 105

Table A1.1. Mean absorption loss (α) and sound speed (c) values between 10 and 130 meters for each mid-inlet acoustic transect between April 2005 and March 2006. 135

Table A1.2. Transducer constants for ASL Water Column Profiler®, s/n 1006. 138

LIST OF FIGURES

Figure 1.1. The difference in echo strength between the zooplankton scattering layer and pelagic fish schools in Saanich Inlet 4

Figure 1.2. Saanich Inlet. The entrance sill at 75m depth restricts circulation in the deep basin and deep waters are typically anoxic. 7

Figure 2.1. Saanich Inlet acoustic transect, CTD stations, ODAS buoy, and IOS sample site. 18

Figure 2.2. The $20*\log_{10}$Range time-varied gain function used by the ZAP to compensate for geometric transmission loss. 22

Figure 2.3. Internal instrument noise generated by the ZAP at gain setting one. 22

Figure 2.4. Example of internal instrument noise, a) before noise removal, and b) after noise removal. 23

Figure 2.5. Sv-frequency histogram for combined monthly transects 28

Figure 2.6. Institute of Ocean Sciences Winkler titration dissolved oxygen data for A) February/March and B) August/September in Saanich Inlet near Bamberton from 1996 to 2005 (solid diamonds are 2005 data) 33

Figure 2.7. Monthly dissolved oxygen profiles for Patricia Bay, Bamberton, and Squally Reach between April 2005 and March 2006. 36

Figure 2.8. Dissolved oxygen (mL L^{-1}) contours and anoxic (0.1 mL O_2 L^{-1}; dashed line) boundary depth for A) Patricia Bay, B) Bamberton, and C) Squally Reach between April 2005 and March 2006. 38

Figure 2.9. Institute of Ocean Sciences temperature data for A) February/March and B) August/September in Saanich Inlet near Bamberton from 1996 to 2005 (solid diamonds are 2005 data). 40

Figure 2.10. Monthly temperature profiles for Patricia Bay, Bamberton and Squally Reach between April 2005 and March 2006. 42

Figure 2.11. Monthly depth of the base of the permanent thermocline and pycnocline between April 2005 and March 2006 44

Figure 2.12. Monthly density anomaly (σ_t) profiles for Patricia Bay, Bamberton, and Squally Reach between April 2005 and March 2006. 46

Figure 2.13. Differences in integrated (0-40m) chlorophyll fluorescence between Patricia Bay and Squally Reach. 49

Figure 2.14. Frequency histograms for A) wind direction, and B) wind speed between April 2004 and June 2006 from the mid-inlet ODAS buoy C46134 in Saanich Inlet (n = 17 840) 50

Figure 2.15. Monthly zooplankton density distribution as measured by backscatter intensity (sv) between 10-130 meters depth along a mid-inlet transect between Patricia Bay and Squally Reach. 51

Figure 2.16. Monthly profiles of integrated volume backscatter between 10-130 meters depth along a mid-inlet acoustic transect from Patricia Bay (0m) to Squally Reach (12 000m). 56

Figure 2.17. Mean integrated volume backscatter between 10-130 meters depth for the Patricia Bay, Bamberton, and Squally Reach sites for each month. 58

Figure 2.18. Zooplankton layer boundaries in relation to anoxic and hypoxic boundary depths.. 62

Figure 2.19. Positive correlation between the depth of the anoxic boundary and the gap-size between the base of the zooplankton layer and the anoxic boundary..... 63

Figure 2.20. Weak positive correlation between anoxic boundary depth and zooplankton layer thickness. 66

Figure 2.21. Dissolved oxygen concentration measured at the A) base and B) top of the daytime zooplankton layer..... 67

Figure 3.1. East to west acoustic transect on March 21, 2006, through Patricia Bay to the middle of Saanich Inlet showing the location of the deep zooplankton scattering layer in relation to Patricia Bay. 84

Figure 3.2. Multibeam acoustic images of Saanich Inlet (A) and Patricia Bay (B). 86

Figure 3.3. Aluminum tripod on the deck of *MSV John Strickland* following recovery on April 21, 2006. 89

Figure 3.4. Example of ascent and descent timing at the shallow site on March 24, 2006. 90

Figure 3.5. Example of qualitative ascent timing at the deep (VENUS) location on March 31, 2006. 91

Figure 3.6. Acoustic backscatter at a shallow site in Patricia Bay between February 7-23, 2006 from an up-looking transducer positioned 0.5m above the seabed. 94

Figure 3.7. Acoustic backscatter at the deep and shallow sites in Patricia Bay between March 22 and April 15, 2006 from up-looking transducers positioned near the seabed. 95

Figure 3.8. Mean day and night integrated volume backscatter for the deep (96m) and shallow (62m) sites between March 22 and April 15, 2006. 97

Figure 3.9. Mean night ascent depth at the deep and shallow sites in Patricia Bay between February 7 and April 15, 2006..... 101

Figure 3.10. Example of near surface zooplankton at the shallow site on March 22, 2006. 102

Figure 3.11. Zooplankton vertical migration timing relative to A) sunset and B) sunrise for zooplankton at the deep and shallow sites in Patricia Bay. 103

Figure 3.12. Location of fish schools and mean zooplankton depth (shallowest depth averaged over the days of deployment) in relation to sunset in Patricia Bay at the deep (A) and shallow sites (B = February; C = March-April). 106

Figure 3.13. Influence of fish schools within one hour of sunset on zooplankton ascent timing at the deep site. 108

Figure 4.1. Summary of trends in the vertical distribution and density of the deep scattering layer (A) and the differences in zooplankton distribution between deep and shallow sites (B).. 120

Figure A1.1. Schematic representation of an acoustic sine wave, showing regions of high and low pressure, position of wavefronts, and the direction of wave propagation. 129

Figure A1.2. Typical beam pattern for a circular transducer..... 133

ACKNOWLEDGEMENTS

I had the pleasure of working with many wonderful people who made my life as a graduate student more interesting and fun. Many thanks to my supervisor, Verena Tunnicliffe, for her encouragement and support as my project evolved from fish to zooplankton. Thanks also to my committee members, John Dower and Richard Dewey, for all their help. The experience I gained working with you has been invaluable.

I was very fortunate to share a lab with so many great people: Mathis Stoeckle, Jen Tyler, Jonathan Rose, Gitai and Ruthy Yahel, Amanda Bates-Bird, Sarah Cook, Kim Davies, Kamira Peters, Dafne Eerkes-Medrano, and Mariken Van Gurp. You all played a role in my success at this endeavour. My sincere thanks also to my family and friends for listening to my rants and not letting me quit when I learned the meaning of nadir.

I would especially like to thank Jonathan for always knowing what was going on; Mathis for his help with maps and figures; Damian Grundle for his help in the field and for sharing his data; Conrad Cooper for his help in the field; Asit Mazumder and Kelly Field for the use of their boat; and 'Super Dave' Smith in the Elliot Machine Shop for always having great ideas.

Working with the VENUS Project team and the CSSF ROPOS guys has been a highlight of my degree. Whether it was stalking herring in Patricia Bay with the ROV, searching for the ZAP I deployed on the seafloor, or helping with the VENUS cable installation, I was exposed to many novel situations that enhanced my graduate experience.

Many people shared their ship time with me and my project would not have been possible without them: Jay Cullen, Tom Pedersen, Diana Varela, Svein Vagle, Damian Grundle, Akash Sastri, Dennis Kramer, and Marina Chong. Captain Ken Brown and the crew of *MSV John Strickland* were excellent and their willingness to work long days was much appreciated. I would also like to thank the Captains and crews of *CCGS John P. Tully* and *CCGS Vector*.

Partial funding for my project was through the King-Platt Fellowship. Additional support and research costs were funded by NSERC Discovery Grant funds to Verena Tunnicliffe.

"We recognize that Saanich Inlet is very weird" - R.E. Pieper. Indeed.

Chapter 1
General Introduction

Zooplankton are an important component of marine food-webs, forming the energetic link between primary producers and higher trophic levels. They are important prey items for a wide range of organisms, including macrozooplankton (Ohman 1984), sessile suspension feeders (Holohan et al. 1998), pelagic fish (Outram and Haegele 1972), and marine mammals (Croll et al. 1998). Zooplankton also have an important role in benthopelagic coupling, facilitating the exchange of biogeochemical material between the pelagic environment and the benthos (Raffaelli et al. 2003). A recently observed effect of vertically migrating macrozooplankton is the generation of turbulence (Kunze et al. 2006). Ascending zooplankton could potentially transport nutrients from below the pycnocline to surface waters, promoting phytoplankton growth. Based on their key role in marine food-webs, factors affecting zooplankton distribution can influence both the distribution of higher level predators and nutrients necessary for primary production.

1.1 Zooplankton Distribution

Zooplankton have patchy distributions in both space and time (Haury et al. 1978; Pinel-Alloul 1995) and their distribution patterns can influence nutrient cycling, predator-prey interactions, and zooplankton population dynamics (Pinel-Alloul 1995). Spatial heterogeneity is caused by complex interactions between physical and biological processes (Mackas et al. 1985). Physical mechanisms that generate spatial heterogeneity in zooplankton distributions include climatic and hydrodynamic processes such as wind and tidal forcing, current interactions with topography, upwelling, internal waves, and surface currents (Pinel-Alloul 1995). Biological processes leading to spatial heterogeneity include phytoplankton patchiness (e.g. Price 1989), diel vertical migrations (e.g. Russell 1928), horizontal migrations (e.g. Webb and Wooldridge 1990), response to environmental gradients (e.g. Stadler and Marcus 1997), and predation (e.g. Swartzman et al. 2002). Horizontal zooplankton migrations are not well documented in the marine environment, but they are an important contributor to spatial heterogeneity in freshwater lakes (e.g. White 1998).

At large spatial scales, physical processes are most important for determining zooplankton distribution patterns, whereas biological processes tend to dominate at smaller scales (Haury et al. 1978). At mega-scales (10^3-10^4 km), zooplankton distributions closely resemble those of oceanic circulation gyres (Haury et al. 1978). Zooplankton behaviour (e.g. vertical migration) will have little influence on distribution patterns at such large scales. At meso-scales (10^1-10^2 km), biological interaction with physical forcing can influence distribution patterns. For example, Simard and Mackas (1989) observed that krill aggregations were strongly associated with upwelling currents along the continental shelf near Vancouver Island. The diel vertical migration behaviour of these krill maintained their position within the upwelling region (Mackas et al. 1997). At coarse (10^0-10^1 km) to fine (10^0-10^3 m) spatial scales, biological processes and environmental conditions will determine the spatial distribution patterns of zooplankton (Pinel-Alloul 1995).

1.2 Zooplankton Behaviour

Many marine animals have specialized as visual predators of zooplankton, including marine birds (e.g. Cassin's auklet; Abraham and Sydeman 2006) and pelagic fish (e.g. Pacific hake (*Merluccius productus*); Outram and Haegele 1972). To avoid visual predators, many pelagic zooplankton species have adopted a diel vertical migration (DVM) strategy, initiated by a change in relative light intensity, to minimize the risk of encounter with visual predators (Ohman 1988). Typical DVM involves spending daylight hours at depth, ascending to surface waters near sunset to feed at night, and then descending to deep dark waters near sunrise (Lampert 1989). Demersal or benthic zooplankton spend daylight hours near or burrowed within surface sediments. Many demersal species of copepods (Teasdale et al. 2004), amphipods (Ingram and Hessler 1983), and mysids (Kringel et al. 2003) also undergo DVM, emerging from the bottom near sunset. The amplitude of vertical migrations can range from less than a meter to hundreds of meters and for macrozooplankton species such as euphausiids, ascent speeds during vertical migrations reach 5 cm s^{-1} (e.g. De Robertis et al. 2003).

Aggregation of pelagic zooplankton at depth during daylight hours following vertical migration results in the formation of acoustically detectable deep scattering layers. A deep scattering layer is a dense concentration of marine organisms that reflects or scatters sound energy back to a receiving device such as a transducer. The first documented observation of a deep scattering layer was in 1942 off the coast of California (Eyring et al. 1948). Acoustic echosounders were first used to detect zooplankton during early investigations into the origin of deep scattering layers.

1.3 Acoustic Sampling

In an active acoustic system, a sound pulse is generated when voltage is applied to piezo-electric ceramic elements in a transducer that cause the elements to physically vibrate at the operating frequency (e.g. 200 kHz). The vibrations generate pressure waves that propagate through the water column (Appendix 1). When a pressure wave encounters an object with a different density than the surrounding seawater (e.g. euphausiid), the wave is scattered and some of the energy is reflected back (backscattered) to the transducer as an echo (MacLennan and Simmonds 1992). When an echo reaches the transducer, the pressure wave causes the ceramic elements to vibrate, generating a voltage that is amplified and recorded by the instrument. The voltage generated by an echo is proportional to its strength. Echo voltages are converted into digital counts using an analogue to digital (A/D) converter where the counts are also proportional to the strength of the received echo. Echo strength is dependent on the density contrast between the reflector and the surrounding seawater, where large density differences result in strong echoes, and the size of the scatterer. For example, echoes from zooplankton are typically much weaker than echoes from pelagic fish (Figure 1.1). The difference in echo strength between these two groups is due to their physical size and the presence of an air-filled swimbladder in many pelagic fish that provides a strong density contrast (Horne and Clay 1998). The identity of acoustic targets can be inferred from these echo strength differences.

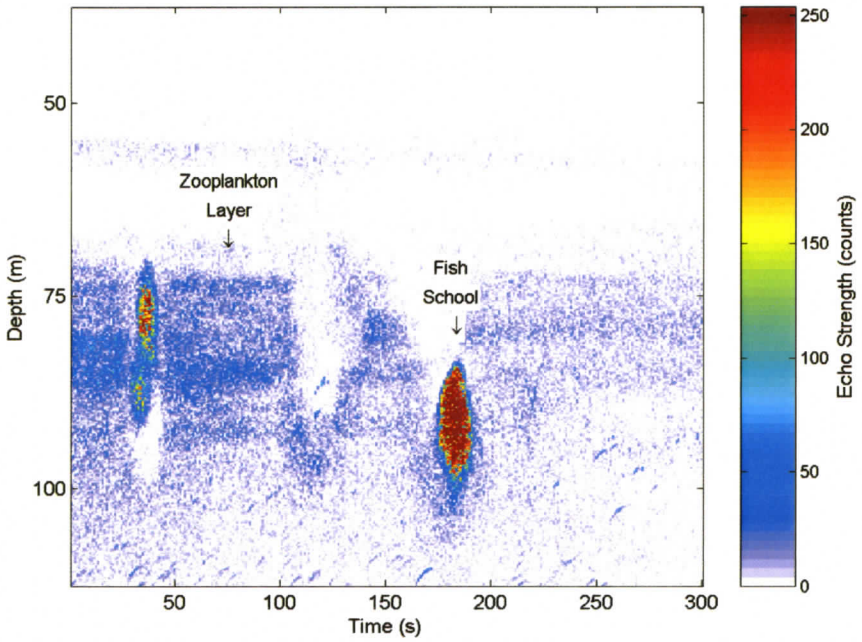

Figure 1.1. The difference in echo strength between the zooplankton scattering layer and pelagic fish schools in Saanich Inlet. Arcs on the echogram are individual fish.

In addition to echo strength, the time elapsed between the transmission of a sound pulse and the reception of an echo is recorded. Using the speed of sound in seawater (c; m s^{-1}), the elapsed time (t; seconds) is converted into a range (R; meters), where:

$$R = ct/2.$$

For a downward-oriented transducer, R is equivalent to the depth of the reflector.

The target resolution of an acoustic instrument is determined by the wavelength (λ; Appendix 1) of the sound pulse, which is related to the operating frequency *(f)* and c as:

$$\lambda = c/f.$$

For example, when c is 1480 m s^{-1}, 38 kHz and 200 kHz transducers will have wavelengths of 39 mm and 7.5 mm, respectively. Generally, individual targets smaller than the wavelength have weak backscatter. Within a volume, echoes from targets smaller than the wavelength will be effectively masked by echoes from larger or stronger acoustic targets. Lower frequencies (e.g. 38 kHz) are typically used for detecting fish and higher frequencies (e.g. 200 kHz) are used for zooplankton. Higher frequencies will also record echoes from fish, whereas zooplankton are not usually detected at low frequencies.

Acoustics provide a non-invasive method to quickly sample large volumes of water with high spatial and temporal resolution. Detailed vertical and horizontal distribution patterns of zooplankton and fish can be obtained along transects from spatial scales ranging from meters to hundreds of kilometers. Acoustic systems can also be used to gather time-series data of zooplankton migration behaviour at a single location (e.g. Trevorrow 2005). The primary disadvantage of acoustic sampling is the lack of species information (Misund 1997). Sampling with multiple frequencies can provide data on a variety of size-classes and, used in conjunction with net samples, can provide detailed descriptions of species distribution. Statistical methods have also been developed for extracting size-class information from single-frequency systems (e.g. Trevorrow 2005).

When zooplankton species composition is known, acoustics can be used to describe small and large-scale distribution patterns (e.g. De Robertis 2002; Kern and Coyle 2000). Where species diversity is low and abundance is dominated by relatively few species, acoustic techniques provide an efficient and effective tool for observing distribution patterns (e.g. Wilson et al. 2002). In Saanich Inlet, British Columbia, the macrozooplankton community is numerically dominated by a few species (De Robertis 2002; Section 1.4.3). Saanich Inlet presents stable oceanographic characteristics (Herlinveaux 1962) coupled with environmental and biological factors that could affect zooplankton distribution patterns, including a biological front at the inlet mouth (Parsons et al. 1983) and an anoxic migration barrier (Devol 1981).

1.4 Saanich Inlet

Saanich Inlet is a coastal fjord located in southeast Vancouver Island and is approximately 24 kilometers in length and ranges in width from approximately 7 km at Patricia Bay to 0.5 km at Squally Reach (Herlinveaux 1962; Figure 1.2). Although the maximum depth is 235 meters, a shallow sill (75m) located at the inlet mouth restricts deepwater circulation and limits mixing with waters located outside of the inlet (Herlinveaux 1962). Coupled with high primary productivity and subsequent organic input (Gargett et al. 2003), the lack of deepwater circulation contributes to anoxic conditions typical of depths below approximately 110 meters (Herlinveaux 1962; Timothy and Soon 2001). Dissolved oxygen rapidly decreases from near-surface maxima to less than 1 mL L^{-1} in a hypoxic zone between approximately 80-110 meters depth. The depth of the anoxic layer varies with the extent of autumn deepwater renewal (Anderson and Devol 1973) but is a consistent feature of the inlet (Bary et al. 1962). Tidal currents, wind-mixing, and upwelling are all relatively weak within Saanich Inlet resulting in an oceanographically stable environment with limited physical forcing (Herlinveaux 1962; Gargett et al. 2003).

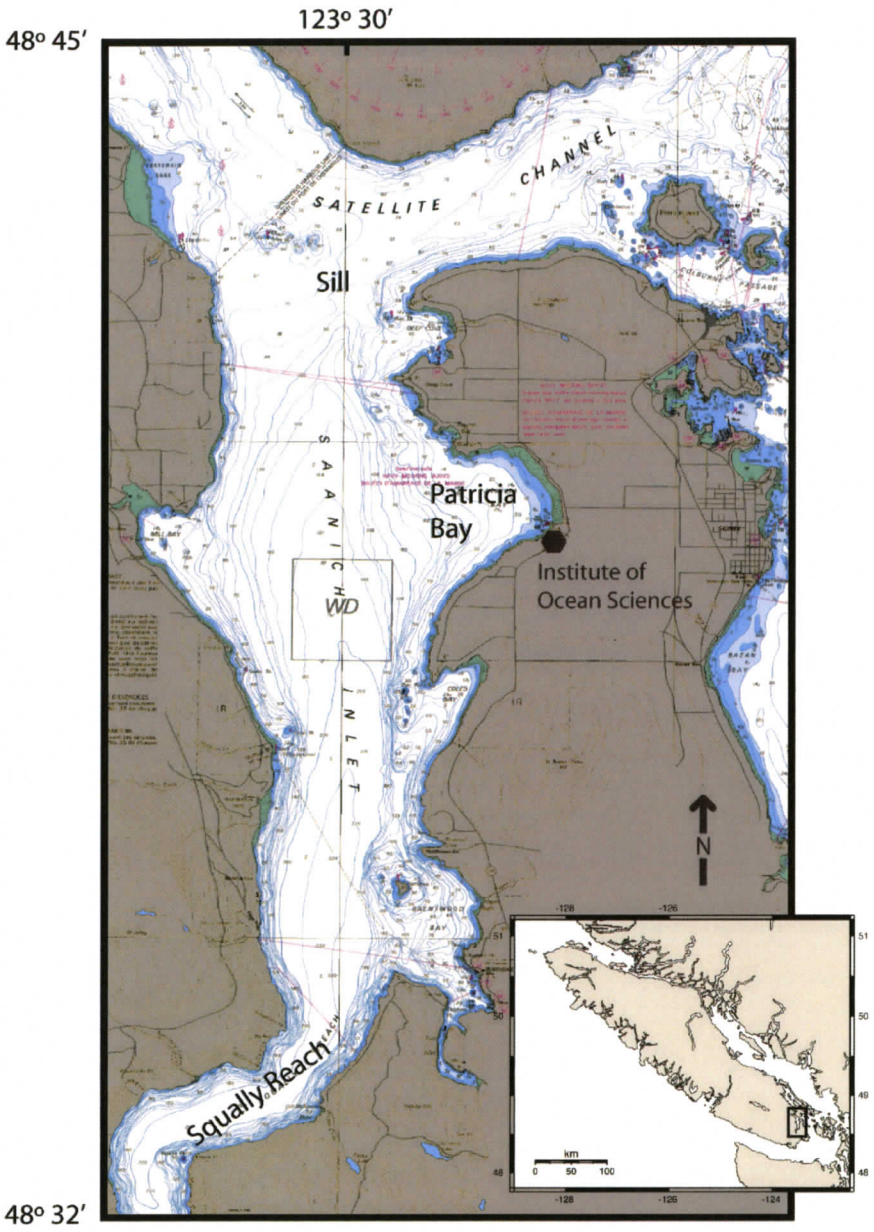

Figure 1.2. Saanich Inlet. The entrance sill at 75m depth restricts circulation in the deep basin and deep waters are typically anoxic.

1.4.1 Physical and Chemical Characteristics

Most fjords are characterized by normal estuarine circulation, where the main source of freshwater input is at the inlet head, causing a net outflow of fresher brackish water at the surface and a compensating inflow of dense nutrient-rich water at depth. Deep inflowing water can be mixed upwards in the water-column to replace the outflowing brackish water. Saanich Inlet, in contrast, is typically characterized by inverse estuarine circulation, where the net flow of fresher water is usually into the inlet (Herlinveaux 1962).

The watershed area draining directly into Saanich Inlet is relatively small and the main sources of freshwater originate seaward of the inlet (Herlinveaux 1962). The Goldstream River drains into the head of the Saanich Inlet, but its freshwater input is minimal relative to outside sources. In winter, the primary freshwater source is the Cowichan River, located about 10 kilometers northwest of the inlet mouth and in summer, a dominant freshwater source is the Fraser River, located in the Strait of Georgia.

The sill restricts circulation within the deep basin, effectively isolating the deep waters for much of the year. Coupled with infrequent oxygen renewal, anoxic conditions arise due to the relatively rapid oxidation of organic materials settling into the deep basin. Oxygen renewal occurs in the late summer/early fall when dense water upwells off the continental shelf and moves through the Strait of Juan de Fuca into Haro Strait. In Haro Strait, the dense offshore water is mixed with outflowing brackish Fraser River water, creating an intermediate water-mass of sufficient density to sink into the deep basin (Anderson and Devol 1973). Oxygen renewal is not a continuous process but rather occurs in pulses that coincide with the spring-neap tidal cycle. During spring tides, turbulent mixing in Haro Strait and connecting passages is greatest and produces the intermediate water-mass necessary for renewal. Anderson and Devol (1973) suggest that pulses of this intermediate water enter Saanich Inlet during flood tides. Upon reaching the sill, the dense water spills into the deep basin, forcing the anoxic boundary upward (Anderson and Devol 1973; Hobson 1983).

The extent of deep-water renewal varies with the extent and timing of freshwater runoff from the Fraser River and with the extent of offshore upwelling along the continental shelf. Despite exposure to anoxic and severely hypoxic conditions, benthic epifauna in Saanich Inlet maintain high species diversity and abundance (Tunnicliffe 1981). In other coastal areas, species diversity and abundance is reduced by periods of anoxia and hypoxia (Diaz and Rosenberg 1995). While low oxygen tolerance of zooplankton has been investigated (e.g. Hoos 1970; Spicer et al. 1999; Stadler and Marcus 1997), the effect of the changing anoxic boundary on pelagic zooplankton distribution patterns is unknown.

Mid-water oxygen is replenished near the inlet mouth through incursions of mixed outside water during flood tides. The density of tidal incursions is insufficient to penetrate the deep basin and the horizontal distance travelled by an incursion is limited by the strength and velocity of the tide. Tidal currents are weak in Saanich Inlet (~5 cm s^{-1}; BC Environment 1996) and incursions typically do not extend beyond about three kilometers into the inlet (Gargett et al. 2003). One consequence of these tidal incursions is that waters near the mouth are well-oxygenated relative to the head of the inlet, creating a horizontal oxygen gradient (Herlinveaux 1962). Herlinveaux (1962) observed that low oxygen levels were found shallower near the head than at the mouth. Similar gradients were not observed for temperature or density (Herlinveaux 1962). I expect the interaction between zooplankton oxygen tolerance and behaviour (e.g. diel vertical migration) to influence zooplankton distribution patterns.

1.4.2 Biological Characteristics

Primary production in Saanich Inlet is high compared with other British Columbia inlets (Timothy and Soon 2001). A large phytoplankton bloom typically occurs during the early spring, followed by several smaller blooms throughout the summer and into the fall (Takahashi et al. 1977). Primary production is highest near the inlet mouth and decreases towards the head (Timothy and Soon 2001). Two factors contribute to this spatial gradient: 1) a biological front (Parsons et al. 1983), and 2) periodic estuarine circulation (Gargett et al. 2003).

A biological front, characterized by high rates of primary production, forms in Satellite Channel (Parsons et al. 1983). Phytoplankton from Satellite Channel are tidally advected into Saanich Inlet (Hobson and McQuoid 2001), contributing to primary productivity in the inlet and adding to the food supply for zooplankton near the inlet mouth. Relatively high rates of primary production have also been measured near the head of Saanich Inlet (Timothy and Soon 2001). To produce these high rates, nutrients must be regularly supplied to the euphotic zone. Tidal currents within the inlet are too weak to deliver nutrients from freshwater input at the mouth to the head of the inlet.

Gargett et al. (2003) suggest an 'action-at-a-distance' mechanism of nutrient delivery that is independent of currents and that has a basin-wide effect. They hypothesize that differences in density stratification between Saanich Inlet and mixed waters outside the inlet generate pressure gradients during spring tides that reverse the typical inverse estuarine circulation. This reversal causes normal estuarine circulation with surface outflow and a compensating inflow of dense nutrient-rich water that is upwelled into the euphotic zone. Gargett et al. (2003) suggest that nutrients associated with this upwelling are responsible for the observed high levels of primary production. The strength of upwelling and the concentration of nutrients brought to the surface decreases with headward distance, which could explain the difference in primary production between the mouth and head of the inlet observed by Timothy and Soon (2001). This spatial difference in primary production was most pronounced between April and September and winter (October to March) production was minimal relative to summer months (Timothy and Soon 2001). In the absence of strong physical forcing, I expect higher phytoplankton biomass near the inlet mouth to result in higher zooplankton abundance relative to the head (e.g. Price 1989).

1.4.3 Species

The macrozooplankton community has low species diversity and is numerically dominated by the Pacific euphausiid (*Euphausia pacifica*) and the gammarid amphipod *Orchomene obtusus* (Bary et al. 1962; De Robertis 2002). Greenlaw (1979) observed

that krill abundance (*E. pacifica*) in Saanich Inlet was 1-2 orders of magnitude higher than in offshore areas. Krill concentrations at day-depth can range between 100 to 10 000 individuals m^{-3} (De Robertis 2002; Mackie and Mills 1983). As acoustic targets, krill and amphipods will dominate zooplankton volume backscatter based on their large size (Appendix 1). Other zooplankton species captured or observed in Saanich Inlet include hydromedusae, siphonophores, ctenophores, pteropods, chaetognaths, and copepods (Mackie and Mills 1983; Table 1.1).

Several fish species have been captured in the Saanich Inlet scattering layer (Table 1.1), but a few species dominate in terms of abundance and acoustic target strength. Abundant pelagic fish captured include Pacific herring (*Clupea pallasi*), Pacific hake, and walleye pollock (*Theragra chalcogramma*) (Bary et al. 1962). Herring, hake, and pollock are planktivorous, feeding extensively on euphausiids as juveniles and adults (Outram and Haegele 1972; Hay et al. 1988; Swartzman et al. 2002). During ROV surveys in Patricia Bay, Saanich Inlet, I observed dense schools of herring and/or pollock on the following dates: July 6, 2005, February 21, 2006, August 3, 2006, and February 4, 2007. I also regularly observed fish schools near the bottom during daytime acoustic transects through Patricia Bay.

Table 1.1. Zooplankton, fish, and other species captured within the deep scattering layer in Saanich Inlet (Bary et al. 1962; Bary 1966).

Zooplankton	**Fish**	**Other**
Euphausia pacifica	*Clupea pallasi* (Pacific herring)	Squid spp
Orchomene obtusus	*Merluccius productus* (Pacific hake)	Medusae spp
Calanus spp	*Theragra chalcogramma* (Walleye pollock)	Shrimp spp
Euchaeta japonica	*Squalus acanthius* (Spiny dogfish)	Ctenophores spp
Oithona spp	*Sebastodes flavidus* (Yellowtail rockfish)	
Microsetella spp	*S. diploproa* (Splitnose rockfish)	
	Lampanyctus leucopsarus (Northern lanternfish)	
	Leuroglossus stilbius (Northern smoothtongue)	

Euphausia pacifica, the dominant macrozooplankton species in the Saanich Inlet scattering layer, has a life-span of 19-22 months in British Columbia (Siegel 2000). Spawning occurs in discrete pulses throughout the growing season (April - October) and

the proximate cause of spawning timing is food availability (Siegel 2000). The greatest spawning intensity occurs in time with the spring phytoplankton bloom (Siegel 2000). The age at first spawning is typically 1+ but fast growing age 0 individuals can also contribute to fall spawning (Bollens et al. 1992). Spawning occurs near the surface and the neutrally buoyant eggs remain in surface waters. When the nauplius hatches from the egg, it passes through a metanauplius, three calyptopis, and six furcilia stages (Siegel 2000). After the last furcilia stage, the juvenile euphausiid is about 6mm in length (Bollens et al. 1992). In Barkley Sound, British Columbia, juvenile recruitment at 12 °C was estimated at 47 days (Tanasichuk 1998), with the rate of development dependent on temperature and food resources (Siegel 2000). Most growth occurs between April and October with negligible growth during winter months (Bollens et al. 1992). Maximum summer and lifetime average growth rates for Strait of Georgia *E. pacifica* have been estimated at 0.094 mm d^{-1} and 0.038 mm d^{-1}, respectively (Bollens et al. 1992). In Saanich Inlet, the largest adults captured are about 24mm (e.g. De Robertis 2001).

1.5 Objectives

Past research describing zooplankton distribution patterns demonstrates the importance of zooplankton response to biological and environmental factors for understanding and predicting distribution patterns (e.g. Sameoto 1976; Bollens and Frost 1989; Price 1989; Stadler and Marcus 1997). In this study, I examine patterns in zooplankton density distribution with respect to inlet position and oxygen concentration over a year. I use acoustic volume backscatter as a proxy for zooplankton density, where volume backscatter is proportional to zooplankton density. I also examine horizontal movements of zooplankton at night and zooplankton migration behaviour in shallower depths than the deep scattering layer.

In the absence of strong physical forcing (e.g. Herlinveaux 1962), I expect zooplankton density to be highest near the mouth of Saanich Inlet due to higher food availability related to the biological front described by Parsons et al. (1983). Further, I expect that zooplankton density will decrease with headward distance based on the primary

productivity gradient described by Timothy and Soon (2001) and the 'action-at-a-distance' model of nutrient distribution proposed by Gargett et al. (2003).

Low oxygen concentration also influences zooplankton distribution (e.g. Stadler and Marcus 1997). Devol (1981) characterized the anoxic layer in Saanich Inlet as a 'false bottom' that limits the descent depth of vertically migrating zooplankton. As the anoxic layer moves upward over time (e.g. Anderson and Devol 1973) and depth refuge from visual predators becomes limited, zooplankton will migrate to the deepest depths accessible, resulting in greater vertical compression of the deep scattering layer. If the anoxic layer is a barrier to vertical migration, then, as the anoxic layer moves deeper following oxygen renewal, I expect zooplankton to descend to greater depths to take advantage of the increasing depth refuge.

The night-time distribution of mid-inlet zooplankton and the migration behaviour at shallow sites have not been studied in Saanich Inlet. The dominant macrozooplankton species in Saanich Inlet undergo diel vertical migrations (Bary 1966; De Robertis 2002). Moored acoustic data suggest that the mid-inlet zooplankton scattering layer moves horizontally over shallow depths at night (ASL Environmental Sciences and R. Yahel, unpublished data). Pelagic zooplankton descending over shallow bottoms could be an important contributor to benthopelagic coupling in Saanich Inlet, but the magnitude of horizontal movements into the shallows is unknown. Vertically migrating benthic zooplankton also contribute to benthopelagic coupling (Raffaelli et al. 2003). Diel vertical migration of benthic mysids was observed at a shallow site in the San Juan Islands in Washington State (Kringel et al. 2003) and I expect similar migrations to occur at shallow depths in Saanich Inlet.

During daytime acoustic transects through Patricia Bay, I observed numerous fish schools close to the deep scattering layer. Studies have shown that planktivorous fish presence can alter the timing and depth of zooplankton vertical migration (e.g. Bollens and Frost 1989; Tjossem 1990). How fish schools influence the migration behaviour of the

zooplankton scattering layer in Saanich Inlet has not been investigated. I expect that the presence of fish schools near the deep scattering layer will delay zooplankton ascent.

In **Chapter 2**, I explore the following concepts:

1. The density of the mid-inlet zooplankton scattering layer decreases with headward distance from the mouth of Saanich Inlet.

2. The vertical extent (depth range) of the zooplankton scattering layer changes with changing anoxic boundary depth.

3. The anoxic layer is a barrier to vertically migrating zooplankton in Saanich Inlet.

In **Chapter 3**, I explore the concepts that:

1. Mid-inlet zooplankton move horizontally over shallow bottoms at night after vertical migration.

2. Zooplankton vertical migrations occur at shallow depths at the Inlet edges.

3. Planktivore presence alters mid-inlet zooplankton migration behaviour.

In **Chapter 4**, I provide a summary of my major findings and suggest directions for future research.

Chapter 2
Mid-inlet Zooplankton Distribution

2.1 Introduction

In the absence of strong physical forcing, zooplankton response to biological and environmental cues will influence distribution patterns. Understanding how zooplankton respond to biological and environmental gradients in coastal systems will assist in understanding pelagic ecosystem responses to changing environmental conditions (Largier 1993). Biological fronts can influence zooplankton distribution patterns by concentrating phytoplankton along or near the front (Parsons et al. 1983). Zooplankton will be attracted to areas of high phytoplankton biomass (e.g. Price 1989), potentially influencing the distribution of planktivores and higher-level predators (Largier 1993). Based on food availability, higher zooplankton abundance is predicted for regions with high phytoplankton biomass. Sameoto (1976) observed a significant positive correlation between euphausiid abundance and chlorophyll concentration in the Gulf of St. Lawrence. I hypothesize that a similar relationship exists in Saanich Inlet as zooplankton respond to the biological front at the inlet mouth and increased phytoplankton biomass through tidal advection.

Zooplankton also respond to environmental cues such as dissolved oxygen gradients (e.g. Devol 1981; Spicer et al. 1999). As zooplankton are the main energetic link between primary producers and higher trophic levels, factors influencing their distribution can have significant ecosystem effects. Rabalais et al. (2002) observed that, during periods of hypoxia, many species normally common to shelf waters in the Gulf of Mexico were either absent or present in low numbers. Forced migrations (Rabalais et al. 2002) or increased spatial overlap between predators and prey through habitat limitation (e.g. Eby and Crowder 2002) could alter community structure and change food web dynamics (e.g. Decker et al. 2004). Breitburg et al. (1997) observed that community composition shifted from crustacean dominance to gelatinous zooplankton during periods of low dissolved oxygen.

The number of coastal and estuarine areas experiencing hypoxia and anoxia is increasing (Diaz and Rosenberg 1995). Most studies on the effects of hypoxia have focused on benthic communities in relatively shallow waters (e.g. Decker et al. 2003), whereas studies on the effects of hypoxia on pelagic communities have been limited. In benthic communities, hypoxia can reduce animal abundance and species richness, leaving only low-oxygen tolerant species present (e.g. Rabalais et al. 2002). However, in Saanich Inlet, Tunnicliffe (1981) observed high species diversity and abundance in a benthic epifaunal community seasonally exposed to anoxia and severe hypoxia. Recovery from hypoxic and anoxic episodes is slow in most benthic communities (Diaz and Rosenberg 1995).

In the pelagic environment, Spicer et al. (1999) observed that the descent depth of northern krill (*Meganyctiphanes norvegica*) was limited by hypoxia, reducing depth refuge. Eby and Crowder (2002) observed that the distribution of various fish species was compressed during hypoxia resulting in an increased overlap between predators, prey, and competitors that did not occur during normoxic conditions with greater habitat availability. As the energetic link between primary producers and higher trophic levels, hypoxic effects on zooplankton distribution could have significant effects on ecosystem function. The absence of zooplankton could lead to the absence of planktivores and top predators. Saanich Inlet provides a stable environment with predictable changes in hypoxic and anoxic conditions to assess changes in zooplankton distribution patterns in relation to changing oxygen concentration. Results from Saanich Inlet should be applicable to other coastal regions where areas of hypoxia could affect distributions of pelagic organisms.

Specifically, I am interested in the following questions:

1) Is zooplankton density higher near the mouth of Saanich Inlet relative to the head as predicted by the biological front and nutrient input, and is this pattern persistent through time?

2) How do changing oxygen conditions affect zooplankton distribution patterns in space and time in Saanich Inlet?

2.2 Methods

2.2.1 Data Collection

2.2.1.1 Acoustic Data

Acoustic data were collected monthly from April 2005 to March 2006 from *MSV John Strickland* on a twelve kilometer mid-inlet transect from Patricia Bay to Squally Reach (Figure 2.1; Table 2.1). Data were collected using a 200 kHz single-beam ASL Environmental Sciences Water Column Profiler® (WCP) with an 8° beam angle (Appendix 1). The WCP is also known as a Zooplankton Acoustic Profiler (ZAP). As a single-beam system, the ZAP records echoes returning from a volume but cannot differentiate single targets within a volume. The ZAP sampled at one hertz (Hz) and had a maximum range of 200 meters. Echoes were automatically binned into preprogrammed vertical bins of 0.125 meters or eight bins per meter. The pulse duration during each sample or ping (Appendix 1) was set to either 300μs or 600μs. Gain setting one (least gain; ASL Environmental Sciences 2004) was used for all transects to limit noise generated at long ranges (e.g. >100m; section 2.2.2.2). The ZAP uses an 8-bit (i.e. 2^8) A/D converter, resulting in a digital resolution of 256 discrete counts, ranging from 0 to 255.

The ZAP transducer was positioned on a mast 2.5 meters below the water line to avoid hull reflections. An aluminum fin was attached to the mast at the waterline to reduce turbulence and limit physical movement of the transducer. The transect was steamed from north to south (Figure 2.1) at a nominal speed of 5 knots (2.6 m s^{-1}) and the total transect time was approximately 1.5 hours (Table 2.1). Data were collected during daylight hours to ensure that vertical zooplankton migrants were at day-depth.

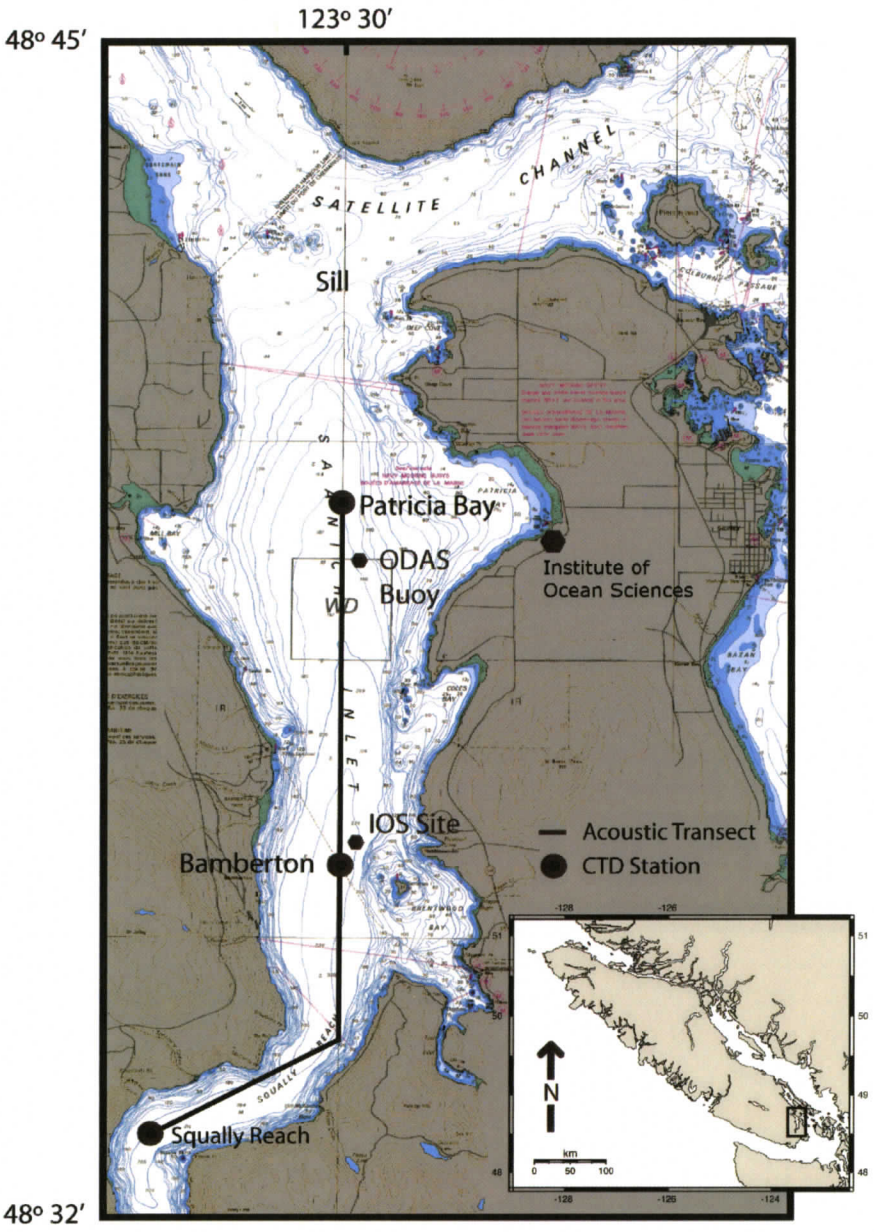

Figure 2.1. Saanich Inlet acoustic transect, CTD stations, ODAS buoy, and IOS sample site.

Table 2.1. Data collection date and time (PST) for mid-inlet transect data between April 2005 and March 2006.

	Date	Sunrise	Transect Start	Transect End
2005	April 26	0502	0805	0930
	May 20	0426	0906	1030
	June 21	0411	0916	1044
	July 20	0433	0914	1041
	August 19	0513	0900	1030
	September 20	0558	0902	1026
	October 18	0639	0923	1044
	November 29	0743	1155	1325
	December 16	0801	1246	1408
2006	January 26	0751	0733	0856
	February 16	0720	0916	1035
	March 21	0615	0935	1109

2.2.1.2 Position Data

Latitude, longitude, speed, and bearing along the transect were collected every six seconds using a Garmin XL 12 global positioning system (GPS) equipped with an external antenna. GPS data were captured as text files using HyperTerminal® software. Position data were accurate to within 15 meters.

2.2.1.3 Environmental Data

Profiles of environmental variables were made at three locations during each transect: Patricia Bay, Bamberton, and Squally Reach (Figure 2.1, Table 2.2). These locations represented the mouth, middle, and head of Saanich Inlet. Data were collected using a SeaBird Electronics SBE 19plus Conductivity-Temperature-Depth (CTD) probe equipped with a Wetlabs WetStar® fluorometer and a SeaBird SBE 43 dissolved oxygen sensor. The CTD was lowered at approximately 1 m s^{-1} to within 15 meters of the bottom while sampling at 4 Hz. Only the downcast was used. Variables measured or derived included:

- temperature (°C)
- salinity (psu)
- density (sigma-t; kg m^{-3})
- dissolved oxygen (mL L^{-1})
- chlorophyll fluorescence (μg L^{-1}).

The Patricia Bay and Squally Reach CTD stations were sampled at the start and end of each transect, respectively. To allow for continuous acoustic data, the Bamberton CTD station was sampled after the acoustic transect was completed.

Table 2.2. Location of Saanich Inlet CTD stations.

Station	Latitude	Longitude	Bottom Depth (m)
Patricia Bay	48° 39.190	123° 30.000	185
Bamberton	48° 35.115	123° 30.370	225
Squally Reach	48° 33.135	123° 32.536	210

Dissolved Oxygen Sensor Accuracy

In February 2005, the SBE 43 dissolved oxygen sensor was calibrated by SeaBird Electronics. The oxygen sensor was recalibrated in June 2006 following completion of field data collection. Drift in the accuracy of oxygen measurements was negligible (<1%). Based on these calibration results, dissolved oxygen measurements were considered accurate and comparable between cruises.

2.2.2 Data Processing

Data processing was completed in Matlab and included: 1) merging GPS and acoustic data sets, 2) removing internal instrument noise, 3) converting digital counts to volume backscattering strength (S_v; Appendix 1), and 4) removing fish school echoes from transects.

2.2.2.1 Merging Acoustic and GPS Files

GPS data (latitude, longitude, speed, and bearing) were merged with acoustic data based on common time. Latitude and longitude were converted into universal transverse mercator (utm) northings (N) and eastings (E). Because the ZAP sampled at 1 Hz and the GPS updated every six seconds, utm coordinates were interpolated between the updated GPS positions to provide a unique position for each acoustic sample.

Due to drift while on station at the Patricia Bay CTD site and the variable time to reach the transect speed of 5 knots among months, transects did not all start from the same position. Data were included in a transect when the vessel speed was greater than 4.7 knots. To ensure the analyses examined the same locations, the start and end northings for each monthly transect were determined and all transects were set to commence at the most southerly start point (5388362N; Patricia Bay) and terminate at the most northerly end point (5378215N; Squally Reach). Data north and south of these positions were excluded from analyses.

2.2.2.2 Internal Instrument Noise

To compensate for geometric transmission loss (Appendix 1), the ZAP applies a 20 log R (MacLennan and Simmonds 1992) time-varied gain (TVG), where more gain (signal amplification) is applied as the time from transmission to detecting an echo increases (Figure 2.2). The addition of gain to backscatter from greater ranges permits direct comparison of echoes by making echo strength independent of range. When high gain levels are applied, the electronics within the instrument begin to generate noise that is detected and recorded by the ZAP (Figure 2.3 and 2.4a). Internal instrument noise below one count is not detected and does not degrade the measured signal. Instrument noise is first detected after about 0.10 seconds (equivalent to 75 meters range when c is 1480 m s^{-1}) and increases rapidly after about 110 meters range (Figure 2.3). At large ranges (e.g. >130m), this noise can potentially mask echoes from weak zooplankton scatterers.

To remove this noise, a curve was fitted to a plot of minimum count per depth bin for ZAP data in calm water with few scatterers (Figure 2.3). This curve was then applied to each depth bin, where the expected noise in counts from the curve was subtracted from the measured counts. This method does not remove all of the noise from every depth bin but it does clean the signal in the depth range of interest (10-130 meters; Figure 2.4b). Because the curve is continuous and does not exactly match the stepped increments of the instrument noise, subtracting the noise curve from measured data results in partial counts. Following noise removal, all counts less than one were removed from the data.

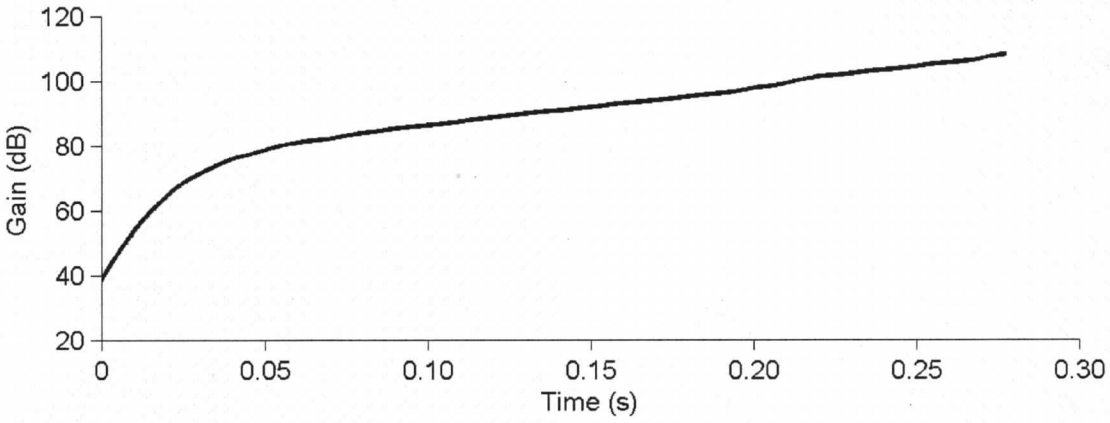

Figure 2.2. The $20*\log_{10}$Range time-varied gain function used by the ZAP to compensate for geometric transmission loss. Range is function of time and more gain is applied as the time between transmission and reception of an echo increases.

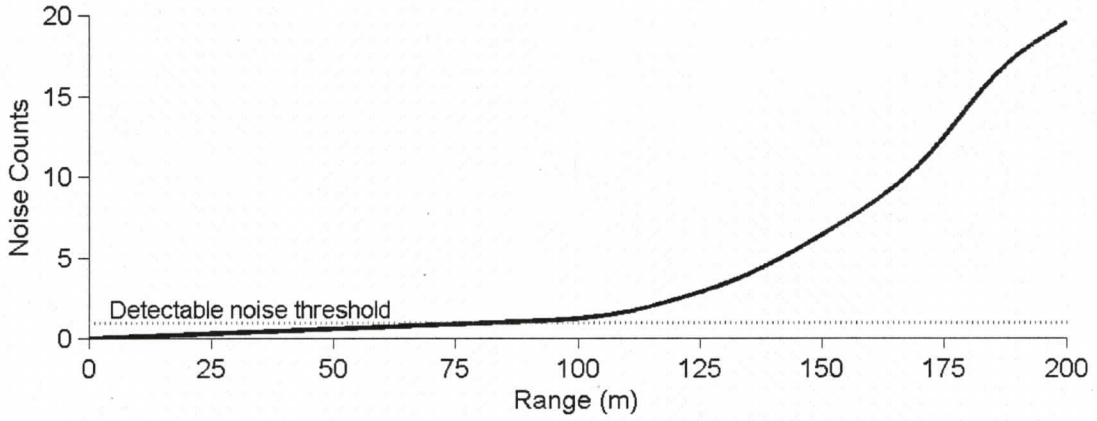

Figure 2.3. Internal instrument noise generated by the ZAP at gain setting one. The detectable noise threshold is one digital count, and beyond 100 meters range, the ZAP generates noise that is recorded by the instrument. At long ranges, the noise counts can potentially mask echoes from zooplankton.

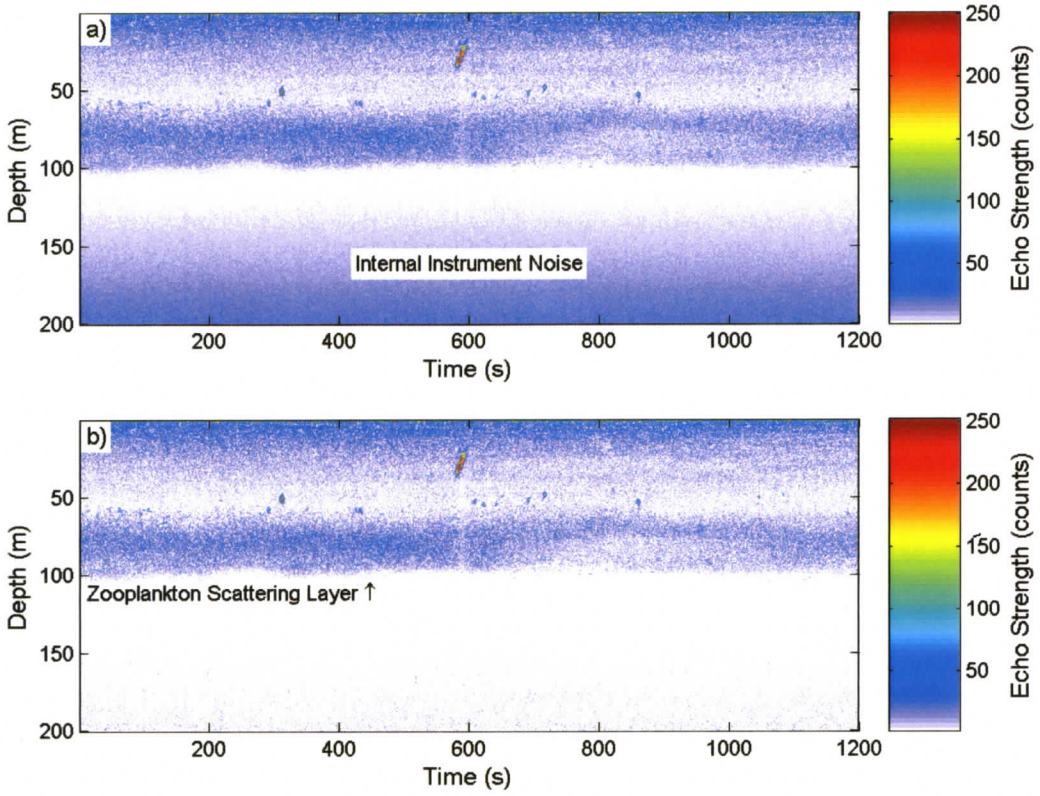

Figure 2.4. Example of internal instrument noise, a) before noise removal, and b) after noise removal. Data are from April 2005 in Saanich Inlet. Echoes from depths greater than 130 meters were not included in analysis.

Further attempts to remove noise would likely start to degrade zooplankton echoes so no further noise removal was conducted.

2.2.2.3 Digital Counts to Volume Backscattering Strength (S_v) Conversion

Digital counts were converted to S_v using the SONAR equation (Clay and Medwin 1977; Appendix 1). The volume insonified by a conical beam increases with range. For example, for an 8° beam and 300 μs pulse width, the insonified volumes at 25 and 75 meters are 2.1 and 19.1 m^3, respectively. The SONAR equation provides a logarithmic measure of volumetric echo strength scaled to one cubic meter for each depth bin. S_v is a common measure for bioacoustic studies, and is expressed as a logarithmic ratio between the energy incident on a volume of targets and the backscattered energy from the volume:

$$S_v = 10 \log (I_e/I_i),$$

where, S_v is measured in decibels (dB), I_e is the backscattered echo intensity at one meter from the volume, and I_i is the intensity of the sound wave incident on the volume (Greenlaw 1979). The echo intensity is always less than the incident intensity so S_v values are negative. Where S_v refers to the echo strength from a volume of targets, the target strength (TS) refers to the echo strength from a single target (e.g. a single euphausiid). Target strengths are also logarithmic ratios expressed as negative numbers.

2.2.2.4 Removing Fish School Echoes

Efforts were made to limit the contribution of fish echoes to S_v used in analyses. Fish schools identified from echograms based on their spherical or elliptical shape (Figure 1.1) and volume backscattering strength were deleted from each transect. Where fish schools were not obvious based on shape, determining the contribution of fish to the S_v from a depth bin was difficult. With a single-beam, single frequency acoustic system, it is not known whether the echoes received from a volume are from a single strong reflector on the acoustic axis (Appendix 1) or from numerous weak scatterers distributed throughout the beam (MacLennan and Simmonds 1992). There can also be overlap in predicted S_v between fish and zooplankton based on known species presence and target strength models.

For example, target strengths for Pacific herring and walleye pollock at 200 kHz can be predicted using the linear regression models of Gauthier and Horne (2004):

$$TS_{herring} = 24.2 \log (L_T) - 74.3,$$

$$TS_{pollock} = 22.5 \log (L_T) - 73.1,$$

where, TS is the target strength (dB) and L_T is fish length in centimeters. For a 20 centimeter fish, the modelled target strengths for herring and pollock are -42.8 and -43.8 dB, respectively. If only one of these fish was present in 1 m^3, then TS and S_v are equivalent. Both of these species are known to form dense daytime schools (e.g. Hay and McKinnell 2002; Brodeur and Wilson 1996). Average fish densities in Atlantic herring schools vary between 0.9 and 5.1 fish m^{-3} for fish 20-28 cm (Misund 1993). Applying the Gauthier and Horne (2004) model to these densities predicts S_v ranging from -44.3 to -35.7 dB, respectively. Dense patches of zooplankton can also reach this S_v range. The daytime densities of euphausiids in Saanich Inlet can vary between about 100 and 10 000 individuals m^{-3} (De Robertis 2002; Mackie and Mills 1983). Assuming an average target strength of -80 dB for euphausiids at 200 kHz (Macaulay 1994), this density range would result in S_v between -60 and -40 dB. The S_v for dense euphausiids and low-density schools (e.g. 1-2 fish m^{-3}) overlap, but without capture data, it is impossible to assign the contribution of fish and zooplankton to volume backscattering.

To separate fish and zooplankton signals effectively, at least two acoustic frequencies should be used. With two frequencies such as 38 kHz and 120 kHz, fish echoes can be separated from zooplankton echoes using the difference in echo strength at the two frequencies (e.g. Miyashita et al. 2004). In some single-frequency studies, it has been possible to filter some fish signals from zooplankton using either a S_v threshold (e.g. De Robertis 2002) or echo statistics (e.g. Trevorrow 2005). Both of these methods require some knowledge of species and size composition through either visual observations or net capture (e.g. Brodeur and Wilson 1996). Neither ground-truthing option was consistently available during this study, although ROV observations and infrequent vertical net tows did confirm published data regarding the dominant zooplankton species present in the Saanich Inlet scattering layer (Table 2.3).

Table 2.3. Zooplankton captured or observed in the deep scattering layer during net tows or during ROPOS ROV operations in Saanich Inlet between November 2004 and February 2007.

Date	Method	Time (UTC)	Depth (m)	Species Captured or Observed
Nov 14, 2004	ROV	0645	90	Euphausiids, copepods
April 15, 2005	*Vertical net	0150	105-65	Euphausiids, amphipods, copepods
Jul 10, 2005	ROV	2204	100	Euphausiids
Jul 12, 2005	ROV	1438	85	Copepods, chaetognaths
Jul 17, 2005	Vertical net	0015	110-65	Euphausiids, amphipods, chaetognaths
Feb 28, 2006	Vertical net	2252	120-60	Euphausiids, amphipods
Aug 5, 2006	ROV	1944	103	Euphausiids
Aug 6, 2006	ROV	0338	93	Euphausiids
Feb 1, 2007	Tucker trawl	0108	154-0	Euphausiids, amphipods
Feb 4, 2007	ROV	2118	101	Euphausiids

* Vertical net tows were conducted using a SCOR net with a 0.57m diameter opening and 236μm mesh.

Although fish have been captured in the deep scattering layer in Saanich Inlet (Bary et al. 1962; Bary 1966), low dissolved oxygen concentrations limit fish access within the scattering layer. De Robertis (2002) observed little daytime overlap between zooplankton and fish at a mid-inlet station near Bamberton. I expect the contribution of fish signals from within the scattering layer to be low based on this limited access and I assume that S_v is dominated by zooplankton. Most fish in the upper water column (i.e. shallower than the deep scattering layer) were observed within schools that were identified and removed from the data.

Where fish schools could not be identified by their spherical or elliptical shape, a -50dB threshold was applied to the data. This S_v threshold corresponds to a euphausiid density of 1000 animals m^{-3} and S_v greater than this threshold were not included in analyses. Relatively few S_v values exceeded this threshold (Figure 2.5) but these values were the strongest recorded and likely included backscatter from fish.

2.2.2.5 Site Selection

Three segments along the transect were selected for analysis of zooplankton scattering layer characteristics among sites and months. Each site was located near a CTD station and the same sites were used for each month. Rather than using a fixed site length, it was

more appropriate to delineate sites based on a constant number of acoustic samples where actual site length varied slightly with average ship speed. Each site, with the exception of Squally Reach in March 2006, consisted of 385 pings at a nominal ship speed of 5 knots (2.6 m s^{-1}), and sites were approximately one kilometer in length. In March 2006, Squally Reach was steamed at 3.1 knots due to problems with the transducer mast and this site consisted of 620 pings. Mean site length was 1018 meters and ranged from 960 to 1093 meters. The variability between the minimum and maximum site lengths was only 12%.

2.2.3 Analysis

I used paired t-tests to compare hypoxic, anoxic, pycnocline, and thermocline depths, and zooplankton density among sites. To correlate zooplankton density and scattering layer characteristics with environmental variables, I used Pearson product-moment correlations.

2.2.3.1 Environmental Variables

For each CTD profile, I averaged density and temperature into one meter depth bins. I defined the base of the permanent thermo- and pycnoclines as the depth where the temperature or density change between descending depth bins was 0.00 and the profile was nearly isothermal or isopycnal.

For dissolved oxygen, hypoxia was defined as less than 2.0 mL O_2 L^{-1} (Diaz and Rosenberg 1995). I defined the anoxic boundary arbitrarily as 0.1 mL O_2 L^{-1} because the oxygen sensor did not actually record zero, even when waters were known to be anoxic (based on the presence of hydrogen sulphide). The instrument is accurate to 2% of saturation. Assuming a temperature and salinity of 10 °C and 30 psu, saturation would be 6.52 mL O_2 L^{-1}, yielding an accuracy of 0.1 mL L^{-1}.

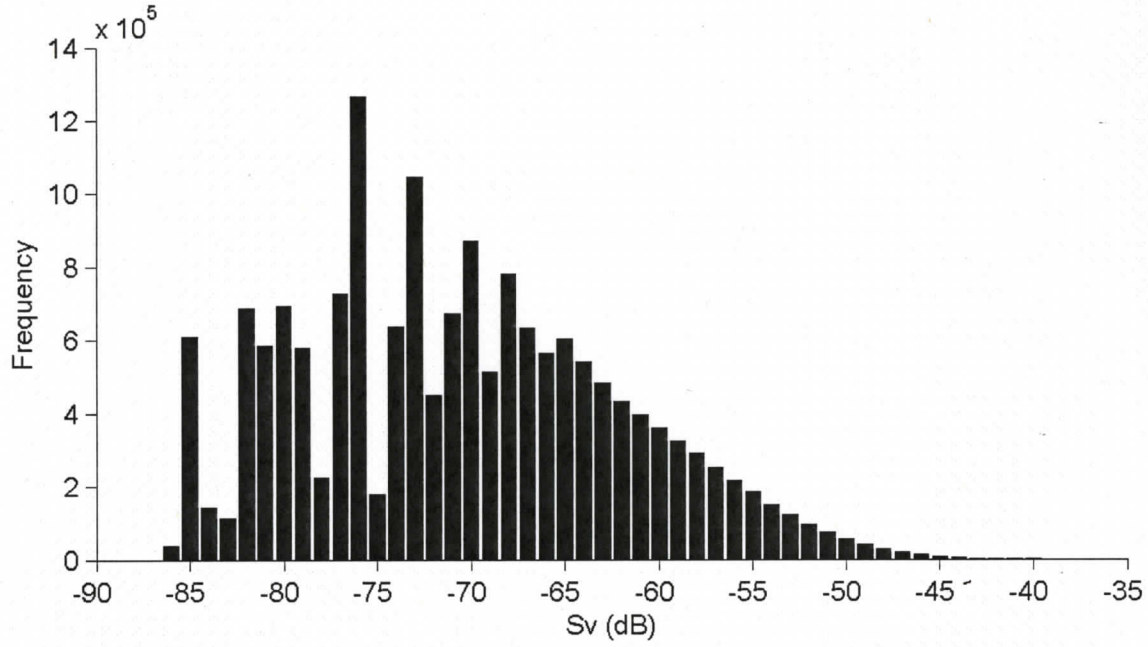

Figure 2.5. Sv-frequency histogram for combined monthly transects. Sv data are for each depth bin of each ping along a transect. Relatively few echoes exceeded -50dB and these echoes were assumed to originate from fish within the scattering layer. Echoes stronger than -50dB were not included in analyses.

2.2.3.2 Zooplankton Distribution

With the exception of the November transect, only data included in the range 10-130 meters were included in the analyses. In November, I collected data from a small boat with twin-outboard engines that generated considerable noise that was recorded by the ZAP. I excluded data below 100 meters for November. This deletion had minimal effect on analysis as the zooplankton scattering layer did not reach below 100 meters in November. Data shallower than 10 meters were excluded to avoid near-surface noise or bubbles generated by the ship. Below 130 meters, the acoustic system generated internal noise that could mask zooplankton targets. The zooplankton scattering layer rarely exceeded 130 meters depth so exclusion of these data avoids including instrument noise and should not bias analyses.

Volume backscattering strength values for each depth bin in each sample (ping) were converted into their linear equivalent, the volume backscattering coefficient (s_v; m^{-1}):

$$s_v = 10^{Sv/10}.$$

The volume backscattering coefficient is a measure of inferred zooplankton density in terms of echo energy (pers. comm., Duncan McGehee, University of Washington, Friday Harbor Laboratories). If the identity of the scatterers is known, s_v can be converted into numeric density (i.e. N m^{-3}). Because of mixed species composition, this conversion was not attempted here.

For each ping, s_v was integrated over the range 10-130 meters, providing a proxy for zooplankton density. To examine the overall trend in zooplankton density along a transect, the integrated volume backscatter for each ping was plotted against transect distance. Each transect consisted of at least 4500 pings and a running average of 39 pings (~100m at 2.6 m s^{-1} ship speed and 1 Hz acoustic sampling rate) was used to smooth the data. Data from the start of Squally Reach where the bottom was shallower than 125 meters were deleted to avoid including bottom reflections in analyses. Zooplankton abundance in this area was typically low due to the relatively shallow bottom (relative to the deep scattering layer in the rest of the inlet).

Gradient

To determine whether a persistent gradient in zooplankton density was present, I calculated mean integrated volume backscatter in the three segments representing the inlet mouth (Patricia Bay), middle (Bamberton), and head (Squally Reach). To test for a persistent horizontal spatial gradient in zooplankton density, I used a nonparametric ranks test (Hollander and Wolfe 1999). Parametric tests assume that the samples are taken from a population with a normal distribution (Potvin and Roff 1993). For small sample sizes (e.g. n = 12), there are usually insufficient data to test this assumption. Nonparametric statistical tests are distribution-free tests where no assumptions are made regarding the underlying distribution of the sampled population. Nonparametric tests are preferred when sample sizes are small and estimates of population parameters are not required (Potvin and Roff 1993).

A number of nonparametric rank tests are available that will test for differences in means between groups. For data sets with at least three groups, the Kruskal-Wallis test is commonly used and is similar to the parametric one-way ANOVA (Hollander and Wolfe 1999). The Kruskal-Wallis test will test for differences between means of groups based on ranks, but it does not determine if group order is monotonic. When the order of groups can be predicted *a priori*, a test is required that will test for significance of group order. Page (1963) developed a modified Kruskal-Wallis rank test for ordered alternatives that included predicted group orders.

The *Page test for ordered alternatives* (Page test) is appropriate for this study because the expected order of zooplankton density can be predicted from the observations of Parsons et al. (1983), Gargett et al. (2003), and Timothy and Soon (2001). Their observations of higher nutrient concentrations and primary productivity near the mouth of the inlet relative to the head suggest that zooplankton, which feed on phytoplankton, should follow a similar gradient. My expectation was that zooplankton density would be highest near the inlet mouth, intermediate in the inlet middle, and lowest at the head of the inlet. Based on this expectation, in order of descending zooplankton density, the three sites can be ordered: 1) Patricia Bay (mouth), 2) Bamberton (middle), and 3) Squally Reach (head).

In the context of this study, the null hypothesis for the Page test can be expressed as:

$$H_0: m_{\text{Patricia Bay}} = m_{\text{Bamberton}} = m_{\text{Squally Reach}},$$

and the ordered alternative hypothesis as:

$$H_A: m_{\text{Patricia Bay}} \geq m_{\text{Bamberton}} \geq m_{\text{Squally Reach}},$$

where m represents mean integrated volume backscatter and there is at least one strict inequality (Page 1963). The Page test calculates an L statistic:

$$L = \sum^{n} (Y_j \sum^{m} X_{ij})$$

where, n is the number of sample sites, m is the number of months, Y_j is the expected rank for the j^{th} sample site, and ΣX_{ij} is the sum of ranks for each site for all months. To calculate L, data were tabulated with monthly ranks in rows and sample sites in columns

(Table 2.6). The L value is compared to l_α from L-tables and if $L \geq l_\alpha$, the result is considered significant at the chosen α level (Hollander and Wolfe 1999). A significant result indicates the presence of a gradient in the data. The Page test has been used in ecological studies to analyze vertical zooplankton gradients over coral reefs (Yahel et al. 2005).

Scattering Layer Boundaries

I delineated the boundaries of the zooplankton scattering layer for each ping along a transect using a custom routine in Matlab. Within each ping, I calculated the s_v difference between adjacent depth bins. I used a s_v threshold of 0.25×10^{-6} to define the scattering layer boundaries. I tried different thresholds and this value provided the best fit to the scattering layer. With increasing depth, the first bin where the change in s_v exceeded this threshold delineated the top scattering layer boundary. I defined the base of the scattering layer as the depth bin where the change in s_v between increasing depth bins exceeded -0.25×10^{-6}. A negative threshold was used to identify changes from high to low s_v with increasing depth expected at the base of the scattering layer. For each of the three sites, I calculated the mean depths of the top and base of the scattering layer for each month.

2.3 Results

2.3.1 Chemical and Physical Characteristics

2.3.1.1 Dissolved Oxygen

Winter and Summer Comparison

Winter and summer dissolved oxygen (DO) data from bottle casts collected by Institute of Ocean Sciences (IOS) researchers near Bamberton (Figure 2.1) between 1996 and 2005 show seasonal variation throughout the water column (Figure 2.6). In the upper 20 meters, winter DO values were within 1.2 mL L^{-1} between years. In summer, near-surface DO declined within an oxycline with values ranging from 10.4 mL L^{-1} at the surface to 3.1 mL L^{-1} at 20 meters depth. Between 20-75 meters depth, winter DO was higher and more constant with depth than in summer. Hypoxic water (<2.0 mL L^{-1}) was

shallower in summer (~65 meters) than in winter (~85 meters). Maximum summer DO (4.1 mL L^{-1}) between 20-75 meter depth was similar to minimum winter values (3.8 mL L^{-1}). Below sill depth, winter DO declined within an oxycline between 75-100 meters depth (Figure 2.6A). I did not observe a deep oxycline in the summer data (Figure 2.6B). Below 100 meters depth, winter DO varied by less than 0.5 mL L^{-1} between years, whereas summer data varied by up to 1.3 mL L^{-1}. IOS recorded anoxia in all years in both winter and summer, except in February 2003 and August 1996. With the exception of March 2000 (219 meters), winter anoxia ranged from 124 to 175 meters depth among years. Summer anoxia ranged between 126 and 217 meters depth. There was no significant difference between winter and summer anoxic depths (paired t-test, p=0.498).

CTD and Bottle Dissolved Oxygen Comparison

CTD oxygen profiles from February 2006 and August 2005 were compared with the IOS bottle data (Figure 2.6). In both winter and summer, CTD profiles had the same overall decreasing DO trend as the IOS bottle data. In the February CTD profile, surface oxygen was within the range of surface bottle data and the CTD data were about 0.5 mL L^{-1} higher than bottle values in the upper 15 meters. Between 15-30 meters, CTD DO was lower than bottle data by about 0.5 mL L^{-1}. Between 30-200 meters, February CTD data were within the range of bottle values, except at 75 meters where the CTD value was about 0.3 mL L^{-1} less than the lowest bottle measurement (Figure 2.6A). In summer, surface DO was within the range of bottle data but was 0.5 mL L^{-1} lower than the 2005 bottle value. In the upper 30 meters, August CTD values were within the range of IOS summer data but between 30-75 meters, the CTD values were about 0.5 mL L^{-1} less than bottle values. The exception was at 50 meters where the 2005 bottle value was at least 0.8 mL L^{-1} lower than both the CTD and the 1996-2004 bottle data. Below sill depth, the CTD data were within the range of bottle values but were highly variable with depth between 75 and 150 meters. Due to natural variability and sample intervals, these differences are deemed not significant.

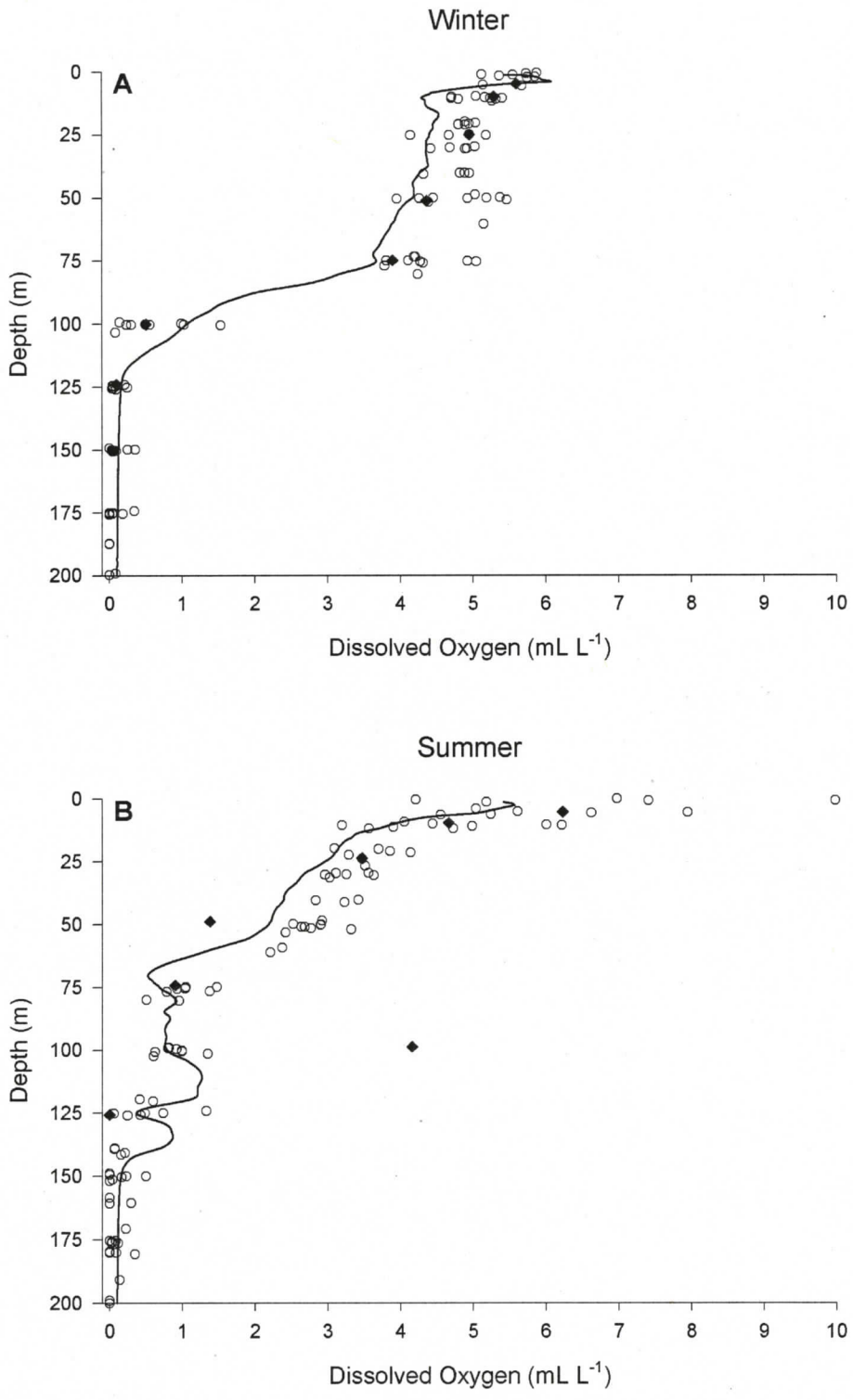

Figure 2.6. Institute of Ocean Sciences Winkler titration dissolved oxygen data for A) February/March and B) August/September in Saanich Inlet near Bamberton from 1996 to 2005 (solid diamonds are 2005 data). The solid lines are the Bamberton dissolved oxygen profiles from this study for February (2006) and August (2005). Sill depth at the mouth of Saanich Inlet is 75 meters.

Monthly Oxygen Profiles

Vertical profiles of DO from the three locations in Saanich Inlet ranged from highly similar (e.g. January) to markedly different throughout the entire profile (e.g. September; Figure 2.7). For most of the year, the oxygen levels from 125 meters to the bottom were within 0.3 mL L^{-1} at the three locations. In all profiles, DO declined from near-surface maxima to anoxia (0.1 mL L^{-1}) in the deep basin.

Maximum DO was recorded at the surface in 61% of profiles. For 39% of profiles, maximum DO was measured at up to 15 meters below the surface (e.g. Figure 2.7D). Below-surface maxima occurred in all seasons. Maximum DO varied seasonally from 14.7 mL L^{-1} in spring (April) to 3.3 mL L^{-1} in autumn (October).

In most months, I observed a surface oxycline where DO changed rapidly with depth. The exceptions were January, which did not have an oxycline, and July where the oxycline occurred between 27-40 meters depth. Surface oxyclines ranged between 3.2 and 21.7 meters depth. In most months, DO decreased by 2 to 4 mL L^{-1} within the oxycline. In April and June, DO increased rapidly with depth in the upper six meters, followed by the rapid decrease observed in other months. Oxygen values at the base of the surface oxycline ranged from 2.7 to 6.6 mL L^{-1} and were highest in the spring.

In mid-water, between the surface oxycline and sill depth (75 meters), DO decreased by up to 3.1 mL L^{-1} with depth. Among sites, mid-water DO decreased the most at Squally Reach. Oxygen decrease was between 0.5 and 3.0 mL L^{-1} greater in Squally Reach than at Patricia Bay, and in most months, Squally Reach DO was less than at Patricia Bay between the oxycline and sill depth (Figure 2.7).

Below sill depth, DO declined steadily to anoxia in spring, autumn, and winter. In summer, DO was variable below sill depth. In June and July, following initial decline, DO increased below sill depth by up to 1.5 mL L^{-1} before becoming anoxic by 125 meters depth at Patricia Bay and Bamberton (Figure 2.7C, D). I did not observe similar increases in Squally Reach in June or July. In August and September, DO increased at

Patricia Bay and Bamberton by up to 1.0 mL L^{-1} below sill depth (Figure 2.7E, F), and this increase extended to greater than 150 meters. In Squally Reach, DO increased slightly below sill depth in August, but I observed no increase in September.

Once anoxia was detected, the water column remained anoxic to the bottom in 89% of profiles. In September and October, I observed an increase in deep-water oxygen below the anoxic layer at Bamberton in September, and at all sites in October (Figures 2.7F, G). The greatest deep-water oxygen increase was 0.3 mL L^{-1} at Bamberton.

Anoxic boundary depth varied among sites and months (Figure 2.8) but was not significantly different between Patricia Bay and Squally Reach (paired t-test, p=0.083). Anoxic boundary depth ranged from 83 to 167 meters depth and was deepest in August at all sites and shallowest in the fall. In contrast, the hypoxic boundary (2.0 mL L^{-1}) occurred significantly shallower at Squally Reach than at Patricia Bay (paired t-test, p=0.002; Table 2.4). Hypoxic boundary depth ranged from 20 to 97 meters depth and was shallowest in late summer and deepest during winter and spring. The hypoxic and anoxic boundaries were most variable in Squally Reach relative to Patricia Bay and Bamberton (Figure 2.8).

Table 2.4. P-values from paired t-tests for comparisons of environmental variables between the Patricia Bay and Squally Reach sites. Only the hypoxic boundary depth was significantly different (α=0.05).

Hypoxic Boundary Depth	**Anoxic Boundary Depth**	***Integrated Chlorophyll Fluorescence**
0.002	0.083	0.836

* Integrated between 0-40 meters.

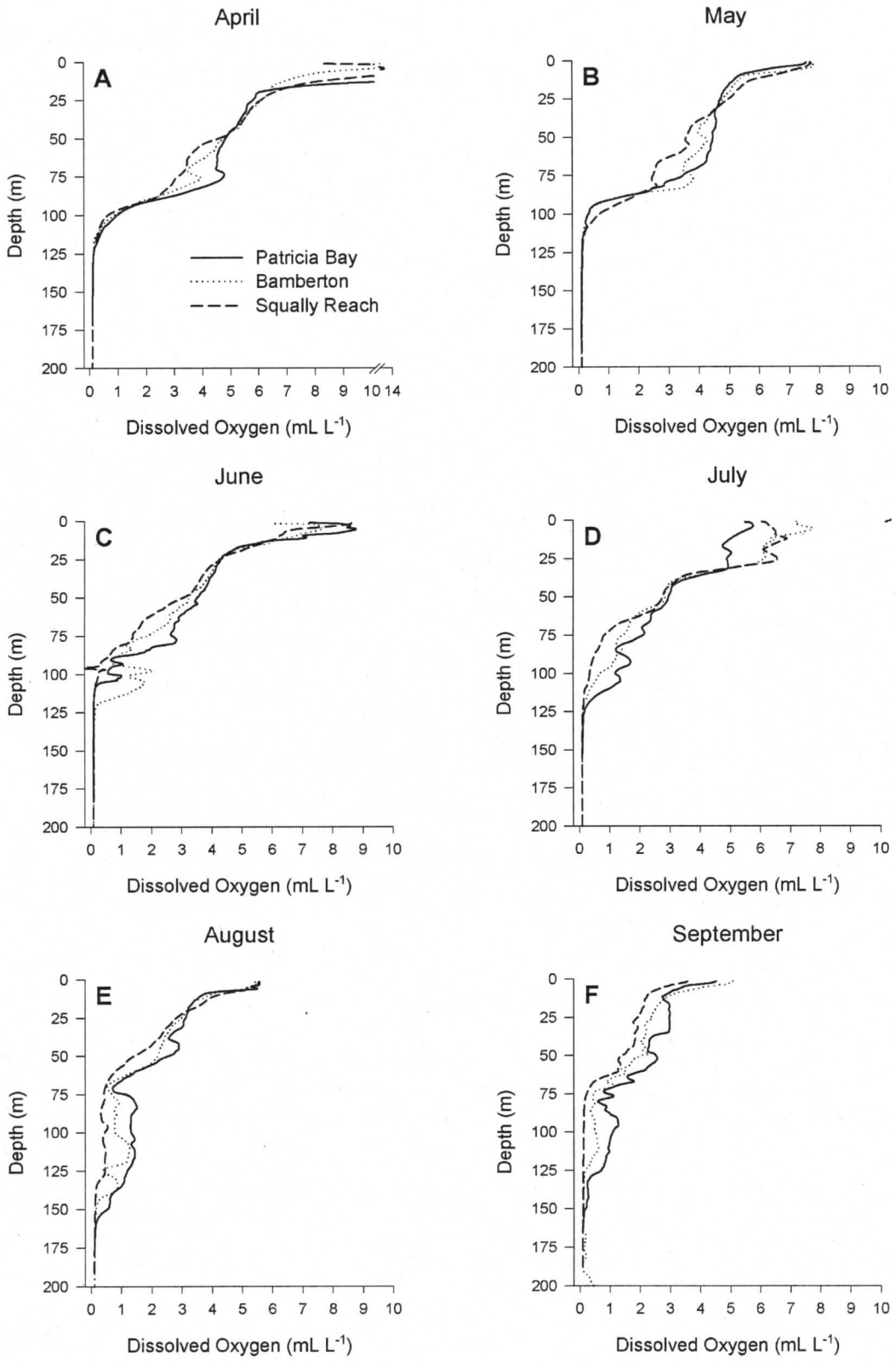

Figure 2.7. Monthly dissolved oxygen profiles for Patricia Bay, Bamberton, and Squally Reach between April 2005 and March 2006. Sill depth at the mouth of Saanich Inlet is at 75 meters.

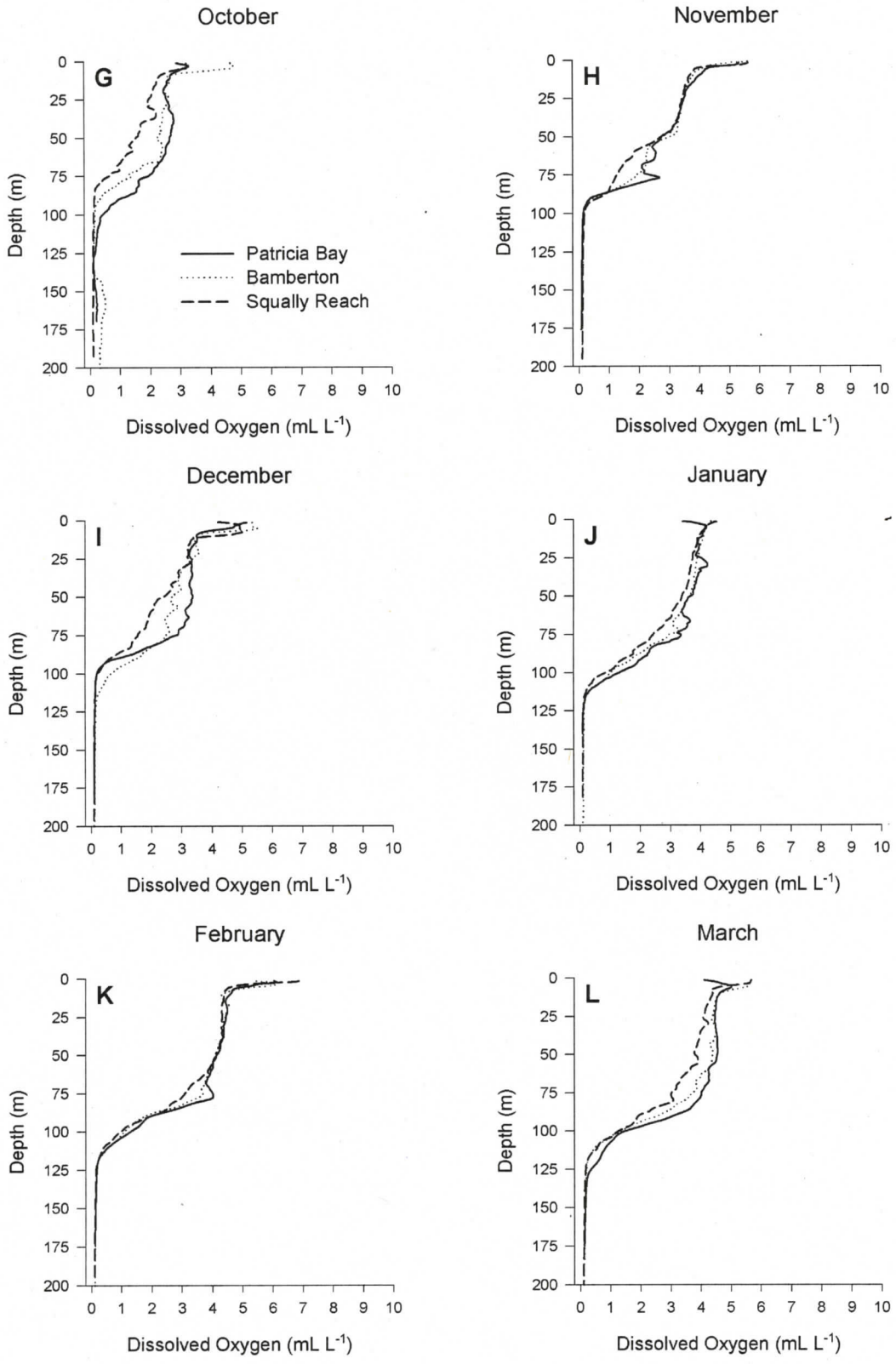

Figure 2.7 continued.

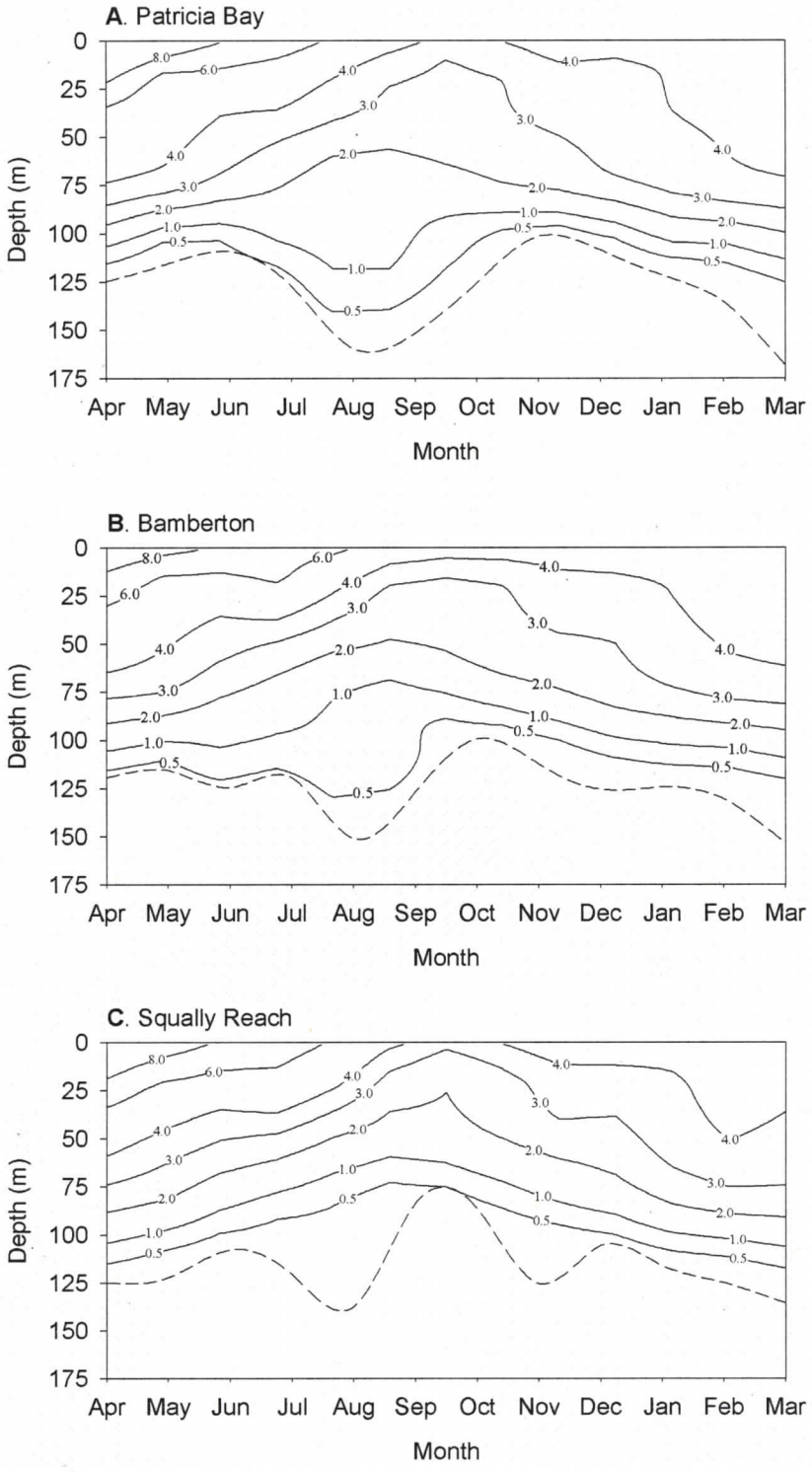

Figure 2.8. Dissolved oxygen (mL L^{-1}) contours and anoxic (0.1 mL O_2 L^{-1}; dashed line) boundary depth for A) Patricia Bay, B) Bamberton, and C) Squally Reach between April 2005 and March 2006.

2.3.1.2 Temperature

Winter and Summer Comparison

Winter and summer temperature data from CTD casts collected by IOS between 1996 and 2005 show seasonal variations above 125 meters depth (Figure 2.9). In winter, temperature increased from a minimum of 7.2 °C at the surface to a maximum of 9.7 °C at 125 meters. Between 125 meters and the bottom, winter temperature was between 9.3-9.7 °C and was isothermal within a year. I did not observe a surface thermocline in the IOS winter data (Figure 2.9A). In contrast, the summer data did have a surface thermocline in the upper 15 meters where temperature decreased rapidly with depth from surface maxima. Surface temperature decreased from a maximum of 17.8 °C to a minimum of 9.1 °C at 100 meters. Below 100 meters, summer temperature was isothermal within a year (e.g. 2005; Figure 2.9B) and ranged between 9.1 and 9.7 °C.

CTD Comparison

CTD temperature profiles from February 2006 and August 2005 from this study were compared with the IOS profiles (Figure 2.9). In both winter and summer, temperature profiles showed the same overall trends as the IOS data. In February, the surface temperature was 5.7 °C, 1.5 °C cooler than the coolest IOS value. The February CTD data had a surface thermocline in the upper 6 meters that was not apparent in the grouped IOS data. Within this surface thermocline, CTD temperature increased to the range of IOS data and remained within this range for the remainder of the profile. CTD temperature increased between the surface and 125 meters and became isothermal at 9.7 °C in the deep basin, following the same pattern as the IOS data (Figure 2.9A).

In August, the CTD data were within the range of IOS data throughout the profile. Summer CTD data had a steep surface thermocline in the upper 15 meters. The CTD data were within 0.8 °C of IOS August 2005 data in the upper 50 meters and were the same as IOS values below 75 meters depth (Figure 2.9B).

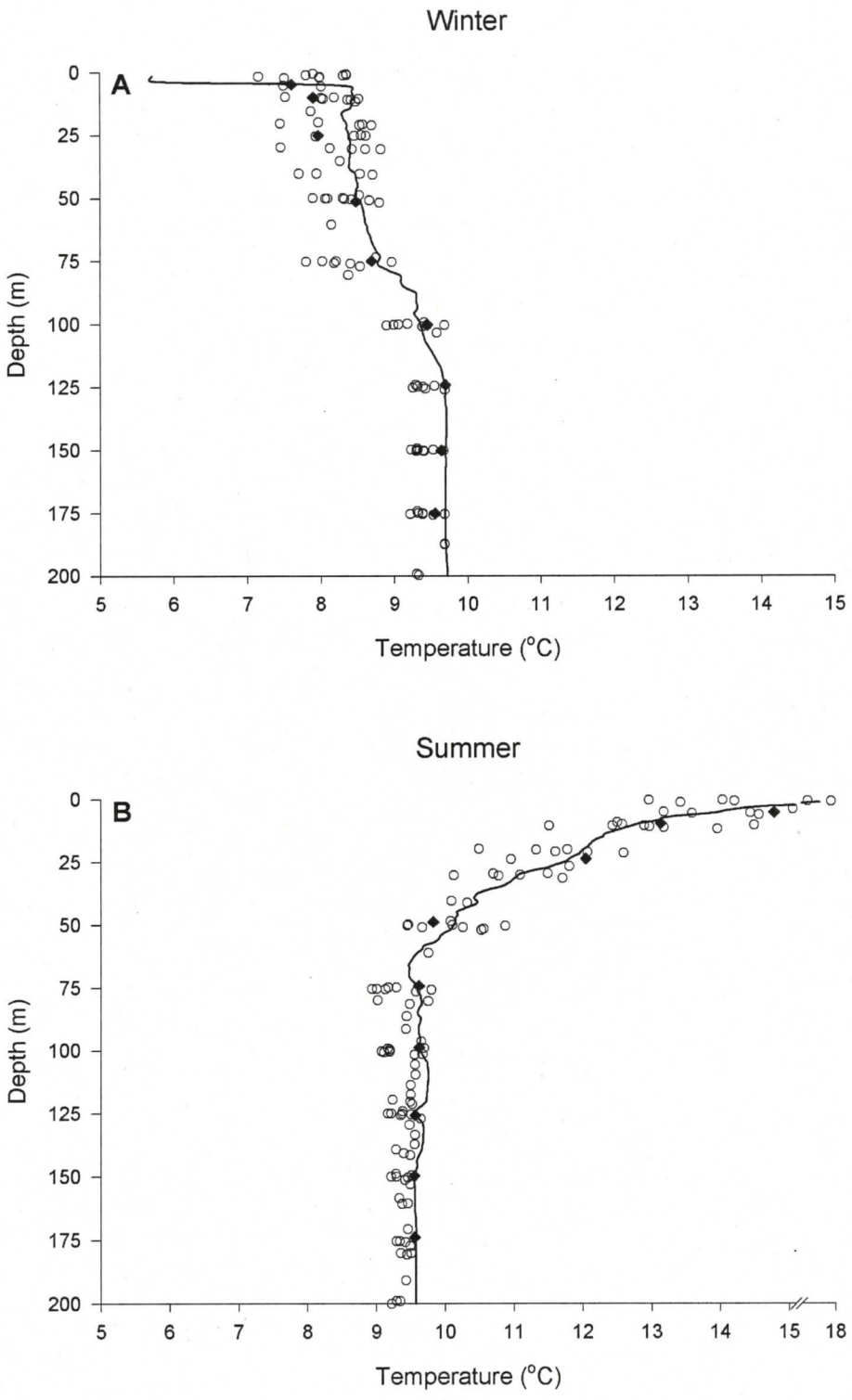

Figure 2.9. Institute of Ocean Sciences temperature data for A) February/March and B) August/September in Saanich Inlet near Bamberton from 1996 to 2005 (solid diamonds are 2005 data). The solid lines are the Bamberton CTD profiles from this study for February (2006) and August (2005). Sill depth at the mouth of Saanich Inlet is at 75 meters.

Monthly Temperature Profiles

Vertical profiles in temperature from my three CTD stations in Saanich Inlet ranged from highly similar (e.g. April) to markedly different throughout the entire profile (e.g. August; Figure 2.10). Over the entire year, temperatures from 125 meters to the bottom were within 0.2 °C at the three locations and each site was nearly isothermal. All profiles had a permanent thermocline. Below this thermocline, the temperature was nearly constant within a month and ranged from 9.4 to 9.7 °C among months. Temperature maxima or minima were measured at the surface in each month. The maximum and minimum temperatures recorded were 17.9 °C in August and 5.6 °C in February.

Profiles in most months were characterized by a surface thermocline where the temperature changed rapidly over a relatively narrow depth range. I did not observe surface thermoclines in October, January, or March. Between April and September, temperature decreased within this thermocline from surface maxima. Spring/summer surface thermocline depth ranged from 4.5 to 13.0 meters. Temperature at the base of the spring/summer surface thermocline ranged from 9.6 °C in April to 14.6 °C in July. I observed the largest temperature decrease within the surface thermocline in April at Squally Reach where temperature declined from 16.4 to 9.8 °C over 9 meters. From November to February, temperature increased within the surface thermocline. Winter surface thermocline depths ranged from 3.5 to 11.3 meters and temperature at the base of this thermocline ranged from 8.3 to 9.9 °C.

Within the permanent thermocline, temperature profiles varied seasonally. During spring and summer, temperature at Patricia Bay was up to a degree warmer than at Squally Reach between May and September (Figure 2.10B-F). This trend reversed in winter when Patricia Bay was slightly cooler than Squally Reach (Figure 2.10I-L). Overall, mid-water temperature decreased with depth from surface values in the spring-summer, and increased with depth in the fall-winter.

The base of the permanent thermocline ranged from 55 to 130 meters depth through the year and was shallowest during the summer and fall (Figure 2.11). Among months, there

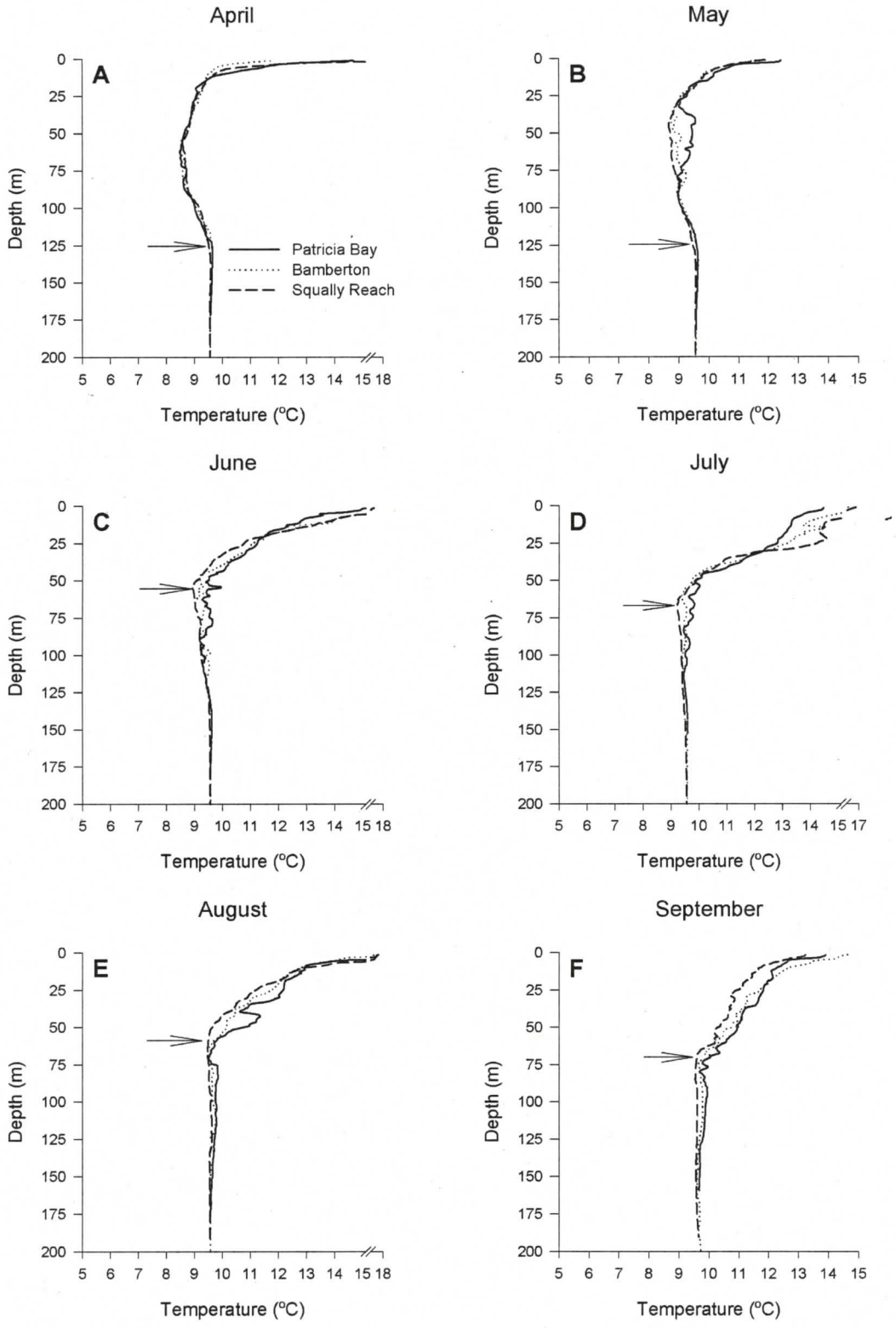

Figure 2.10. Monthly temperature profiles for Patricia Bay, Bamberton and Squally Reach between April 2005 and March 2006. Sill depth at the mouth of Saanich Inlet is 75 meters. The arrows delineate the base of the permanent thermocline.

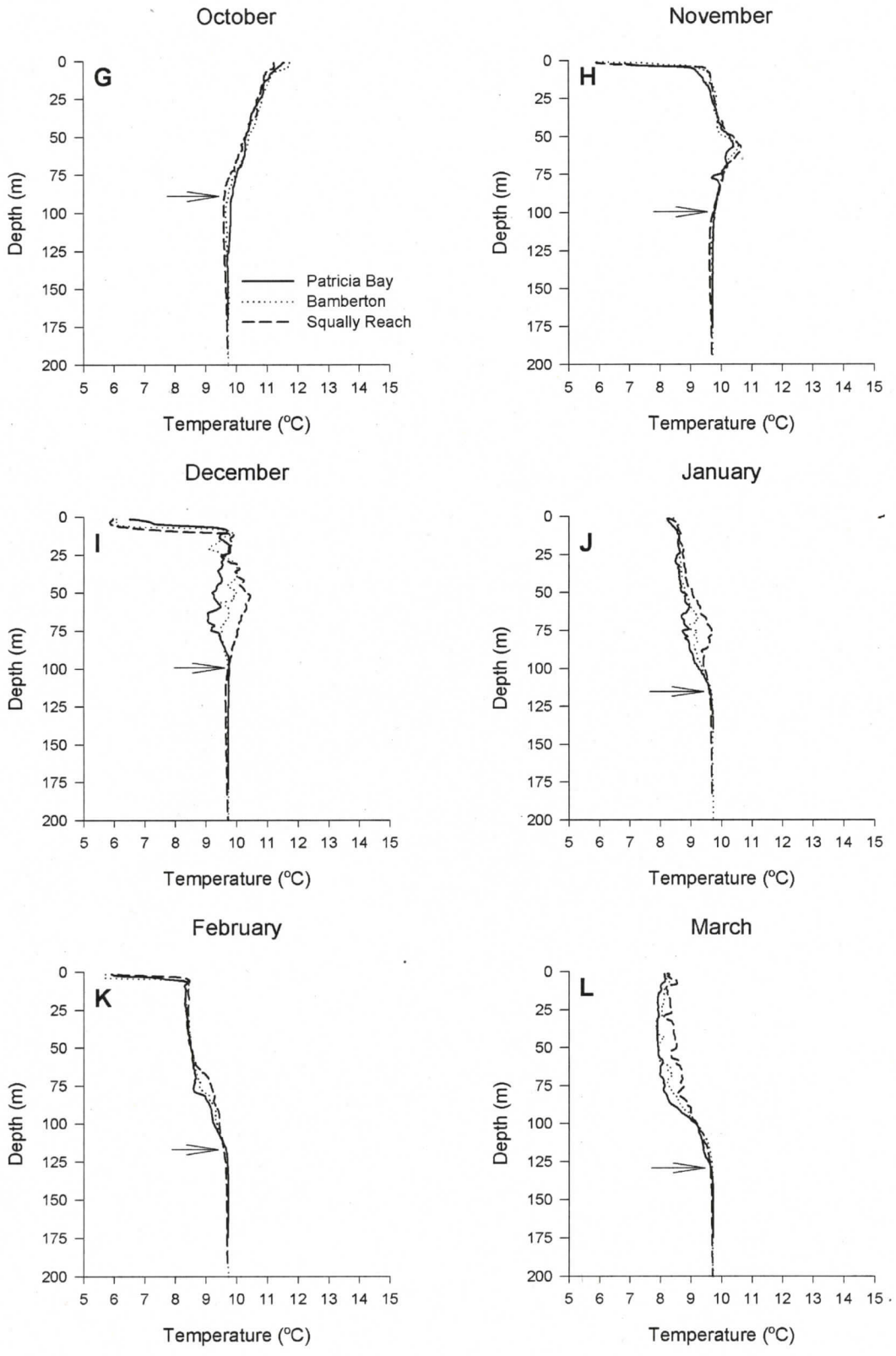

Figure 2.10 continued

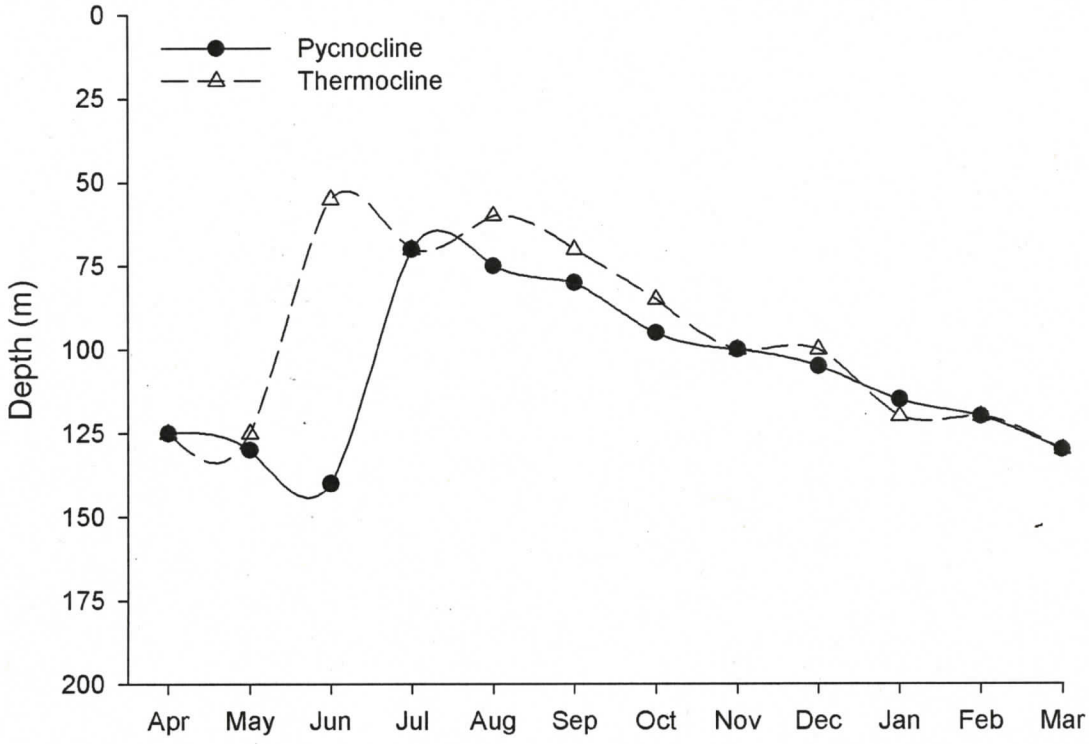

Figure 2.11. Monthly depth of the base of the permanent thermocline and pycnocline between April 2005 and March 2006. There was no difference in cline base depth among sites within months.

was no difference in permanent thermocline depth between Patricia Bay and Squally Reach (Figure 2.10). Deep-basin temperature increased slightly (0.1 °C) in Bamberton and Squally Reach below 160 meters in September (Figure 2.10F). No temperature change was associated with deep-water oxygen in October (Figure 2.10G; section 2.3.1.1).

2.3.1.3 Density

Density and salinity profiles followed the same patterns so only density profiles are described. I define density anomaly (σ_t) as actual density minus 1000 kg m^{-3}. Vertical density anomaly profiles were characterized by a positive gradient from surface minima to maximum density anomaly in the deep basin (Figure 2.12) and a permanent pycnocline. Surface density anomaly ranged from 13.8 kg m^{-3} in February to 22.8 kg m^{-3} in October, and in the deep basin, the density anomaly was isopycnal at 24.1 kg m^{-3} in all profiles. Profiles were highly similar among months and sites. Density difference among sites was less than 0.6 kg m^{-3} throughout the entire profile in all months.

I observed surface pycnoclines in most months. Only September and October did not have surface pycnoclines. Surface pycnocline depth ranged from 3.2 to 11.6 meters and varied among sites and months. Within the pycnocline, density increased by 0.6 kg m^{-3} (December) to 8.2 kg m^{-3} (February). Density anomaly at the base of the surface pycnocline ranged from 20.2 kg m^{-3} (July) to 23.0 kg m^{-3} (December). Within the permanent pycnocline, density increased steadily with depth at all sites. I did not observe a change in density in September or October during the increase in deep-water oxygen (Figures 2.12F, G).

The depth of the permanent pycnocline varied seasonally, but there was no difference in this depth between Patricia Bay and Squally Reach (Figure 2.12). The base of the permanent pycnocline ranged from 70 to 140 meters (Figure 2.11). The pycnocline base was shallowest between July and October, and was usually less than 95 meters depth during these months. During the rest of the year, the base of the permanent pycnocline was usually at greater than 100 meters depth, reaching a maximum of 140 meters in June.

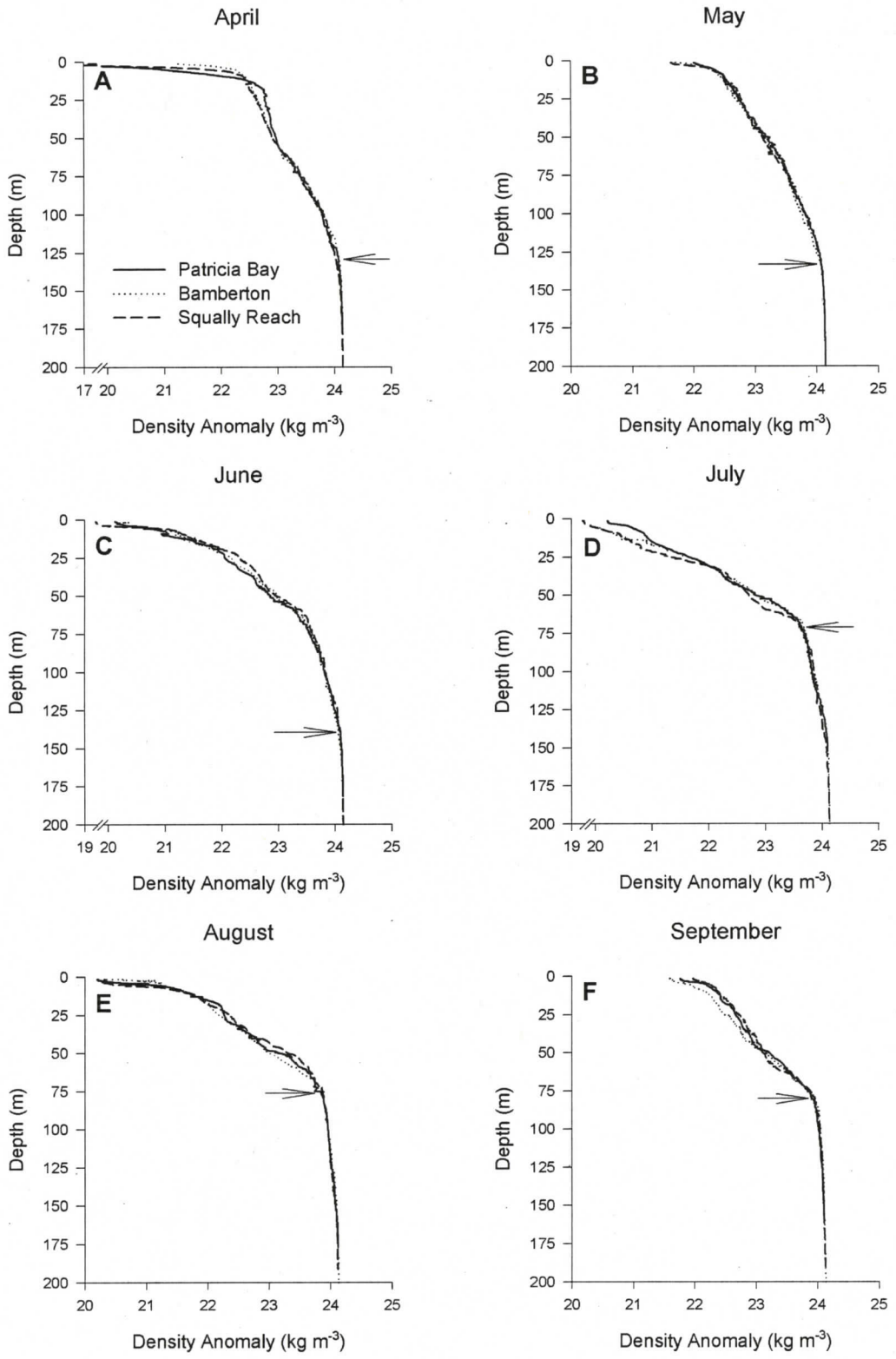

Figure 2.12. Monthly density anomaly (σ_t) profiles for Patricia Bay, Bamberton, and Squally Reach between April 2005 and March 2006. Sill depth at the mouth of Saanich Inlet is 75 meters. The arrows delineate the base of the permanent pycnocline.

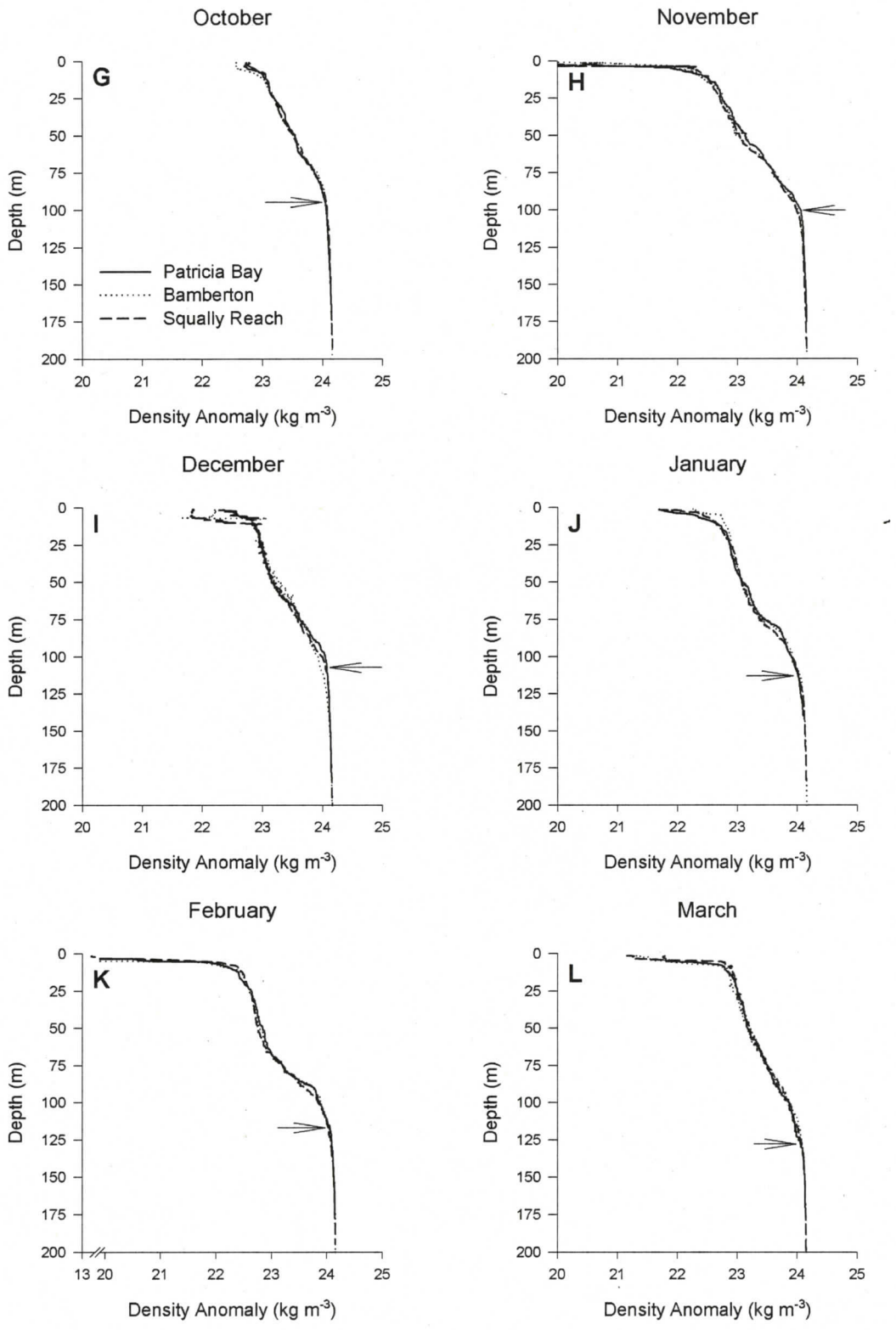

Figure 2.12 continued.

2.3.1.4 Chlorophyll Fluorescence

I integrated chlorophyll fluorescence over the upper 40 meters of the water column and considered this value as representative of available zooplankton food. I found no statistically significant difference in integrated chlorophyll fluorescence between Patricia Bay and Squally Reach over the year (paired t-test, n=11, p=0.836; Table 2.4). However, large differences did occur in spring and summer (Figure 2.13). During winter, integrated chlorophyll fluorescence was nearly the same at Patricia Bay and Squally Reach.

2.3.1.5 Wind and Currents

Between April 2004 and June 2006, 17 840 windspeed and direction measurements were recorded from the mid-inlet ODAS buoy (buoy # C46134) off Patricia Bay (Figure 2.1). Only 10% of wind direction measurements were on-axis (i.e. from the North (350° to 10°) or South (170° to 190°); Figure 2.14A). Most wind in Saanich Inlet was from the east or west and windspeeds were typically low. Fewer than 10% of measurements were greater than 21 km h^{-1} (Figure 2.14B).

Currents in Saanich Inlet during spring 2006 measured at about 95 meters depth from the VENUS 300 kHz ADCP ranged between 5 - 15 cm s^{-1} and tidal flows were typically oriented North-South (Richard Dewey, VENUS Project, pers. comm.). Summer surface currents average about 5 cm s^{-1} (BC Environment 1996).

2.3.2 Zooplankton Distribution

I used volume backscatter intensity as a proxy for zooplankton density, where high backscatter intensity indicated high zooplankton density. I observed a deep scattering layer during each monthly transect, but near-surface scattering only occurred between April and July (Figure 2.15). Minimum and maximum depths of the deep scattering layer were 56m (April) and 116m (September), respectively. I did not observe biological backscatter below 130 meters depth. In most months, I observed the highest densities between Patricia Bay and Bamberton (Figure 2.15). Zooplankton density and scattering layer thickness varied spatially and temporally.

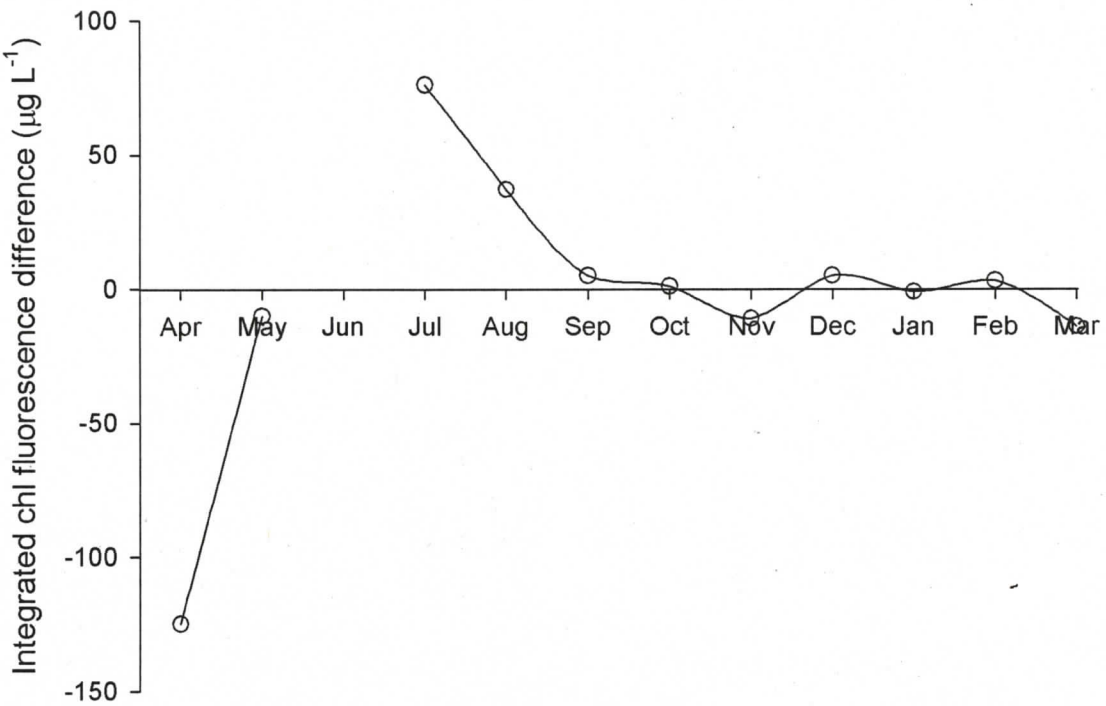

Figure 2.13. Differences in integrated (0-40m) chlorophyll fluorescence between Patricia Bay and Squally Reach. A positive difference indicates greater chlorophyll fluorescence at Patricia Bay. The greatest differences occurred in the summer.

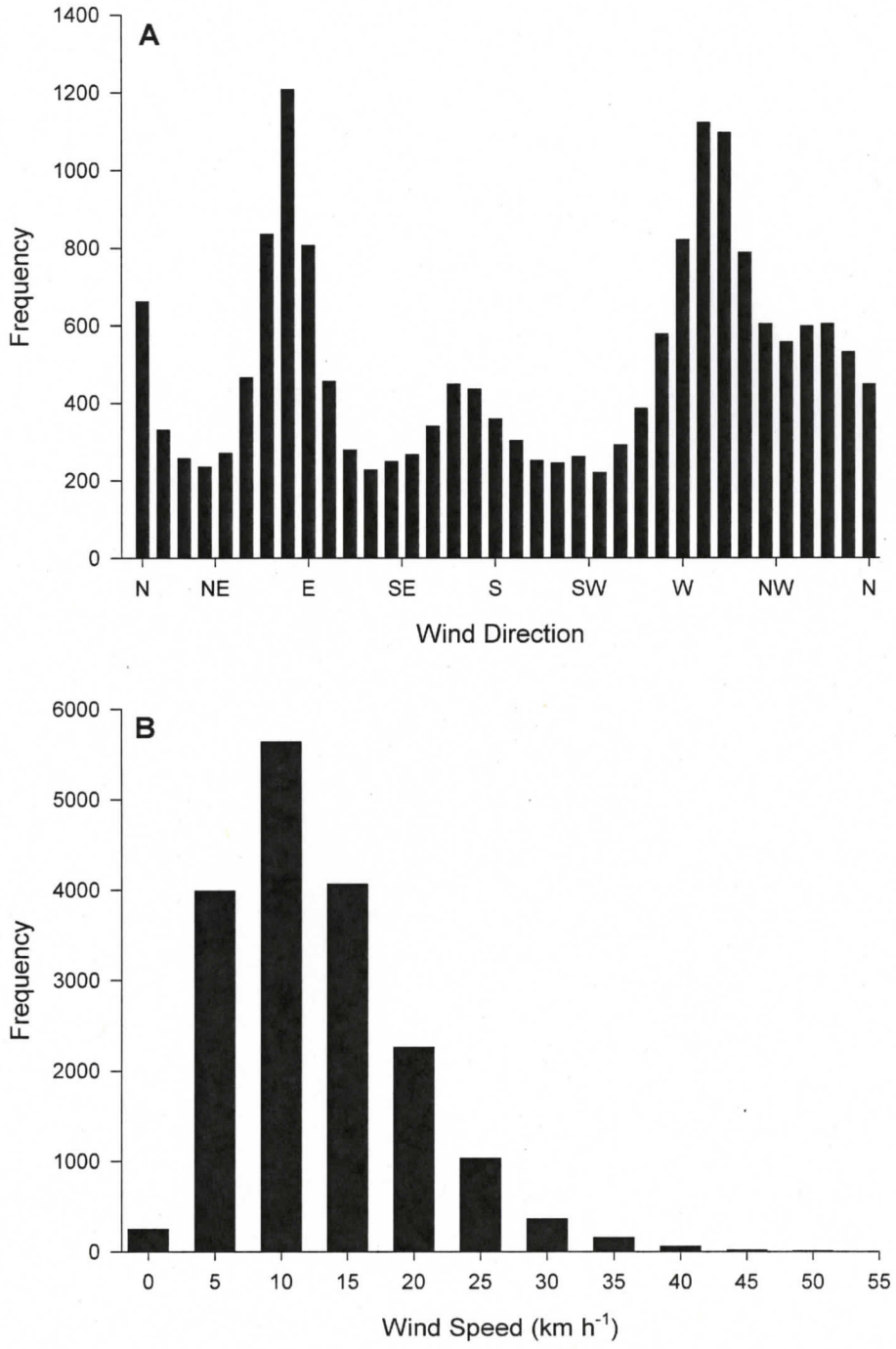

Figure 2.14. Frequency histograms for A) wind direction, and B) wind speed between April 2004 and June 2006 from the mid-inlet ODAS buoy C46134 in Saanich Inlet (n = 17 840). Winds were generally from the east or west and were typically weak.

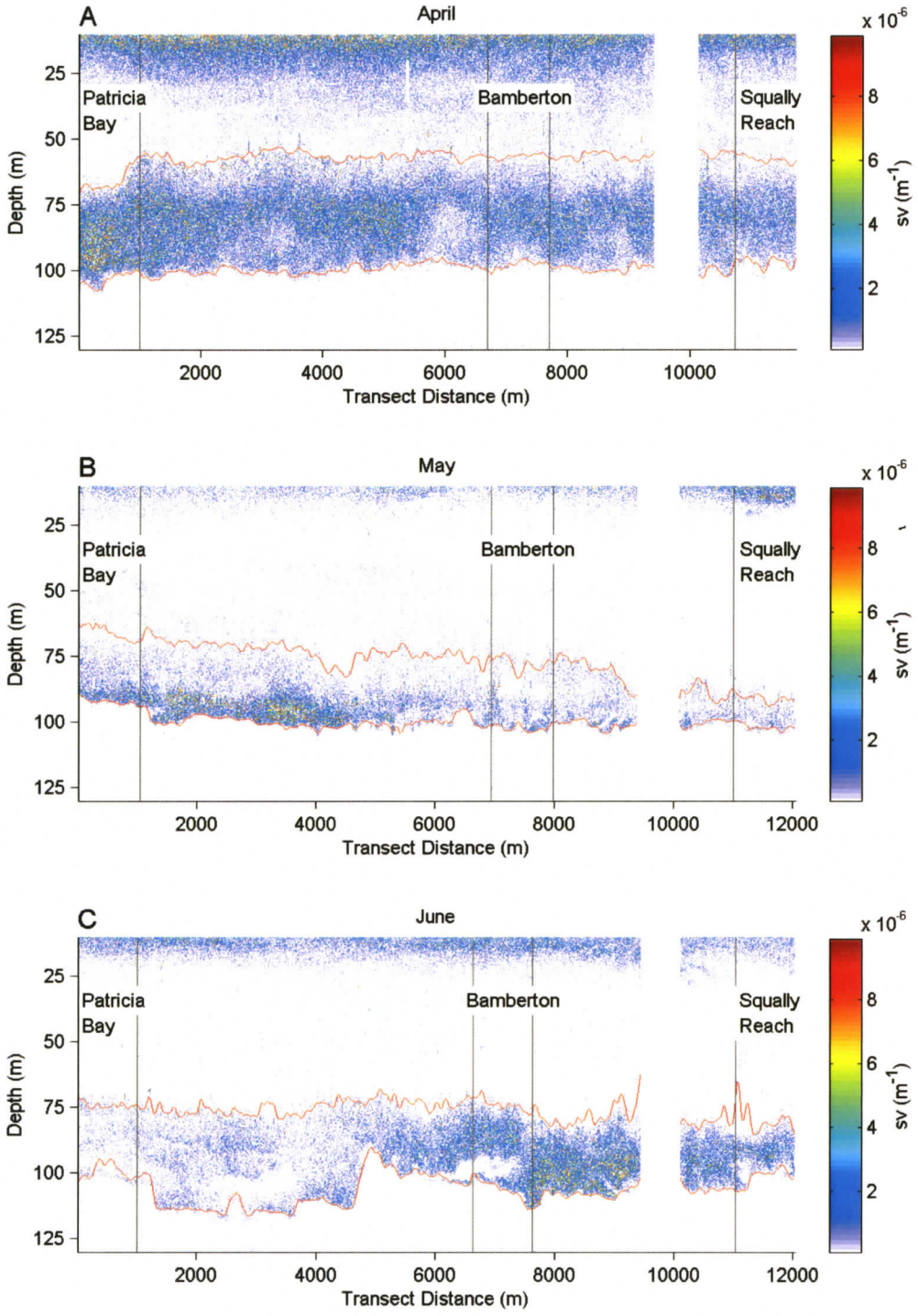

Figure 2.15. Monthly zooplankton density distribution as measured by backscatter intensity (sv) between 10-130 meters depth along a mid-inlet transect between Patricia Bay and Squally Reach. The red lines delineate scattering layer boundaries and the vertical lines delineate the location of three sites along the transect. The gap at the start of Squally Reach represents deleted data where the bottom echo was shallower than 125 meters.

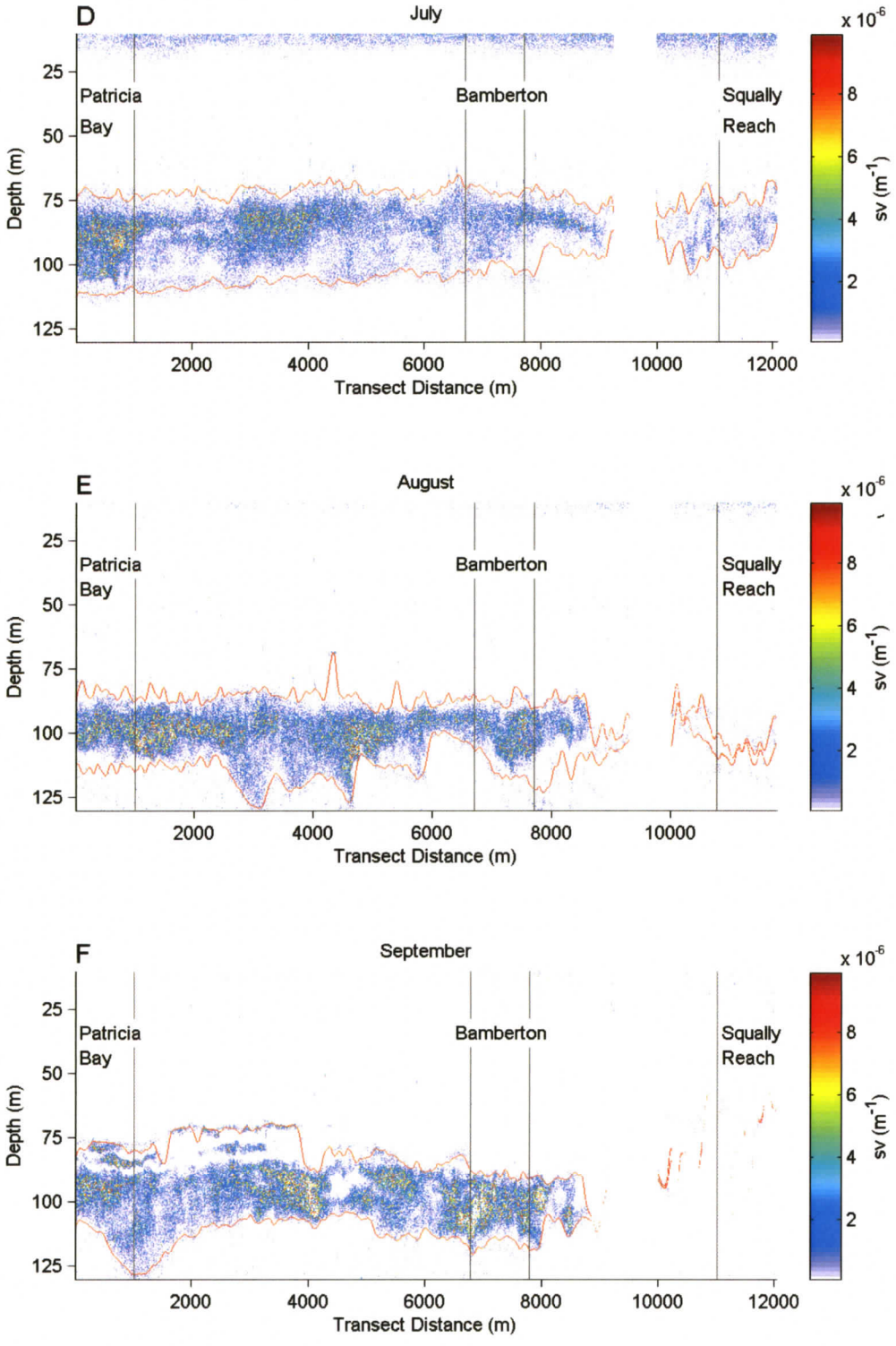

Figure 2.15 continued

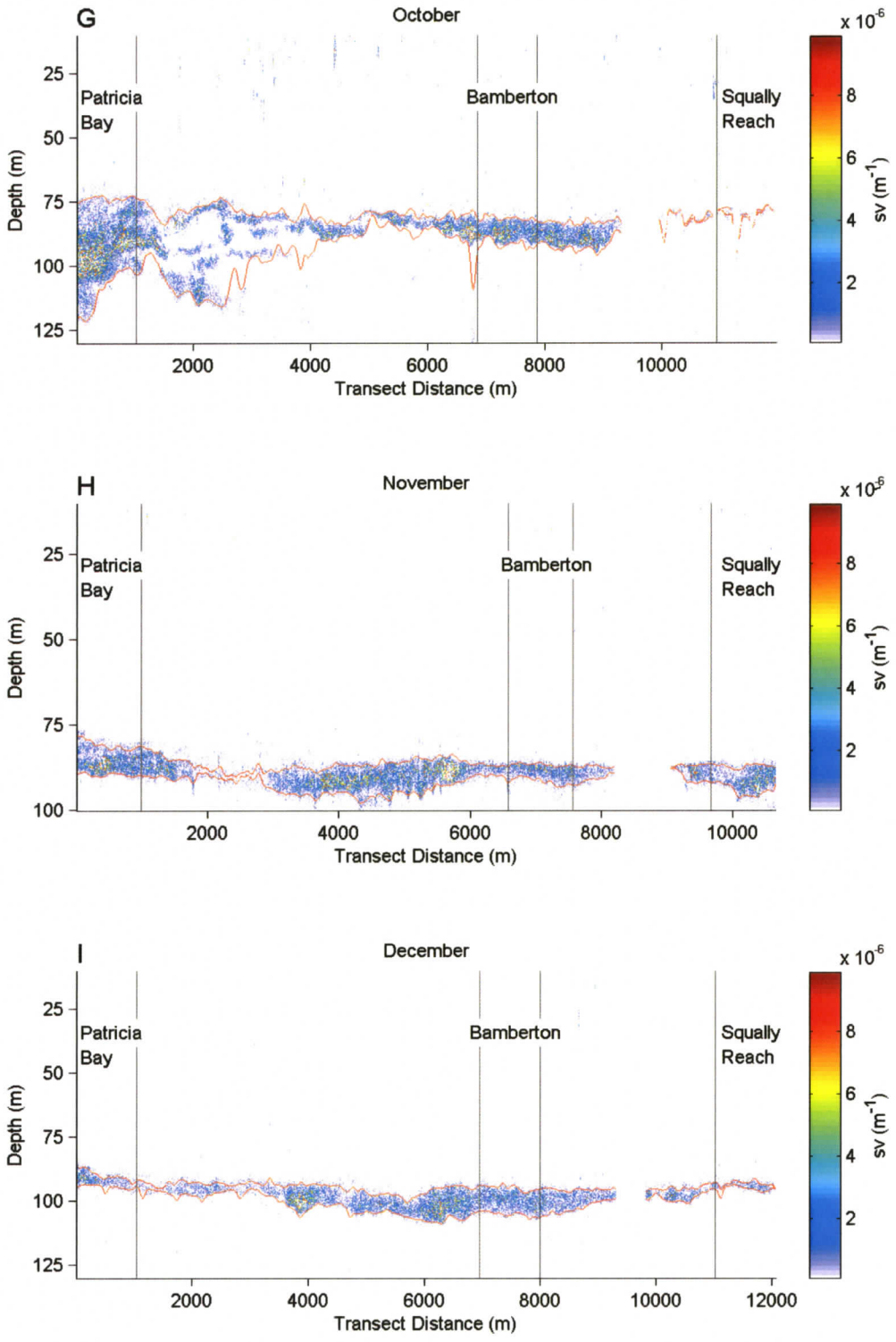

Figure 2.15 continued.

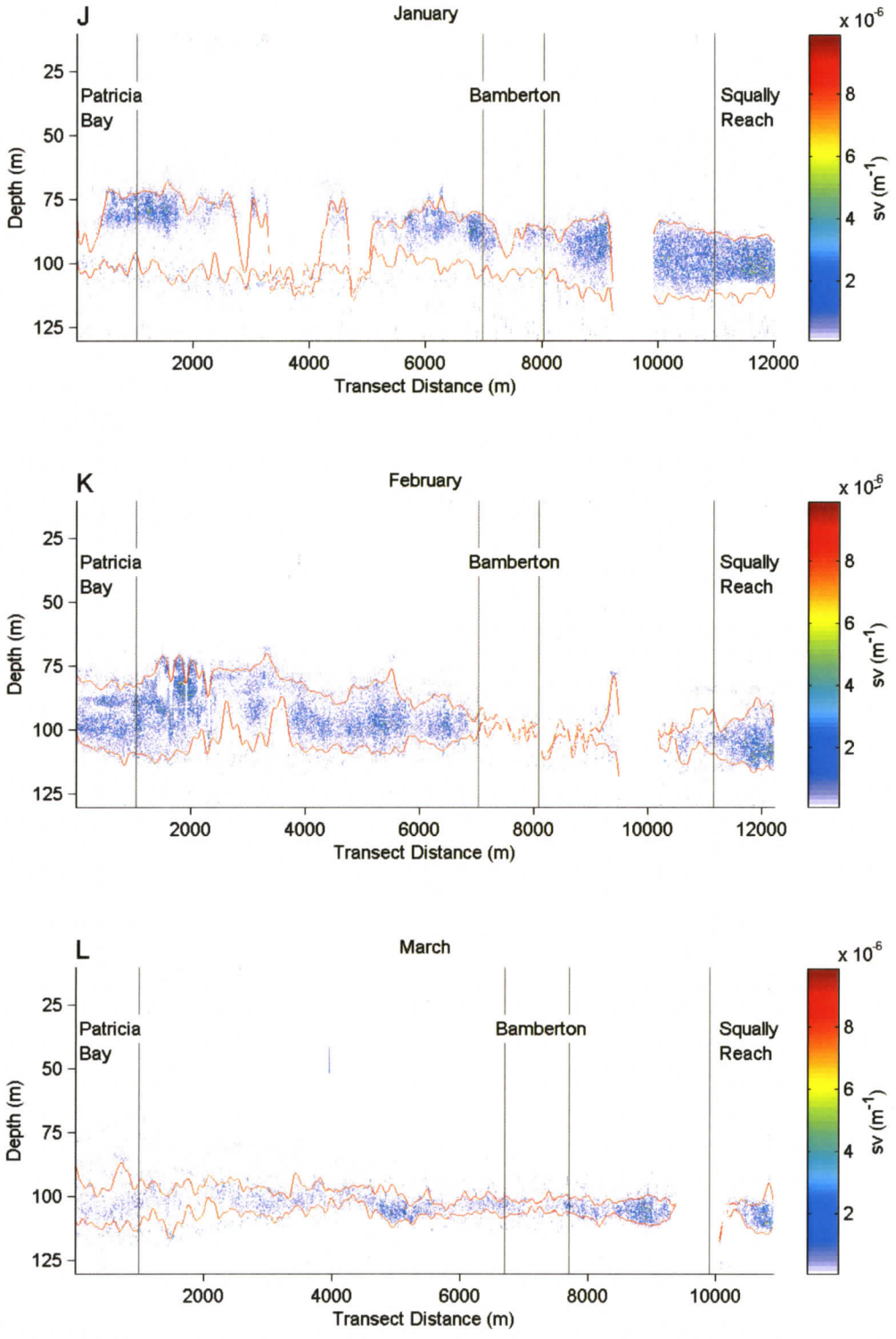

Figure 2.15 continued.

Monthly profiles of volume backscatter integrated between 10-130m were variable in space and time (Figure 2.16). I observed relatively high zooplankton densities between April and September (Figure 2.16A-F), compared with the fall and winter months (Figure 2.16G-L). The location of peak density varied among months (e.g. Figure 2.16A,C), but was located between Patricia Bay and Bamberton in 75% of transects. Density minima occurred in Squally Reach between August and October. In some months, zooplankton density decreased along a gradient from Patricia Bay to Squally Reach (e.g. Figure 2.16A,D). In June and August, zooplankton density peaked near the middle of the transect (Figure 2.16C,E). In March, zooplankton density was evenly distributed along the transect (Figure 2.16L).

Integrated volume backscatter profiles were characterized by one to five large peaks that were separated by between one and six kilometers (Figure 2.16). The mean distance between these large peaks was approximately 2.5 km. Superimposed on this pattern were regular and repeated smaller peaks. These smaller peaks were observed every 200-900 meters along transects and were observed in all months (Figure 2.16).

2.3.2.1 Site Comparison

Zooplankton Density (Backscatter Intensity)

I compared monthly mean integrated volume backscatter from three sites along each transect (Figure 2.17). The highest densities occurred at each site in April and the lowest densities were recorded in Squally Reach in August, September, and October despite maintaining relatively high values at the Patricia Bay site. In 11 months, zooplankton density was highest at either Patricia Bay (n=7) or Bamberton (n=4), and was lowest at Squally Reach in 7 months. Overall, a general decline in backscatter intensity took place over the year of observation.

Zooplankton density was significantly higher at Patricia Bay than Squally Reach (paired t-test, $p=0.042$; Table 2.5). The greatest density differences between Patricia Bay and Squally Reach occurred during the summer and early fall when Squally Reach zooplankton density was nearly zero (Figures 2.15E-G).

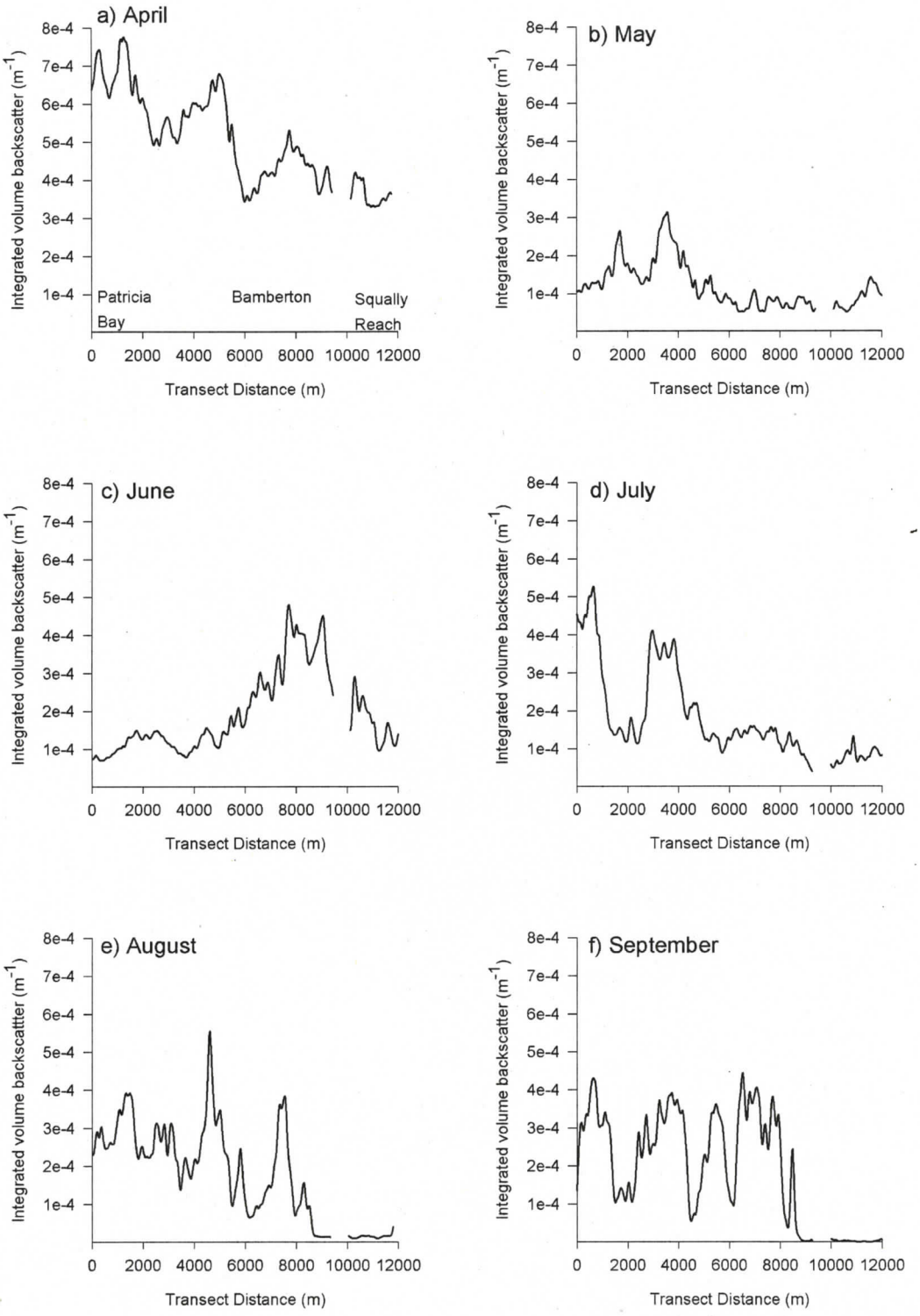

Figure 2.16. Monthly profiles of integrated volume backscatter between 10-130 meters depth along a mid-inlet acoustic transect from Patricia Bay (0m) to Squally Reach (12 000m). Data were smoothed over approximately 100 meters. The gap in the profiles represents deleted data at the start of Squally Reach where the bottom echo was shallower than 125 meters.

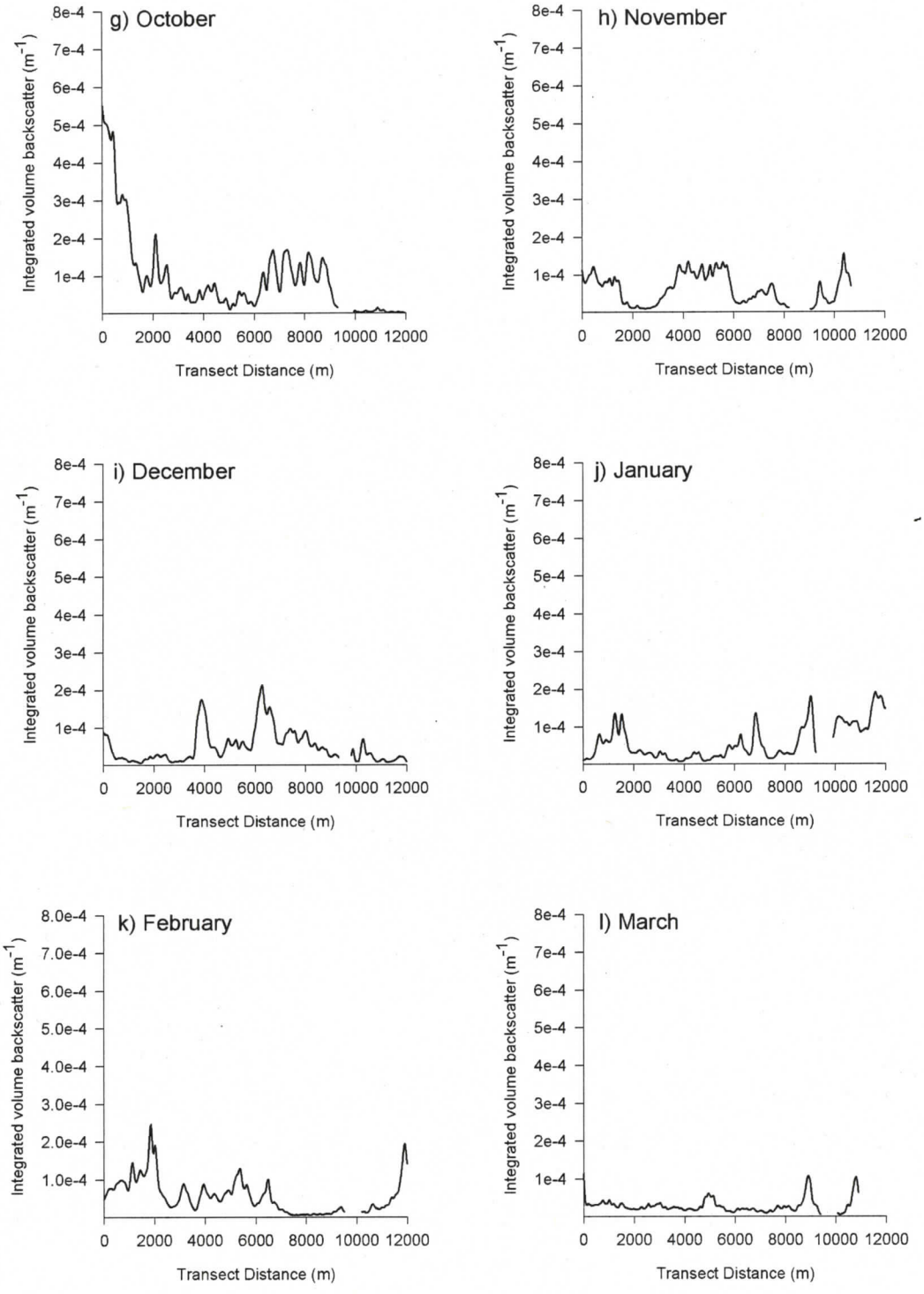

Figure 2.16 continued.

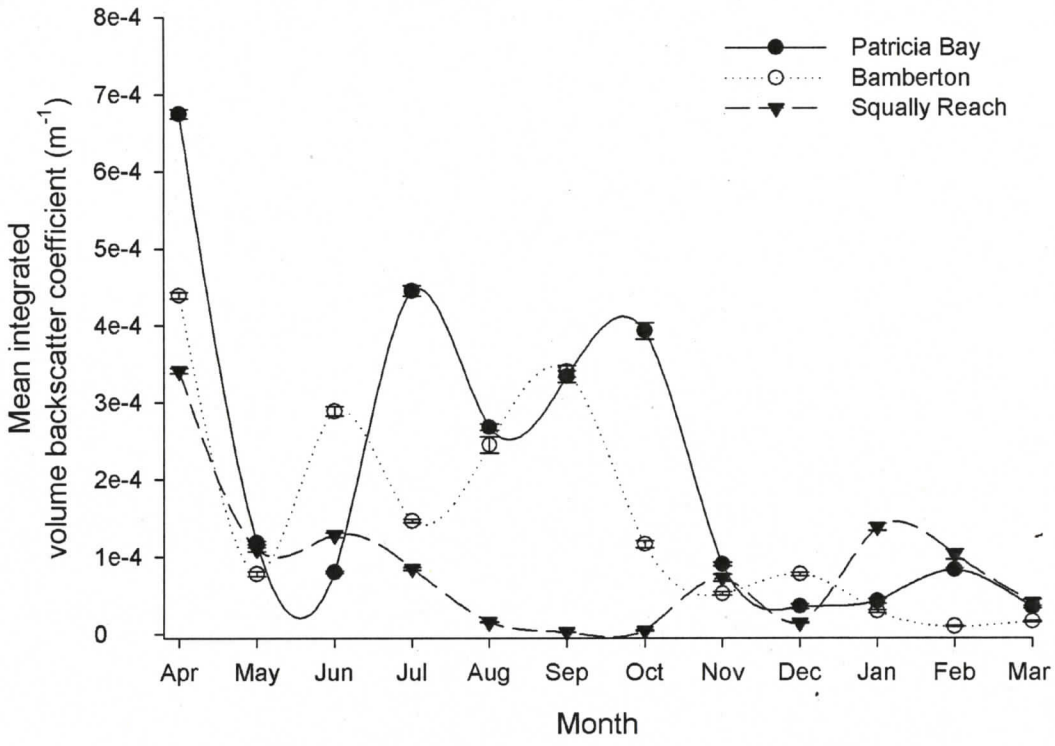

Figure 2.17. Mean integrated volume backscatter between 10-130 meters depth for the Patricia Bay, Bamberton, and Squally Reach sites for each month. Each site was approximately one kilometer in length and consisted of 385 acoustic measurements. Error bars are 95% confidence intervals of the mean.

Table 2.5. P-values from paired t-tests for comparisons of scattering layer characteristics between the Patricia Bay and Squally Reach sites. Zooplankton density was significantly (α=0.05) higher at Patricia Bay. The scattering layer was also significantly thicker at Patricia Bay.

Zooplankton Density	Scattering Layer Base Depth	Scattering Layer Thickness
0.042	0.235	**0.020**

I used the nonparametric Page test for ordered alternatives (Page 1963) to determine if a gradient in zooplankton density between Patricia Bay and Squally Reach was present in the monthly mean integrated volume backscatter data. The Page test was significant ($L > l_{\alpha}$, α=0.05) for a decreasing zooplankton density gradient from Patricia Bay to Squally Reach (Table 2.6). However, this gradient only occurred in four months: April, July, August, and October.

Zooplankton Layer Depth

Among months, the top of the scattering layer can change as much as 46 meters at any one site while the base depth can differ by up to 42 meters (Figure 2.18). The greatest variation in scattering layer boundary depths occurred in Squally Reach (Figure 2.18C). The Patricia Bay site was the least variable among months, with maximum changes in top and base depths of 29m and 27m, respectively. Within a month, the top and base of the scattering layer varied among sites by 25 and 45 meters, respectively. The greatest top boundary variation occurred in May, whereas the base of the layer was most variable in September (Figure 2.18). The top of the scattering layer was deepest at Squally Reach in 58% of transects and shallowest at Patricia Bay in 67% of transects.

Monthly mean depths of the base of zooplankton layer were 104.0 ± 2.6, 103.1 ± 1.9, and 98.6 ± 3.0 meters for Patricia Bay, Bamberton, and Squally Reach, respectively. There was no significant difference in zooplankton layer base depth between Patricia Bay and Squally Reach (paired t-test, p=0.235; Table 2.5). The depth of the base of the scattering layer was positively correlated with depth of the anoxic boundary (n=36, r=0.794, p<0.001; Table 2.7). I found no correlation between the base of the scattering layer and

the depth of the hypoxic boundary (n=36, r=0.280, p=0.099), permanent thermocline depth (n=36, r=-0.021, p=0.904), or permanent pycnocline depth (n=36, r=-0.006, p=0.971; Table 2.7). I also found no correlation between the depth of the top of the scattering layer and the hypoxic boundary (n=36, r=0.001, p=0.996; Figure 2.18).

Maximum zooplankton depths occurred when the anoxic boundary was deepest (Figure 2.18) and were 116.0, 116.1, and 113.4 meters for Patricia Bay, Bamberton, and Squally Reach, respectively. The base of the zooplankton layer was shallowest at each site when the anoxic boundary was shallowest (Figure 2.18). The base of the zooplankton layer was shallowest in Squally Reach in September (71m) and October (81m).

Table 2.6. Page test for ordered alternatives (α=0.05) for a zooplankton density gradient between Patricia Bay and Squally Reach. Mean volume backscatter integrated between 10-130 meters depth at the Patricia Bay (PB), Bamberton (B), and Squally Reach (SR) sites were ranked from high to low and tested against their *a priori* predicted rank (*Y*).

	Mean Integrated Volume Backscatter				**Ranks**		
Month	**Patricia Bay**	**Bamberton**	**Squally Reach**		**PB**	**B**	**SR**
				Y	*1*	*2*	*3*
April	6.75E-04	4.39E-04	3.41E-04		1	2	3
May	1.18E-04	7.83E-05	1.10E-04		1	3	2
June	8.03E-05	2.89E-04	1.28E-04		3	1	2
July	4.45E-04	1.46E-04	8.50E-05		1	2	3
August	2.68E-04	2.45E-04	1.56E-05		1	2	3
September	3.34E-04	3.41E-04	2.83E-06		2	1	3
October	3.93E-04	1.16E-04	4.59E-06		1	2	3
November	9.03E-05	5.25E-05	7.29E-05		1	3	2
December	3.60E-05	7.75E-05	1.45E-05		2	1	3
January	4.27E-05	2.94E-05	1.38E-04		2	3	1
February	8.30E-05	9.94E-06	1.03E-04		2	3	1
March	3.50E-05	1.63E-05	2.31E-05		1	3	2
				Σ	18	26	28
				$Y\Sigma$	18	52	84
				$L = \Sigma(Y\Sigma)$	154		
				Critical Value (α = 0.05), l_α	153		
				$L > l_\alpha$, significant at α			

When the depth of the anoxic boundary increased at all sites in August, the depth of the base of the zooplankton layer increased only slightly (Figure 2.18). Zooplankton depth also increased only slightly during a spring increase in anoxic boundary depth. In Squally Reach, the depth of the base of the zooplankton layer decreased slightly in March even though anoxic boundary depth increased (Figure 2.18C). The zooplankton layer did not follow the higher oxygen levels into deeper water. A significant correlation exists ($n=36$, $r=0.865$, $p<0.001$) between the depth of the anoxic boundary and the gap between the anoxic boundary and the zooplankton layer (Figure 2.19). Gap-size was greatest when the anoxic boundary was greater than 150 meters.

For 17% of observations, zooplankton at the base of the layer were not associated with the anoxic boundary but were in relatively oxygenated waters (1.0 to 2.0 mL L^{-1}; Figure 2.18).

Zooplankton Layer Thickness

Zooplankton layer thickness varied among sites, with the greatest variability observed in Squally Reach (Figure 2.18). Squally Reach thickness ranged from 0.3 to 39.2 meters, with a mean of 13.5 meters. The extremely low value occurred in September when the scattering layer was nearly absent. Scattering layer thickness was the least variable at Patricia Bay over the twelve months of observation (range: 4.7-38.0m; mean: 25.7m). The scattering layer at Patricia Bay was significantly thicker than at Squally Reach (paired t-test, $p=0.020$, $df=9$; September and October data were excluded due to the near absence of the scattering layer from Squally Reach).

At each site, the scattering layer was most compressed when the anoxic boundary was shallowest (Figure 2.18), with the exception of the Bamberton site in February and March. Zooplankton density was concentrated in a narrower vertical band when the anoxic boundary was shallow. For example, at Patricia Bay, anoxic boundary depth increased from 109m in December to 124m in January. Zooplankton layer thickness increased from 4.7m to 21.9m, although mean integrated volume backscatter at each site was nearly the same in the both months (3.6×10^{-5} and 4.3×10^{-5} m^{-1}).

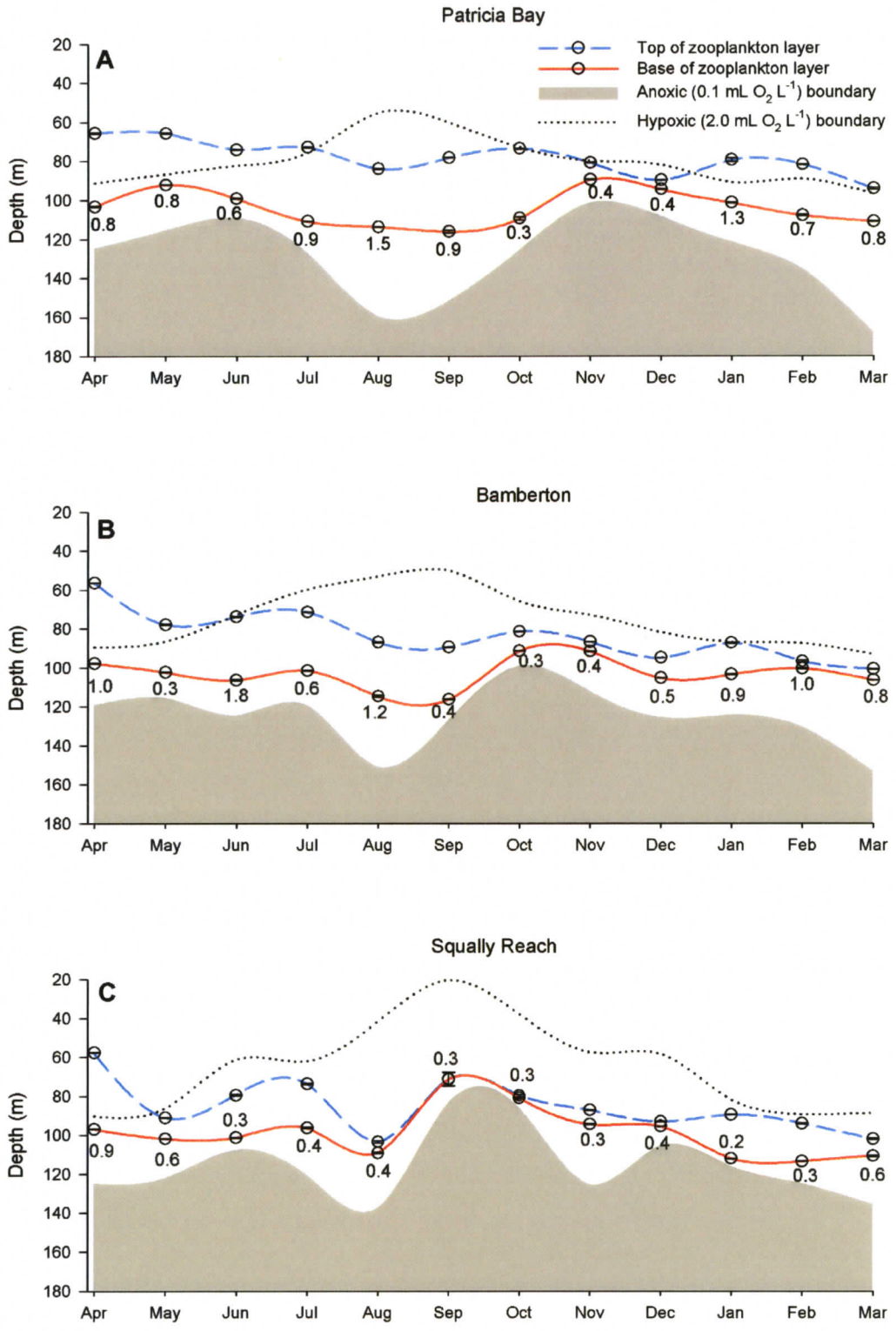

Figure 2.18. Zooplankton layer boundaries in relation to anoxic and hypoxic boundary depths. Error bars are 95% confidence intervals of the mean zooplankton layer boundaries. Values are the dissolved oxygen concentration (mL L^{-1}) at the base of the zooplankton layer.

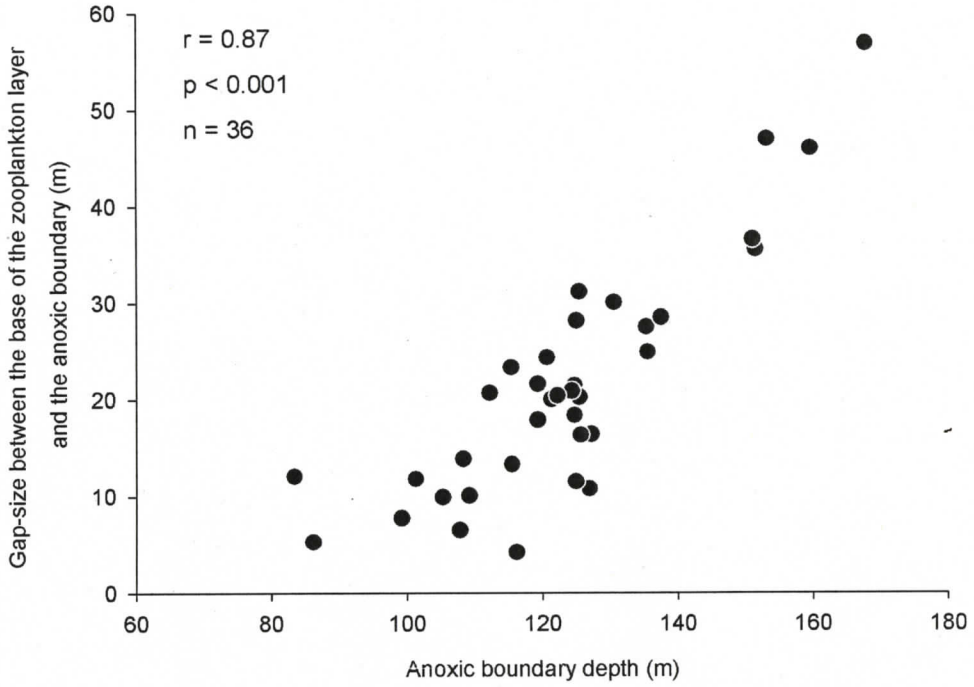

Figure 2.19. Positive correlation between the depth of the anoxic boundary and the gap-size between the base of the zooplankton layer and the anoxic boundary. When the anoxic boundary deepens, the gap between the zooplankton and anoxic layers increases, indicating that the zooplankton do not follow increased oxygen concentrations into deeper waters.

Table 2.7. Pearson product-moment correlations between zooplankton scattering layer characteristics and environmental variables. Statistically significant (α=0.05) results are shown in bold. The hypoxic boundary depth was significantly correlated with each scattering layer characteristic in Squally Reach. The depth of the anoxic boundary was significantly correlated with the depth of the base of the zooplankton layer.

Scattering Layer Characteristic		**Hypoxic Boundary Depth (n=12 per site)**			**Anoxic Boundary Depth (n=36)**	**Permanent Thermocline Depth (n=36)**	**Permanent Pycnocline Depth (n=36)**	***Integrated Chlorophyll Fluorescence (n=33)**
		PB	**Bam**	**SR**				
Mean integrated volume backscatter	r	-0.277	-0.428	0.612	0.203	-0.128	-0.103	0.546
	p	0.383	0.165	**0.034**	0.234	0.458	0.551	**0.001**
Base of zooplankton layer depth	r	-0.440	-0.379	0.741	0.794	-0.021	-0.006	-
	p	0.152	0.224	**0.006**	**<0.001**	0.904	0.971	
Zooplankton layer thickness	r	-0.314	-0.295	0.646	0.325	-0.126	0.009	-
	p	0.279	0.352	**0.023**	0.053	0.465	0.960	

* Integrated between 0-40 meters.

A weakly significant positive correlation exists between the depth of the anoxic boundary and scattering layer thickness (n=36, r=0.325, p=0.053; Table 2.7; Figure 2.20). In Squally Reach, a significant positive correlation exists between the depth of the hypoxic boundary and the thickness of the zooplankton layer (n=12, r=0.646, p=0.023) but no significant correlations exist at Patricia Bay (n=12, r=-0.341, p=0.279) or Bamberton (n=12, r=-0.295, p=0.352).

2.3.2.2 Environmental Correlations

Chlorophyll Fluorescence

Mean integrated volume backscatter was positively correlated with chlorophyll fluorescence integrated between 0-40 meters (n=33, r=0.546, p=0.001).

Temperature and Density

No significant correlation exists between the depth of the permanent thermocline (n=36, r=-0.128, p=0.458) or pycnocline (n=36, r=-0.103, p=0.551) and mean integrated volume backscatter (Table 2.7).

Dissolved Oxygen

During daylight hours, zooplankton at the base of the scattering layer in Squally Reach occupied severely hypoxic (<0.5 mL L^{-1}) water in 67% of transects (Figure 2.21A). Only in April was dissolved oxygen greater than 1.0 mL L^{-1} at the base of the zooplankton layer in Squally Reach. The top of the Squally Reach scattering layer occurred in normoxic (>2.0 mL L^{-1}) water in April only (Figure 2.21B). During the rest of the year, oxygen at the top of the Squally Reach scattering layer ranged from 0.3 to 1.6 mL L^{-1}. At Bamberton and Patricia Bay, oxygen concentrations at the base of the zooplankton layer were usually in the moderate (0.5-1.0 mL L^{-1}) to mild (1.1-2.0 mL L^{-1}) hypoxic range (Figure 2.21A). The top of the scattering layer was in normoxic water at Patricia Bay and Bamberton in 58% and 17% of transects, respectively.

No significant correlation exists between the depth of the anoxic boundary and mean integrated volume backscatter (n=36, r=0.203, p=0.234). Hypoxic boundary depths were

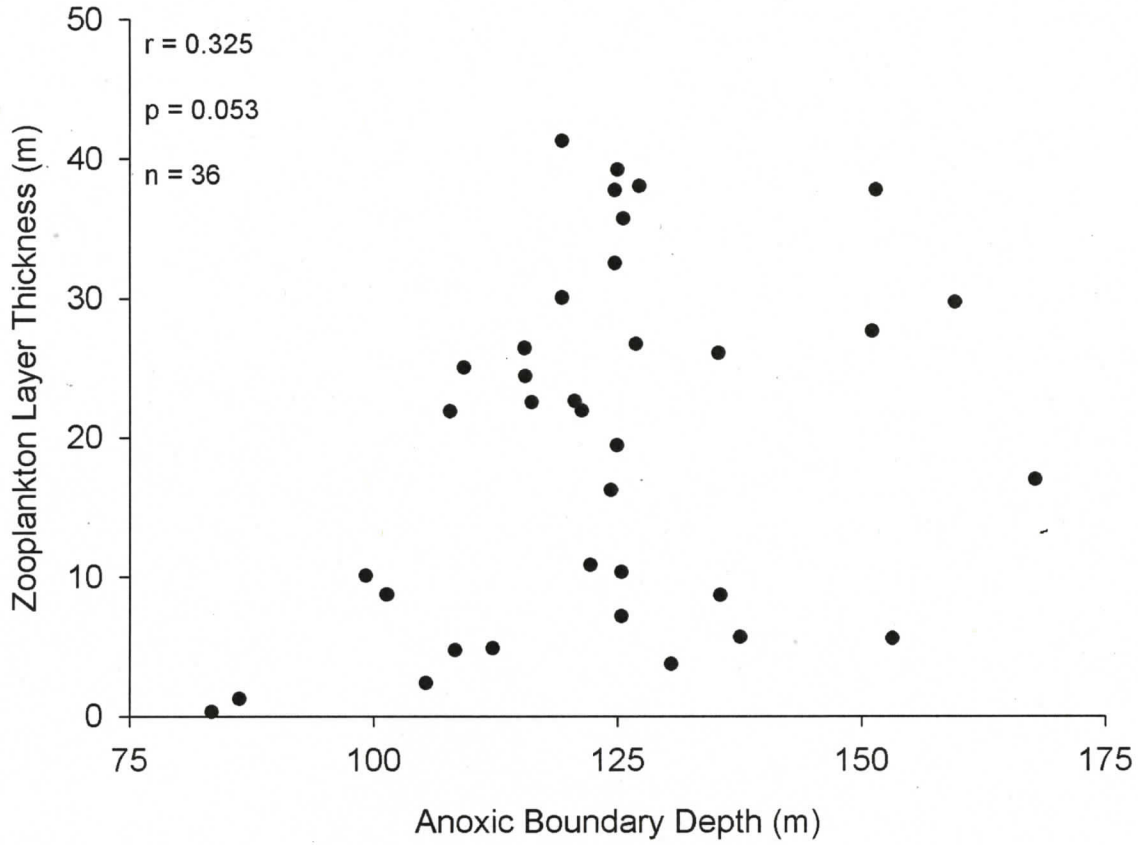

Figure 2.20. Weak positive correlation between anoxic boundary depth and zooplankton layer thickness. The zooplankton layer becomes more compressed when the anoxic boundary is shallow.

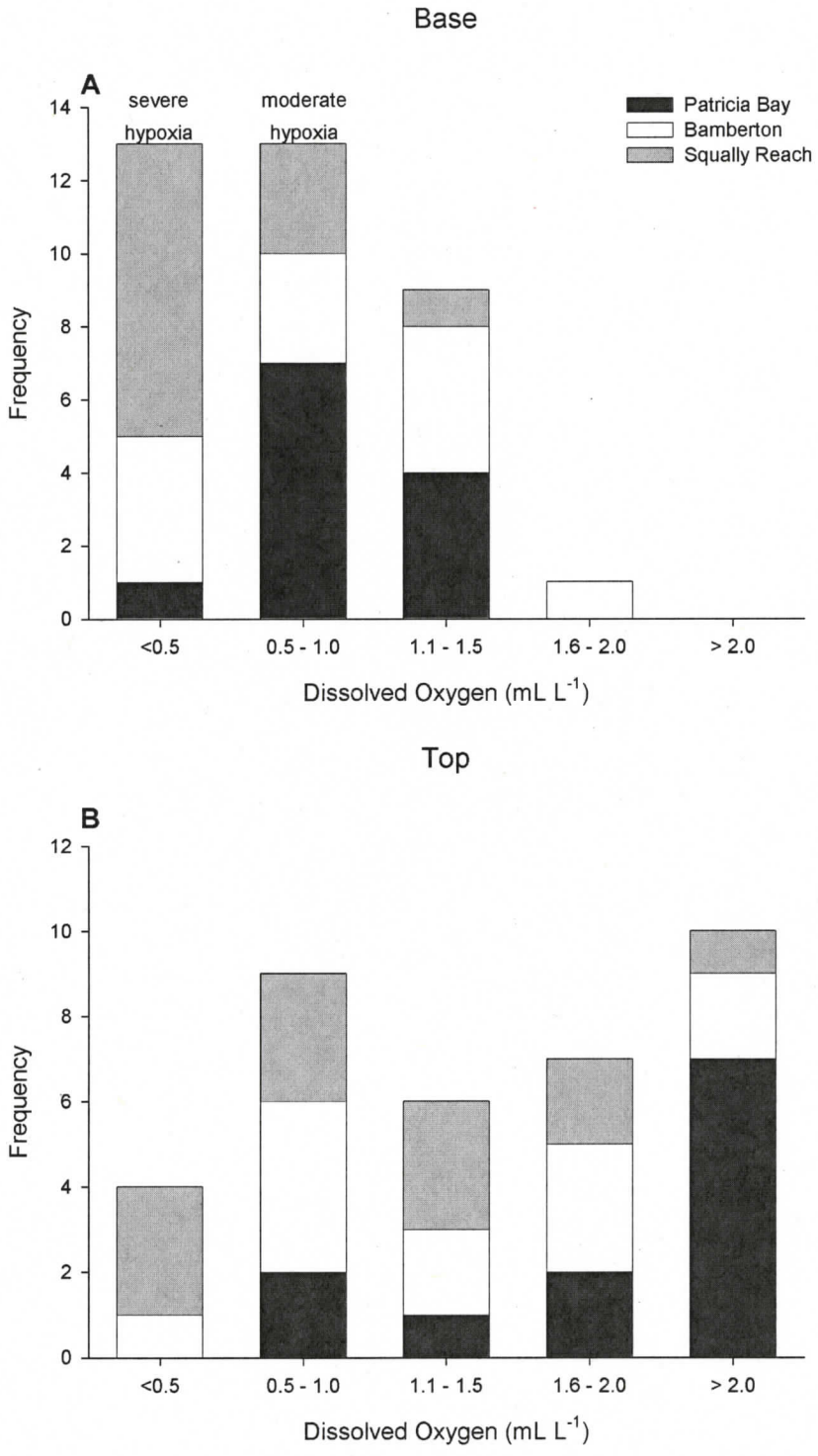

Figure 2.21. Dissolved oxygen concentration measured at the A) base and B) top of the daytime zooplankton layer. Squally Reach zooplankton descended into severely hypoxic water in most months. For 28% of observations, zooplankton at the base of the scattering layer occupied relatively oxygenated (>1.0 mL L^{-1}) waters.

significantly different between sites so correlation between this depth and zooplankton density were analyzed separately for each site (Table 2.7). No significant correlation exists between zooplankton density and hypoxic boundary depth at Patricia Bay (n=12, r=-0.277, p=0.383) or Bamberton (n=12, r=-0.428, p=0.165), but a significant correlation does exist at Squally Reach (n=12, r=0.612, p=0.034).

2.4 Discussion

2.4.1 Physical and Chemical Characteristics

2.4.1.1 Dissolved Oxygen

Anoxia was observed in all oxygen profiles. Anoxia and severe hypoxia is not uncommon in fjords with shallow sills and is not uncommon in British Columbia fjords (Pickard and Stanton 1980). However, the depth where anoxia occurs is much greater in Saanich Inlet compared to other British Columbia fjords (Pickard and Stanton 1980) and this deep anoxic layer can influence the distribution of diel vertically migrating zooplankton. Devol (1981) suggested that the hypoxic zone is a barrier to the vertical migration of the Saanich Inlet scattering layer.

Intermediate depth (<75m) dissolved oxygen was lower in Squally Reach than at Patricia Bay and the hypoxic boundary was significantly shallower at the inlet head compared to the mouth. Similar spatial gradients in dissolved oxygen have been observed in other British Columbia fjords characterized by low runoff (Pickard and Stanton 1980). In Saanich Inlet, this spatial oxygen gradient can be explained by a combination of: 1) limited oxygen delivery at the inlet head due to low runoff, and 2) tidal incursions of oxygenated water moving across the entrance sill.

Tidal currents are weak in Saanich Inlet (Herlinveaux 1962), limiting tidal incursions to within about three kilometers of the inlet mouth (Gargett et al. 2003). As an incursion of oxygenated water progresses towards Squally Reach, it is mixed into the water column. During this mixing, oxygen is consumed and the potential for elevated oxygen concentrations reaching and renewing mid-water oxygen at the inlet head is very low. In

contrast, tidal incursions occur during flood tides, constantly renewing mid-water oxygen near the mouth. The density (σ_t) of these tidal incursions is insufficient to penetrate into the isopycnal deep-basin and they do not affect anoxic boundary depth.

The anoxic boundary was always deeper than sill depth and there was no significant difference in anoxic boundary depth between the mouth and head. Anoxic boundary depth is determined by the extent of deep-water oxygen renewal. During winter and spring, as oxygen is consumed in the deep-basin, the anoxic boundary becomes shallower (Figure 2.8). Oxygen renewal occurs in late summer/autumn when the density of mixed waters outside of the inlet is greater than the density of the deep-basin. During renewal, anoxic water is forced upward by the higher density oxygenated water spilling over the sill into the deep-basin. The depth of the anoxic boundary was shallowest (<90 meters) in Squally Reach during September and October, indicating that the anoxic boundary was forced shallower by an incursion of dense oxygenated bottom water (Anderson and Devol 1973; Hobson 1983). As the renewed oxygen is mixed into the water column, the anoxic boundary depth increases. When the renewed oxygen in consumed, the anoxic boundary again becomes shallower until deep-water renewal occurs.

Deep-water oxygen renewal occurred in August, September, and October. In August and September, dissolved oxygen between 75-150m depth increased by up to 1.0 mL L^{-1} at Patricia Bay and Bamberton. A shallower (to ~140m) and weaker (0.2 mL L^{-1}) dissolved oxygen increase was observed in Squally Reach in August but not in September. The decreasing oxygen concentration with distance from the mouth suggests that a bolus of water from outside the inlet caused the increase in deep-basin oxygen. As the water-mass moved south towards the head, oxygen concentration decreased with headward distance, likely due to respiration and mixing. The water-mass did not extend to the bottom when observed on August 19. Renewal events where a pulse of oxygenated water stayed at intermediate depths within the deep basin have been previously observed (Anderson and Devol 1973). Further, Hobson (1983) observed an August increase of 1.5 mL O_2 L^{-1} between 90 and 190 meters near Bamberton.

The temperature and salinity at the depths of increased oxygen were also slightly elevated at the Patricia Bay and Bamberton sites, further suggesting a propagating water-mass. Temperature (9.7 °C) and salinity (31.3) characteristics at the depth of increased deep-water oxygen suggest that the water originated from outside the inlet. These values are similar to the temperature and salinity of the intermediate water-mass formed in Haro Strait that results in the high densities necessary to initiate deep-water renewal in Saanich Inlet (Anderson and Devol 1973).

An alternate explanation for the increase in deep-water oxygen is an intrusion of oxygenated surface water. An intrusion of surface water is possible if reduced freshwater input is coupled with evaporation, increasing surface salinity and density. Freshwater inputs from the Goldstream, Cowichan, and Fraser Rivers would be at summer minima in August, increasing surface salinity. Further, between July 13 and August 19, total rainfall in Saanich Inlet was only 21.6mm. Maximum surface temperatures were recorded in August and surface salinity increased from 27 psu in July to 29 psu in September. For an intrusion of surface water to sink below sill depth would require a density (σ_t) > 24.1 kg m^{-3}, representing a salinity of 31.8 psu at 12 °C. Based on surface salinity values measured in August and September, the necessary density cannot be achieved at the recorded temperatures. An intrusion of surface water in August and September can not explain the oxygen increase below sill depth.

2.4.1.2 Temperature and Density

Saanich Inlet temperature and density profiles from this study were similar to profiles from other Vancouver Island fjords (Pickard 1963) and the Strait of Georgia (Pickard and Stanton 1980), respectively. Saanich Inlet did not present unusual temperature or density conditions. Temperature and density profiles were similar among sites and months, and unlike dissolved oxygen, there was no significant spatial gradient in temperature or density between the mouth and head of the inlet. The bases of the permanent thermo- and pycnoclines did not limit zooplankton day-depth. When these clines were shallow in the summer and fall, I observed the zooplankton layer at greater depth.

2.4.2 Zooplankton Distribution: Patricia Bay to Squally Reach

In most months, I observed the highest zooplankton densities at either the Patricia Bay or Bamberton sites. The significant difference in zooplankton density between the mouth and head suggests that conditions at the Patricia Bay site were more favourable for zooplankton and that differences between the two locations influences distribution patterns. Advection of zooplankton from Satellite Channel also likely contributes to the higher densities I observed near the mouth. Zooplankton distribution can be influenced by phytoplankton biomass (e.g. Sameoto 1976), wind and currents (e.g. Mackas et al. 1985), or environmental conditions (e.g. Diaz and Rosenberg 1995).

2.4.2.1 Food Availability

I used chlorophyll fluorescence as a proxy for phytoplankton biomass or zooplankton food availability. Despite the presence of a biological front at the inlet mouth (Parsons et al. 1983), the absence of a significant difference in chlorophyll fluorescence between the mouth and head of the inlet suggests that food availability was similar at both locations. However, the lack of a significant difference could be due to the relatively few observations (n=11) and the limited power of the paired t-test. Further, primary productivity, and presumably phytoplankton biomass, is minimal in winter compared with summer (Timothy and Soon 2001) and a large winter spatial difference is not expected. I observed the largest integrated chlorophyll fluorescence differences between the mouth and head in summer. Timothy and Soon (2001) observed similar spatial differences in primary productivity during summer months. This spatial gradient can be explained by: 1) tidal advection of phytoplankton across the sill from the biological front in Satellite Channel (Parsons et al. 1983; Hobson and McQuoid 2001), and 2) increased summer nutrient input to the inlet from the Fraser River (Herlinveaux 1962).

Surface incursions of Fraser River water are limited to within about three kilometers of the inlet mouth by tidal velocity (Gargett et al. 2003). However, the summer spring-neap tidal cycle produces alternating periods of mixed water and surface stratification. Mixing of Fraser River water with deep dense water outside the inlet during spring tides produces a surface density gradient between Saanich Inlet and adjoining passages that reverses the

inverse estuarine circulation typical of the inlet. This pressure-driven gradient results in surface outflow and deep inflow and upwelling of nutrient-rich water (Gargett et al. 2003). The concentration of nutrients decreases with headward distance from the mouth through mixing, causing the spatial gradient in primary productivity and integrated chlorophyll fluorescence.

Mean integrated volume backscatter (proxy for zooplankton density) was positively correlated with integrated chlorophyll fluorescence, suggesting that areas with higher chlorophyll support higher densities of zooplankton. For example, Sameoto (1976) observed a similar relationship between krill density and chlorophyll fluorescence in the Gulf of St. Lawrence. Sameoto (1976) suggested that this relationship was likely due to euphausiids seeking out and remaining in areas with high food concentration. According to the Page test for ordered alternatives (Page 1963), a significant headward gradient of declining zooplankton density was present between Patricia Bay and Squally Reach. This indicates that favourable conditions for zooplankton declined with distance from the mouth. However, the Page test was only just significant and I only observed this declining pattern in 4 of 12 transects. The four months where the declining gradient occurred were April, July, August, and October. The largest integrated chlorophyll fluorescence differences between the mouth and head occurred in July and August (Figure 2.13), suggesting that zooplankton in these months were responding to the summer gradient in food availability. In October, the low zooplankton density at Squally Reach was likely due to the shallow anoxic boundary limiting habitat (section 2.4.2.4). Further, between April and September when zooplankton growth and reproduction occur (e.g. Bollens et al. 1992), zooplankton density was highest at Patricia Bay in all months but June and September. These observations support my hypothesis of a zooplankton gradient between the mouth and head of Saanich Inlet in the summer. The absence of a winter gradient can be explained by low primary productivity (Timothy and Soon 2001), the absence of a winter primary productivity gradient between the mouth and head (D. Grundle, pers. comm.), and reduced feeding by zooplankton throughout the system.

2.4.2.2 Wind and Currents

Wind and currents in Saanich Inlet are both weak and winds are rarely on the North-South axis. The potential for wind to influence zooplankton distribution patterns between Patricia Bay and Squally Reach is very low. Currents should have minimal effect on zooplankton distribution patterns between the mouth and head. For example, the low current velocity is within the swimming capabilities of *Euphausia pacifica* (De Robertis et al. 2003), one of the dominant macrozooplankton species within the scattering layer. Assuming an average current speed of 5.0 cm s^{-1} and twelve hours of darkness, krill feeding near the surface at night could potentially drift 2.2 kilometers before descending to day depth. Mean swimming speeds for *E. pacifica* range from 0.3 to 10 cm s^{-1} and maximum swim speeds recorded in Saanich Inlet were 17 cm s^{-1} (De Robertis et al. 2003). At these speeds, euphausiids could easily maintain position in these weak currents. While at day-depth, krill are quiescent (Jaffe et al. 1999), with a median swimming speed of 1.8 cm s^{-1} (De Robertis et al. 2003). Assuming krill swim against the 5.0 cm s^{-1} current, they could drift up to 1.4 kilometers over twelve hours. This distance is not sufficient to change the overall distribution patterns that I observed. Observations by Tarling et al. (1998) of Nordic krill in the Kattegat Channel maintaining position in favourable habitats despite tidal currents supports my conclusion that macrozooplankton in Saanich Inlet can remain in preferred habitats within weak currents.

2.4.2.3 Temperature and Density

Temperature and density profiles were similar between Patricia Bay and Squally Reach and there was no difference in the base depth of the permanent thermocline and pycnocline between these locations. No significant correlations exist between the depth of the base of the permanent thermo- or pycnocline and zooplankton density. Temperature and density do not influence the distribution of zooplankton between the mouth and head of Saanich Inlet.

2.4.2.4 Dissolved Oxygen

In contrast to temperature and density, dissolved oxygen did affect zooplankton density distribution. The depth of the hypoxic boundary was significantly shallower at the inlet

head compared to the mouth, and zooplankton density was significantly correlated with hypoxic boundary depth in Squally Reach. When the hypoxic boundary was shallow, zooplankton density was low. A similar correlation does not exist at Patricia Bay nor Bamberton, indicating that oxygen concentration has a strong influence on zooplankton density near the head of Saanich Inlet. Zooplankton density in Squally Reach was very low and the scattering layer was nearly absent between August and October. During this period, the hypoxic boundary was shallow (<50m) and in September and October, the anoxic boundary was also very shallow (<90m). During this same period, the hypoxic boundary at Patricia Bay and Bamberton was deeper (>50m) and zooplankton abundance remained high. The difference in integrated chlorophyll fluorescence between Patricia Bay and Squally Reach in September and October was low (Figure 2.13), indicating that a lack of food was likely not the cause of zooplankton absence in Squally Reach.

The lower zooplankton density in Squally Reach could be due to poor survivorship caused by physiological stress associated with the low oxygen environment (e.g. Richmond et al. 2006). While there was no significant difference in the day-depths of the scattering layer between the mouth and head of the inlet, the scattering layer was almost always in severely hypoxic water in Squally Reach. Oxygen levels at day-depth were usually below the low-oxygen tolerance of *Euphausia pacifica* (0.7 mL L^{-1}; Lasker 1966). Spicer et al. (1999) observed that Nordic krill use anaerobic metabolism to survive at day-depth in hypoxic conditions. While at day-depth, Nordic krill incur a substantial oxygen debt in the form of accumulated L-lactate, the end product of anaerobic metabolism. Recovery from this oxygen debt likely reduces growth and survivorship of northern krill. It is unknown whether *E. pacifica* can undergo anaerobic metabolism or how the respiratory metabolism of Saanich Inlet krill compares with *E. pacifica* from normoxic coastal areas. Laboratory experiments by Hoos (1970) suggest that *E. pacifica* have not developed the ability for anaerobic metabolism. Hoos (1970) observed 100% mortality after two hours of exposure to 0.4 mL O_2 L^{-1}. However, the oxygen levels within the zooplankton layer, especially in Squally Reach, suggest that these krill can tolerate low oxygen levels for several hours.

In a laboratory experiment, Stadler and Marcus (1997) found that dissolved oxygen levels lower than 0.7 mL L^{-1} were lethal for three species of marine calanoid copepod. Tolerance for hypoxia was higher in a species collected from Chesapeake Bay where seasonal hypoxia is common and predictable (Stadler and Marcus 1997). Chesapeake Bay copepods also avoided hypoxic water. Species collected from areas without seasonal hypoxia had much lower tolerance and did not avoid areas of hypoxia (Decker et al. 2003). This suggests that populations regularly exposed to hypoxic events can detect and respond to poor oxygen conditions through active avoidance (Pihl et al. 1991). In Chesapeake Bay, Keister et al. (2000) observed that copepods avoided bottom water hypoxia, but returned to bottom habitats when normoxic conditions resumed. A similar pattern may occur in Squally Reach and could explain the low zooplankton density, especially when the hypoxic and anoxic boundaries were shallow. When zooplankton were nearly absent from Squally Reach between August and October, the hypoxic boundary was less than 50 meters deep and became as shallow as 24 meters. Zooplankton could be responding to this shallow depth and avoiding areas where a shallow anoxic boundary (and therefore insufficient depth refuge) is likely to occur.

2.4.3 Zooplankton Distribution Within the Water Column

2.4.3.1 Zooplankton Layer Depth

Zooplankton undertake diel vertical migrations seeking depth refuge in deep dark waters during daylight to avoid visual predators (Lampert 1989). Insufficient depth refuge caused by physical (e.g. Genin 2004) or physiological (e.g. Spicer et al. 1999; Keister et al. 2000) barriers could concentrate migrants at light levels sufficient for visual predation (Ohman 1988). No physical barriers to vertical migration exist mid-inlet but the anoxic boundary has long been considered a likely vertical migration barrier (Bary 1966; Devol 1981; De Robertis 2002). Low oxygen concentrations limit the descent depth of zooplankton in other regions. For example, in Gullsmarfjorden (Sweden), hypoxia limited the depth of northern krill vertical migration (Spicer et al. 1999). The strong correlation between the zooplankton layer base depth and the anoxic boundary depth supports the hypothesis that the anoxic boundary limits the day-depth of the scattering layer in Saanich Inlet. However, two observations suggest the anoxic boundary is not a

persistent barrier to zooplankton migration, and that other factors contribute to determining day-depth.

If the anoxic boundary is a persistent barrier in Saanich Inlet, the depth of the zooplankton layer should track the depth of the anoxic boundary. When anoxic boundary depth increases, the depth of the scattering layer should also increase to take advantage of the greater depth refuge (Lampert 1989). The significant positive correlation between the depth of the anoxic boundary and the gap size between the base of the zooplankton layer and the anoxic boundary (Figure 2.19) indicates that beyond a certain depth, the anoxic boundary does not limit zooplankton day-depth. When the anoxic boundary was greater than 150m depth in August and September, the zooplankton layer did not descend much deeper than in previous months when the anoxic boundary was shallower (Figure 2.18), indicating that sufficient depth refuge was available. The preferred depth of the scattering layer was about 115 meters, indicating that the zooplankton were responding to another variable, likely light level. More observations during oxygen renewal events are needed to determine to what extent the anoxic boundary limits migration and what other factors are influencing day-depth.

In 17% of observations, the base of the scattering layer was in relatively well-oxygenated water (>1.0 mL L^{-1}; Figure 2.18). Relative to months where I observed the base of the zooplankton layer in severe or moderately hypoxic water, the layer could have migrated deeper than observed, assuming that the species composition of the layer was similar between months. Plankton sampling within the layer has established that *E. pacifica* and *O. obtusus* are the dominant macrozooplankton species and acoustic scatterers present (Bary et al. 1962; De Robertis 2000). These two species are vertically separated within the scattering layer, with *O. obtusus* located at the base of the layer and *E. pacifica* located in the mid and upper layer (Mackie and Mills 1983). This separation is related to the low oxygen tolerance of each species. *Orchomene obtusus* has a much greater low oxygen tolerance than *E. pacifica* (De Robertis et al. 2001; Hoos 1970). In Squally Reach, the base of the scattering layer was always in severely hypoxic water, suggesting that amphipods may dominate the zooplankton community at the inlet head. Detailed net

sampling of seasonal species composition, with concurrent oxygen measurements, is necessary to determine if species composition is an important factor is controlling zooplankton day-depth.

However, dissolved oxygen values at 100 meters depth near the mouth of Saanich Inlet were observed to fluctuate over a period of hours by up to 2.5 mL L^{-1} (Thomson et al. 1988). Similar oxygen fluctuations have been observed in Patricia Bay at the VENUS observatory (VENUS 2006). It is unknown whether similar oxygen fluctuations occur at the head of the inlet, but the absence of higher oxygen levels in Squally Reach suggests that these fluctuations are limited to the Patricia Bay and Bamberton areas. The relatively well-oxygenated measurements at the base of the scattering layer could be due to the point sampling capturing a temporary moment of elevated oxygen.

It is also possible that vertical migration was not completed when these relatively well-oxygenated measurements at the base of the zooplankton layer were made, but this possibility is remote. All transects were completed during daylight, and were usually started two hours after sunrise. Assuming descent rate is the same as ascent (2.5 to 3.5 cm s^{-1}; De Robertis et al. 2003), vertical migration to 100 meters depth should be completed in about one hour. Data from the VENUS observatory in Patricia Bay confirm that vertical migration is completed within an hour of sunrise. Incomplete migration does not explain the relatively oxygenated depth of these observations. This suggests that the anoxic boundary was not limiting zooplankton day-depth and that factors other than dissolved oxygen concentration, such as light, were controlling vertical migration depth, even when the anoxic boundary was relatively shallow. Changes in relative light intensity are known to initiate vertical migration in zooplankton (Lampert 1989) and light level has been suggested as controlling descent depth for *E. pacifica* along the continental shelf off Vancouver Island (Simard and Mackas 1989).

The near absence of a scattering layer from Squally Reach when the anoxic boundary was less than 90 meters deep suggests that this depth is a threshold for predation risk for Saanich Inlet zooplankton. If limited to such a shallow depth, the scattering layer would

be concentrated in relatively well-illuminated waters with high predation risk. Increased predation would negate the benefits of vertical migration and zooplankton should avoid areas of shallow low oxygen. The absence of the layer suggests either active avoidance (e.g. Decker et al. 2003), mass mortality caused by exposure to anoxic water, high predation rates (e.g. Genin 2004), or an absence of food. Direct mortality through exposure to anoxic water would require that the anoxic boundary depth decrease rapidly over several hours while zooplankton are concentrated at day-depth. Anoxic boundary depth decreases as anoxic water is forced upward during deep-water oxygen renewal, a process that occurs over a period of weeks (Anderson and Devol 1973). A rapid decrease in the anoxic boundary depth is unlikely. Mass mortality through high predation is possible but the most likely cause is active avoidance of the shallow hypoxic conditions (e.g. Decker et al. 2003).

2.4.3.2 Zooplankton Layer Thickness

The zooplankton layer was significantly thicker at Patricia Bay compared with Squally Reach. The difference is likely due to: 1) the higher density of zooplankton near the mouth of the inlet relative to the head, and 2) the greater variability in thickness of the Squally Reach scattering layer over the twelve months of observation (Figure 2.18). Scattering layer thickness was least variable at Patricia Bay, probably due to more favourable oxygen levels at day-depth, higher abundance due to greater food supply, or an influx of zooplankton from outside of Saanich Inlet.

When anoxic boundary depth increases, scattering layer thickness should increase as larger zooplankton take advantage of the greater depth refuge while smaller zooplankton remain at shallower depths (De Robertis et al. 2000). Conversely, a shallow anoxic boundary will force the base of the scattering layer into shallow depths and increase compression of the scattering layer as individuals attempt to access the darkest waters possible. Although weak, the positive correlation between anoxic boundary depth and scattering layer thickness supports this hypothesis (Figure 2.20).

The increased compression as the anoxic boundary becomes shallower suggests that light levels at these depths are sufficient for visual predation by planktivorous fish. Boden and Kampa (1965) observed that light levels between 85-100 meters in Saanich Inlet were 2-3 orders of magnitude higher than light levels observed at *E. pacifica* day-depth (250-300m) off the coast of California. These light levels could be sufficient for visual predation by Pacific herring. In laboratory experiments, Atlantic herring (*C. harengus*), a closely related species, were observed feeding visually at light levels as low as 0.01 lux (Batty et al. 1990). Herring are also capable of filter feeding (Batty et al. 1990). Of the 186 fish schools observed along transects, 123 were observed within or near the scattering layer at oxygen levels as low as 0.5 mL O_2 L^{-1}. Fish schools within the scattering layer indicates that zooplankton cannot completely avoid visual predators during the day.

2.4.4 Conclusions

A zooplankton density gradient between the mouth and head of Saanich Inlet was present during the summer months. This result met my *a priori* expectation based on the presence of a biological front at the mouth of Saanich Inlet and historically higher primary productivity at the mouth relative to the head. The difference in chlorophyll fluorescence was greatest in summer which corresponded to months where zooplankton density was greater at either Patricia Bay or Bamberton relative to Squally Reach.

Zooplankton may respond to horizontal oxygen concentration gradients between the mouth and head of Saanich Inlet by avoiding areas of shallow hypoxic water. This behaviour was most apparent in Squally Reach between August and October when the zooplankton scattering layer was nearly absent. Further, zooplankton also avoid areas where the anoxic boundary is less than 90 meters deep. I interpret the absence of zooplankton when the anoxic boundary is shallow as an avoidance response to insufficient depth refuge from visual predators.

The zooplankton scattering layer has a preferred depth in Saanich Inlet of about 115 meters. My expectation was that zooplankton would follow increased oxygen levels into

deeper water to take advantage of increased depth refuge. However, when anoxic boundary depth increased by up 32 meters depth in late summer, zooplankton day-depth increased by less than 15 meters relative to months with shallower anoxic boundaries, indicating that sufficient depth refuge from visual predators is available at 115 meters depth.

Some zooplankton can tolerate severely hypoxic conditions while at day-depth. This result is consistent with observations of *Orchomene obtusus* deep in the scattering layer and known low-oxygen tolerance of this amphipod. It also suggests that euphausiids and other scattering layer zooplankton may have greater low-oxygen tolerances than previously described.

Chapter 3

Zooplankton Distribution in Patricia Bay

3.1 Introduction

3.1.1 Zooplankton Migration Behaviour

Diel Vertical Migration

In pelagic ecosystems, where refuge habitats from visual predators are limited, many species have developed diel vertical migration (DVM), during which species ascend to surface waters near sunset and descend to deep, dark waters near sunrise. In shallow habitats, many benthic zooplankton species such as mysids (Kringel et al. 2003) and copepods (Teasdale et al. 2004) also undergo DVM, emerging from bottom sediments near dusk and returning to the seafloor at dawn. Diel vertical migration is considered a predator-avoidance response, initiated by a change in relative light intensity (Lampert 1989). In support of the predator-avoidance hypothesis, De Robertis et al. (2000) found that smaller euphausiids initiate migration to surface waters earlier and at higher light levels than larger conspecifics. De Robertis et al. (2000) suggest that because smaller euphausiids are less visible to visual predators, they can initiate migration earlier without increased risk of detection by planktivorous fish. The trade-off for diel migrating species is that although predation risk is reduced, feeding opportunities and growth are also reduced. Typically, DVM species do not feed during the day while at depth.

Diel vertical migration behaviour in zooplankton can be influenced by planktivore presence. In laboratory experiments, Tjossem (1990) found that *Chaoborus* (midge) larvae altered their vertical migration behaviour in response to water containing chemical cues from planktivorous fish. Offshore acoustic observations by Thomson and Allen (2000) suggest that zooplankton modify their rate of ascent/descent in the presence of planktivorous fish. In a coastal fjord, Bollens and Frost (1989) observed that a lower proportion of a population of *Calanus pacifica* vertically migrated when actively feeding planktivorous fish were abundant. In contrast, De Robertis (2002) observed that planktivorous fish within 100 meters of euphausiids had no influence on their migration behaviour.

Horizontal Migration

Horizontal migrations in zooplankton can occur in near-surface waters in freshwater and marine environments. Horizontal migrations of crustacean zooplankton are common in freshwater lakes and are usually interpreted as predator avoidance responses (e.g. White 1998; Wojtal et al. 2003). In lakes, larger zooplankton such as *Daphnia* typically move from littoral areas with dense macrophytes to open waters when littoral planktivores are abundant. In the marine environment, horizontal migrations of gelatinous (e.g. Hamner and Hauri 1981) and crustacean (e.g. Webb and Wooldridge 1990) zooplankton have been documented. Hamner and Hauri (1981) observed diel horizontal migrations of up to one kilometer in scyphomedusae and suggested predator avoidance as a possible explanation of this behaviour. Hamner et al. (1982) also suggested that these migrations could be related to nutrient requirements of a symbiont. Webb and Wooldridge (1990) observed that a species of mysid (*Mesopodopsis slabberi*) undertook diel horizontal migrations of up to one kilometer and suggested that this mysid was responding to changes in food availability. In Hawaii, Benoit-Bird and Au (2004) observed a diel offshore-onshore horizontal migration of a deep scattering layer of micronekton into shallow waters during DVM. These horizontal migrants are likely exploiting near-shore resources such as phytoplankton or vertically migrating benthic species.

Horizontal zooplankton movement can occur by swimming (e.g. Hamner and Hauri 1981) or through advection by currents (Genin 2004). For less motile groups such as crustacean zooplankton, a consequence of horizontal movement through migration or advection is becoming trapped on a shallow bottom during descent. This 'topographic blockage' results in very high predation mortality for the trapped zooplankton and has been documented at seamounts (Genin 2004). Bottom trapping could potentially occur in coastal fjords where vertically migrating pelagic zooplankton (e.g. euphausiids) actively swim or are advected over shallow bottoms prior to descent. Descending zooplankton trapped by the bottom could be an important contributor to benthopelagic coupling (Marcus and Boero 1998).

3.1.2 Patricia Bay

In Saanich Inlet, acoustic observations from a Patricia Bay buoy moored over a 60m bottom in 2000 suggest that the deep scattering layer (Chapter 2) can move horizontally over shallow depths at night (ASL Environmental Sciences and R. Yahel, unpublished data). Patricia Bay is the largest bay in Saanich Inlet and is located on the east side of the inlet about four kilometers south of the entrance sill (Figure 1.1). Maximum depth is approximately 120 meters where the bay merges with the main body of Saanich Inlet. West of the 120m isobath, bottom depth increases to about 185 meters in the mid-inlet. Dissolved oxygen concentrations in the deeper areas of Patricia Bay vary with changes in tidal intrusions of oxygenated water across the sill and the depth of the mid-inlet anoxic layer. At the Patricia Bay VENUS site, located at 96 meters depth, oxygen varies by as much as 2.5 mL L^{-1} over a period of hours (VENUS 2006). Tidal currents in Patricia Bay are typically weak (~5 cm s^{-1}) and winds are usually from the east or west (Chapter 2).

The deep zooplankton scattering layer extends eastward into Patricia Bay to about 80 meters depth (Figure 3.1). In addition to these zooplankton, Patricia Bay supports pelagic planktivorous fish including Pacific herring and walleye pollock. During daytime acoustic transects through Patricia Bay, I observed these schooling species most often near the bottom or in deep waters in close proximity to the deep scattering layer (Figure 3.1). Benthic fish include slender sole (*Lyopsetta exilis*), eelpout (*Lycodopsis* spp), and plainfin midshipman (*Porichthys notatus*; personal observation). In some areas of Patricia Bay, high densities of suspension feeders such as sea whips (*Halipteris* or *Virgularia*) occur. Regular input of zooplankton into Patricia Bay is necessary to support these communities. Strong westerly winds could potentially advect zooplankton vertically migrating from the deep mid-inlet into the shallower waters of the bay, providing a food source for these planktivorous fish and invertebrates.

3.1.3 Objectives

Several studies have focused on the behaviour and species composition of the daytime deep scattering layer in Saanich Inlet (e.g. Bary et al. 1962; Mackie and Mills 1983; De

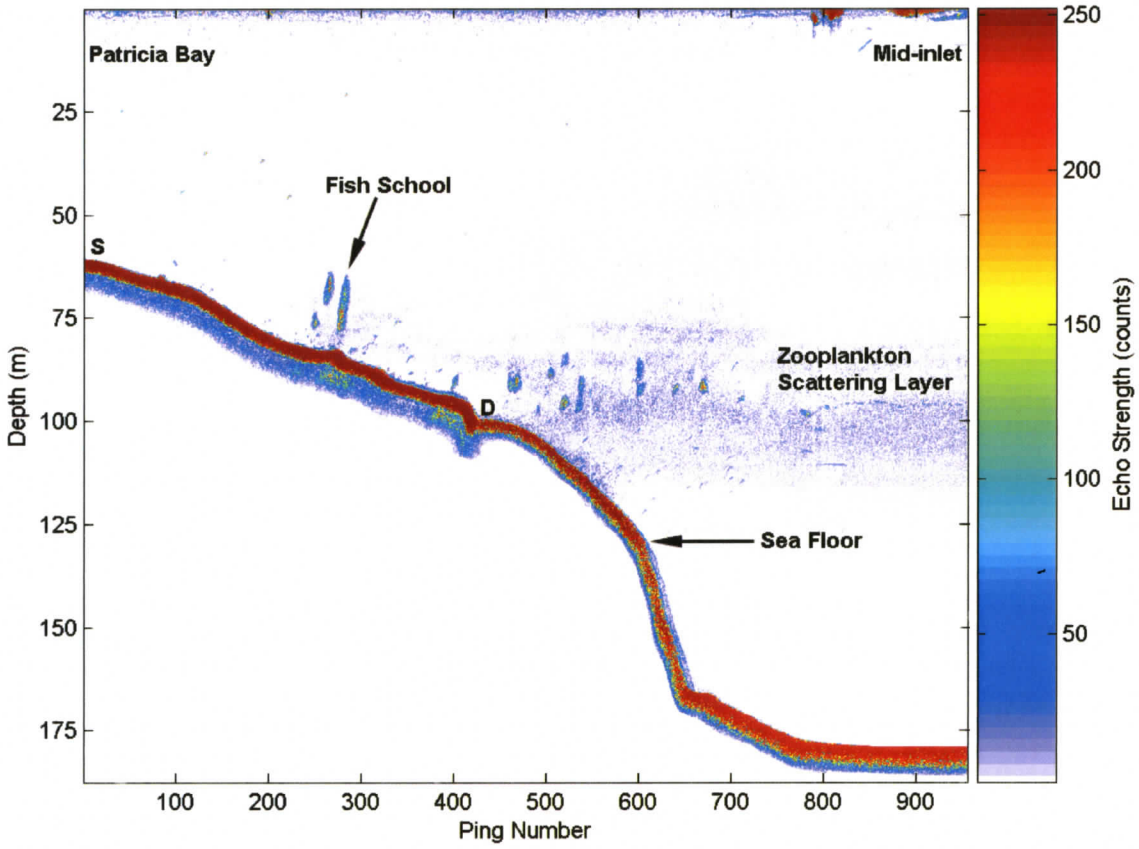

Figure 3.1. East to west acoustic transect on March 21, 2006, through Patricia Bay to the middle of Saanich Inlet showing the location of the deep zooplankton scattering layer in relation to Patricia Bay. The approximate locations of the shallow (S) and deep (D) acoustic sample sites are also shown.

Robertis et al. 2000). Night-time zooplankton dynamics in the shallower waters of the inlet have not been studied.

I am interested in the following questions:

1) Do mid-inlet zooplankton move horizontally over shallow depths in Patricia Bay during DVM or at night?
2) Do zooplankton at shallow depths vertically migrate?
3) Do all vertically migrating reflectors move at the same time?
4) Does the presence of planktivorous fish change zooplankton migration patterns?

3.2 Methods

3.2.1 Data Collection

Acoustic data were collected from deep and shallow locations in Patricia Bay between February and April 2006 (Figures 3.1, 3.2). Data from the deep site were collected by the VENUS observatory (48° 39.079, 123° 29.161). At the shallow site (February: 48° 39.109, 123° 28.358; March-April 48° 39.122, 123° 28.334), I collected data using an autonomous acoustic system. Data were collected simultaneously at both locations between March 22 and April 15, 2006, but only data from the shallow site were available in February.

3.2.1.1 Deep Site: VENUS Observatory

An upward-oriented 200 kHz ASL Water Column Profiler™ (aka ZAP) collected acoustic data from the VENUS instrument platform. The VENUS platform was located at 96.5 meters depth and the acoustic transducer was located 1.5 meters above the seabed. Volume backscatter data were collected at 1 Hz and were automatically binned into 0.125 meter vertical bins. The pulse duration of each ping was 300μs. The VENUS ZAP collected data at gain setting two (ASL Environmental Sciences 2004), a higher energy setting than used at the shallow site.

A

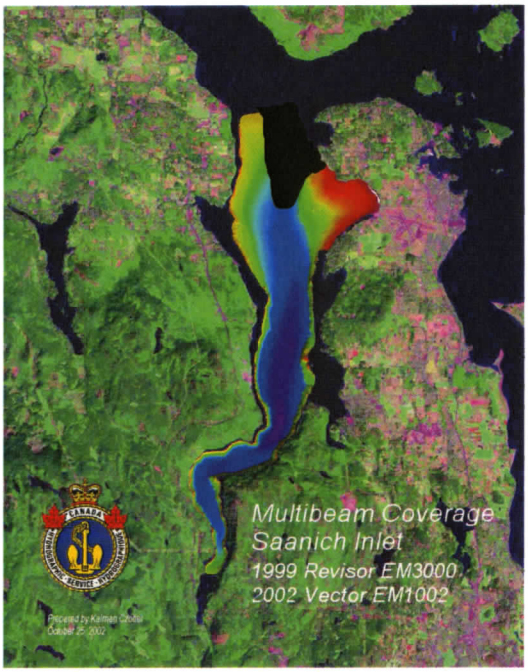

B

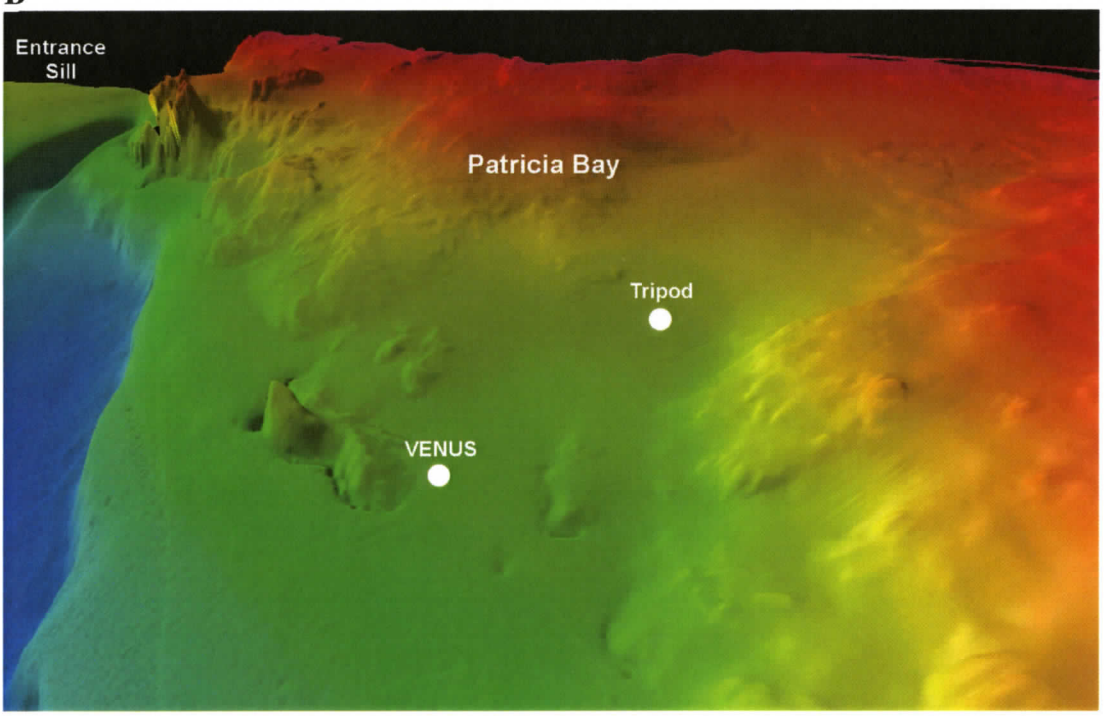

Figure 3.2. Multibeam acoustic images of Saanich Inlet (A) and Patricia Bay (B). The location of the VENUS observatory (96m depth) and the shallow tripod deployment site (62m depth) are shown. Vertical relief is exaggerated by 6:1. Images courtesy of the Canadian Hydrographic Service.

3.2.1.2 Shallow Site

The shallow site was located one kilometer east of the VENUS observatory at a depth of 62 meters. The area selected was first surveyed by ROV and was rich in benthic animals. Further, the site was shallower than the preferred day-depth of the deep scattering layer (Chapter 2). A battery-powered ZAP was attached to a weighted aluminum tripod with the transducer oriented upwards (Figure 3.3). Following deployment, the transducer was about 0.5 meters above the seabed. The tripod was deployed from *MSV John Strickland* on two occasions: February 7 and March 21, 2006. For the February deployment, the tripod was lowered with ropes to the bottom and left on the seafloor. The position where the tripod reached the bottom was recorded and the instrument was recovered February 23 using the ROPOS ROV. In March, the tripod was lowered using a rope with a float at the surface end of the line and 15 kg of lead weight located about 20 meters from the tripod. Once the tripod was on the bottom, the position was recorded and the weighted rope was moved approximately 20 meters from the tripod so the attached float would not be within the acoustic beam. The attached float was submerged 10 meters below the surface and recovery was from *MSV John Strickland* on April 21 using divers.

On both deployments, the tripod ZAP collected data at 0.05 Hz or one ping every 20 seconds, and the pulse duration of each ping was 300μs. Data were binned into 0.125 meter vertical bins to be consistent with VENUS data. Gain setting one was used (ASL Environmental Sciences 2004), which was a lower energy setting than used with VENUS. I used these settings to maximize the number of days of data collection. Due to memory limitation, the ZAP only recorded data to April 15. I used data collected between March 22 and April 15 in comparisons between the two locations.

3.2.2 Data Analysis

3.2.2.1 Processing

February data at the shallow site extended from 12:00 (PST) February 7 to 11:59 February 23. VENUS data were unavailable during this period. March-April data extended from 00:00 (UTC) March 22 to 23:59 April 15. To limit file size and permit comparison, I extracted VENUS data matching the tripod sample times for analysis.

Following this extraction, both data sets contained data collected at the same time and each data set consisted of 108,000 pings. I also averaged data into one meter vertical bins to further reduce file size.

3.2.2.2 Near-Surface Zooplankton

I define near-surface zooplankton as night-time scatterers within 20 meters of the surface. The time when near-surface zooplankton appeared at the shallow site was assessed qualitatively by reviewing daily echograms. I used the first appearance of zooplankton in the upper 20 meters of the water column at the shallow site to determine arrival time.

3.2.2.3 Zooplankton Density

Volume backscatter coefficient (sv m^{-1}) is a reasonable proxy for zooplankton density (Chapter 2). For each site, I integrated volume backscatter through the water column for each ping and then calculated mean day and night integrated backscatter values for each deployment day. At both sites, I ignored the first depth bin above the transducer to avoid including values associated with near-field effects (Appendix 1).

3.2.2.4 Vertical Migration Timing

I determined the timing of zooplankton ascent and descent using a custom routine in Matlab. For each ping, I calculated the difference in acoustic counts between adjacent 1m bins with increasing height above the transducer. At the shallow site, I used a threshold of 0.45 counts to determine the height of scatterers above the transducer. At the deep site, I used a threshold of 2.4 counts due to the higher count values associated with the higher gain setting. The timing of ascent and descent was defined as the start of rapid and sustained increase (ascent) or decrease (descent) in the height of the vertical migrants (Figure 3.4).

The high amount of daytime backscatter at the deep site prevented using this method for determining ascent timing. Instead, I determined ascent timing qualitatively by reviewing daily echograms near sunset. I considered ascent started when scatterers nearest to the transducer began to move upwards in the water column (Figure 3.5).

Figure 3.3. Aluminum tripod on the deck of *MSV John Strickland* following recovery on April 21, 2006. The acoustic transducer was located 0.5 meters above the seabed.

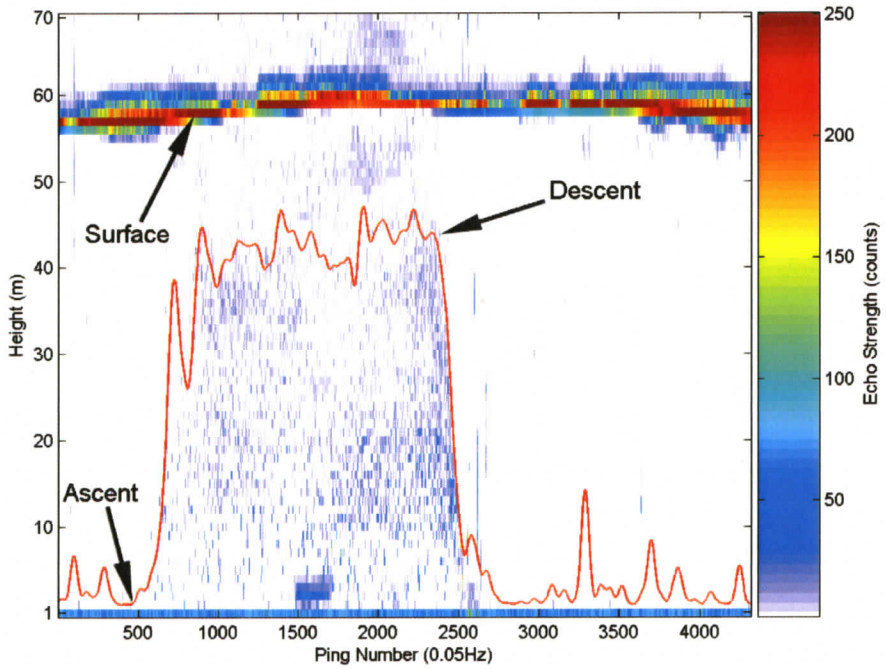

Figure 3.4. Example of ascent and descent timing at the shallow site on March 24, 2006. The red line represents the smoothed height of zooplankton above the transducer.

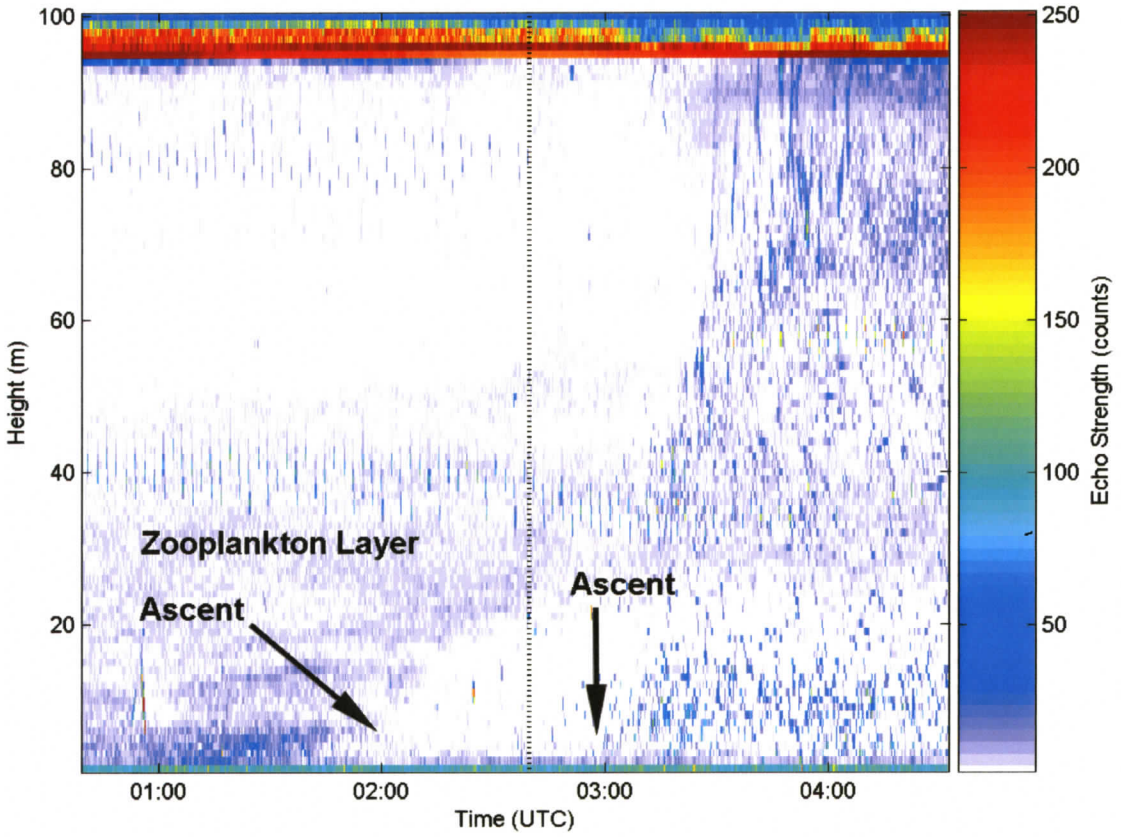

Figure 3.5. Example of qualitative ascent timing at the deep (VENUS) location on March 31, 2006. Two ascents occurred at the deep site. The first ascent consisted of the deep scattering layer and the second ascent originated near the transducer. The dashed line represents sunset. The vertical bands centred at 40 and 80 meters height above the transducer are interference from a 300 kHz acoustic Doppler current profiler.

Ascent times at the shallow site were determined quantitatively and qualitatively and values were within 3%. I assume a similar accuracy for ascent timing at the deep site.

3.2.2.5 Vertical Migration Depth

I used a custom Matlab routine to determine mean night-time depth of migrating zooplankton at each site. I only considered data between sunset and sunrise and I used a count threshold of 2.4 for both sites. I tried different thresholds and found that this count value most closely tracked ascent depth. I inverted each data matrix so that bin one was near the surface, rather than at the transducer. Within each ping, I calculated the acoustic count difference between adjacent depth bins starting at bin one. With increasing bins (depth), the first bin where the change in acoustic counts exceeded the threshold delineated zooplankton ascent depth. At the deep site, I excluded the first 10 bins to avoid including surface reflections. At the shallow site, I excluded the first 16 bins for the same reason. I smoothed ascent depth over 45 pings or 15 minutes at both sites.

3.2.2.6 Fish School Identification

To identify fish schools, I converted digital backscatter count data into volume backscatter strength (Sv; Chapter 2). I applied a -50dB threshold to the data and only data with Sv greater than this threshold were displayed. I defined fish schools as being at least 3 vertical bins (i.e. 3 meters) by 2 horizontal bins (i.e. 20 seconds). The -50dB threshold and the 3x2 contiguous bins limited the potential for including zooplankton as fish targets. I defined school depth as the base or deepest part of the school.

3.3 Results

3.3.1 Day-night Distribution

I observed day-night differences in the vertical distribution of volume backscattering and in the abundance of scatterers. At both sites, I found a significant difference between day and night mean integrated volume backscatter (paired t-test, $p<0.001$ for both sites). At the shallow site, daytime volume backscattering was nearly absent (Figures 3.6, 3.7, 3.8). I observed very few scatterers during the day and the mean of daytime mean integrated

volume backscatter was 4.68×10^{-7} m^{-1}. At night, the mean of mean integrated volume backscatter increased to 6.74×10^{-6} m^{-1}, a 14-fold increase over daytime values. Night-time scatterers at the shallow site first appeared at or near the level of the transducer and were concentrated within 40 meters of the seabed (Figures 3.6, 3.7). There was no difference in mean of mean night-time integrated backscatter between February (6.60×10^{-6} m^{-1}; n=16) and April (6.82×10^{-6} m^{-1}; n=15).

In contrast to the shallow site, high concentrations of daytime scatterers occurred within 20 meters of the transducer at the deep site (Figure 3.7). Between 72-90% of daytime volume backscatter was concentrated within this 20m range. Few daytime scatterers were detected above 20m height. The mean of daytime mean integrated volume backscatter within 20m of the transducer was 1.89×10^{-5} m^{-1}, whereas mean integrated volume backscatter above 20m was 4.51×10^{-6} m^{-1}. During each day, the concentration and the height above the transducer of daytime zooplankton decreased between sunrise and sunset (Figure 3.7).

At night at the deep site, scatterers occurred throughout the water column, with the highest concentrations within 20m of the surface on most days. The mean of mean night-time integrated volume backscatter was 3.13×10^{-5} m^{-1} and between 14-54% of the volume backscatter occurred in the upper 20m of the water column. There was no correlation between night-time mean integrated backscatter at the deep and shallow sites ($r=0.027$, $p=0.899$, n=25). During the last week of observation, mean integrated volume backscatter increased relative to the start of observation in March (Figure 3.8).

At the deep site, beginning on March 29, a band of weak scattering was present between the seafloor and 60 meters above the bottom (Figure 3.7). This band did not vertically migrate and was present within this depth range both day and night through the final observation on April 15. I did not observe a similar band at the shallow site.

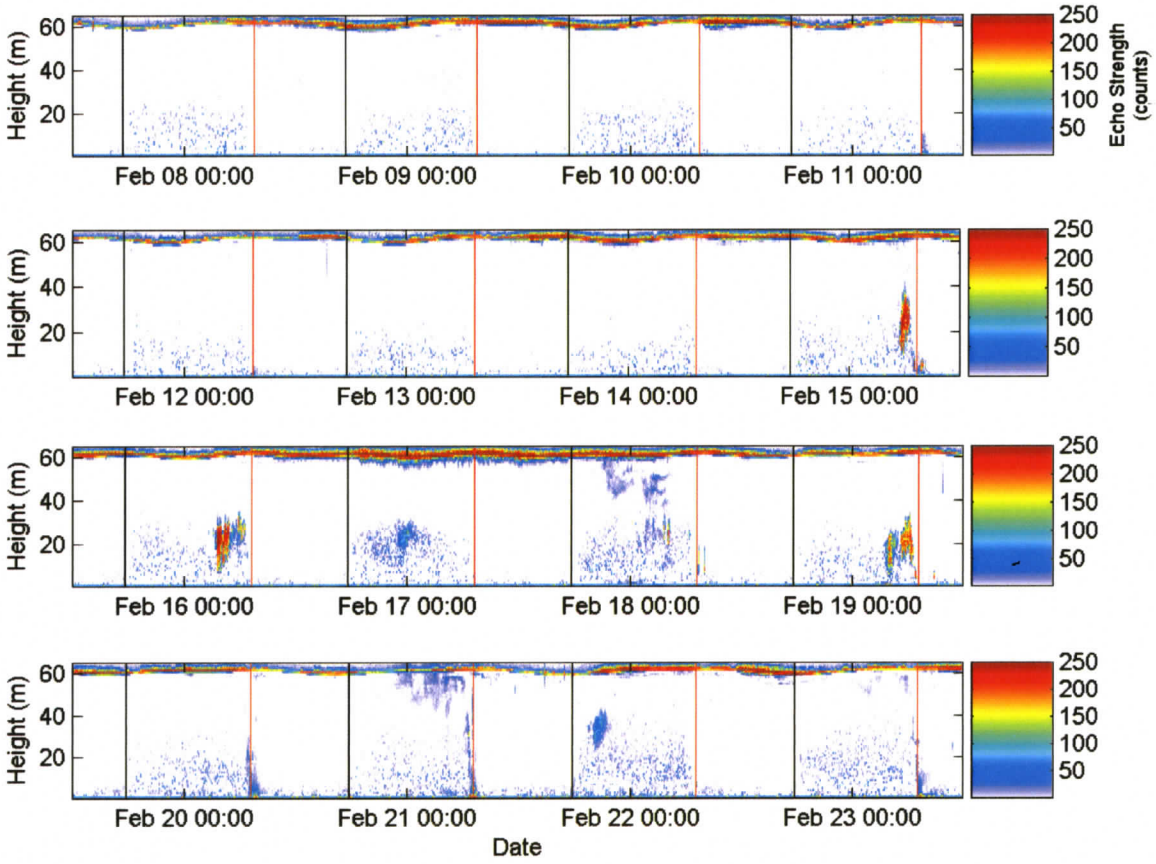

Figure 3.6. Acoustic backscatter at a shallow site in Patricia Bay between February 7-23, 2006 from an up-looking transducer positioned 0.5m above the seabed. Height is the distance above the transducer. Time is PST and sunset and sunrise are shown as black and red lines, respectively. Zooplankton migrants first appear at the level of the transducer each evening near sunset. Near surface zooplankton only occurred during the nights of February 17-18 and 20-21. The strong band at about 60m height is due to strong echoes from the surface.

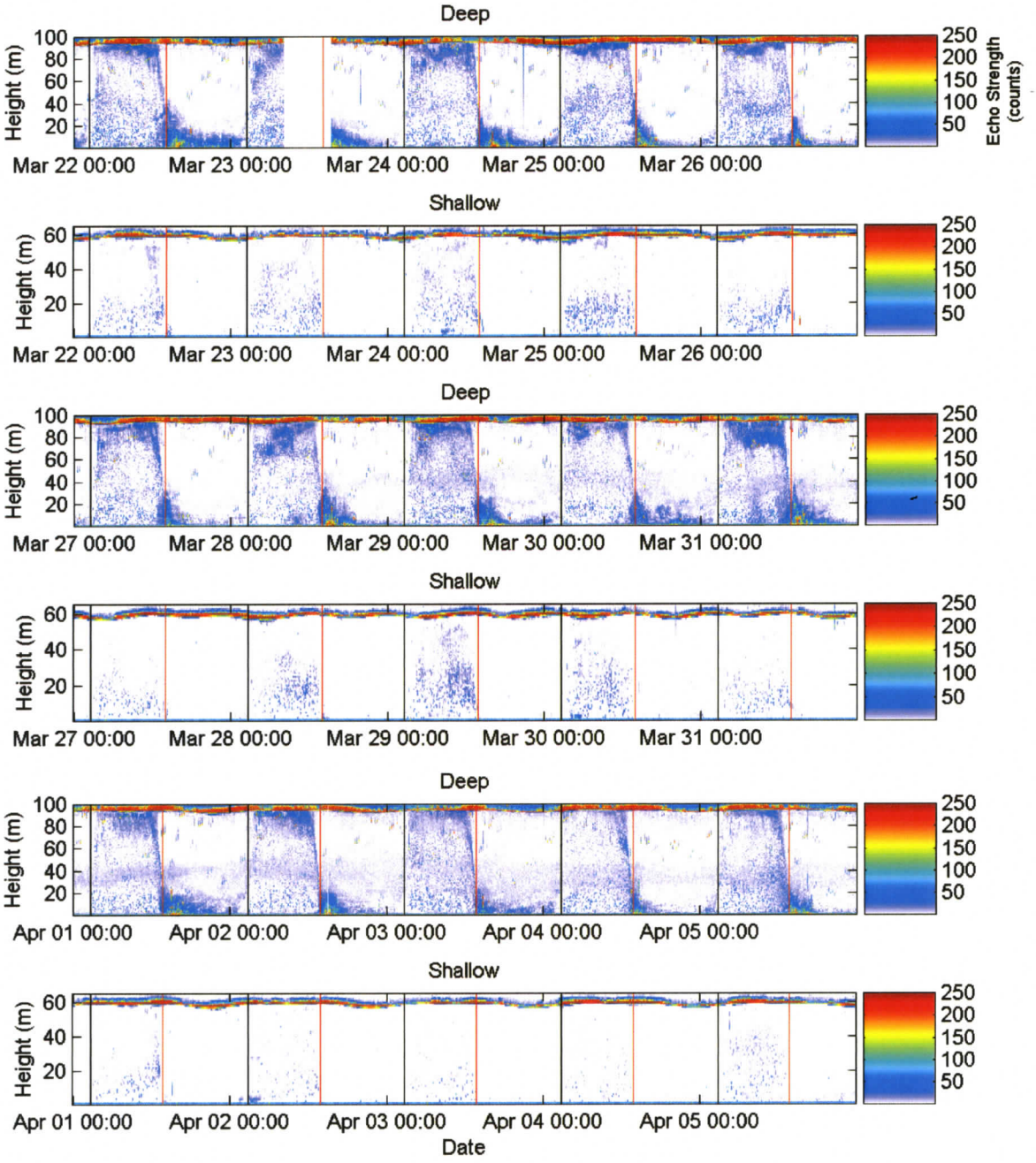

Figure 3.7. Acoustic backscatter at the deep and shallow sites in Patricia Bay between March 22 and April 15, 2006 from up-looking transducers positioned near the seabed. Transducers were located about 1.5m and 0.5 m above the seabed at the deep and shallow sites, respectively. Height is the distance above the transducer. Time is UTC and sunset and sunrise are shown as black and red lines, respectively. Zooplankton migrants at the shallow site first appear at the level of the transducer each evening near sunset. Near surface zooplankton were infrequent at the shallow site. The strong bands at about 95m and 60m height at the deep and shallow sites, respectively, were due to strong echoes from the surface.

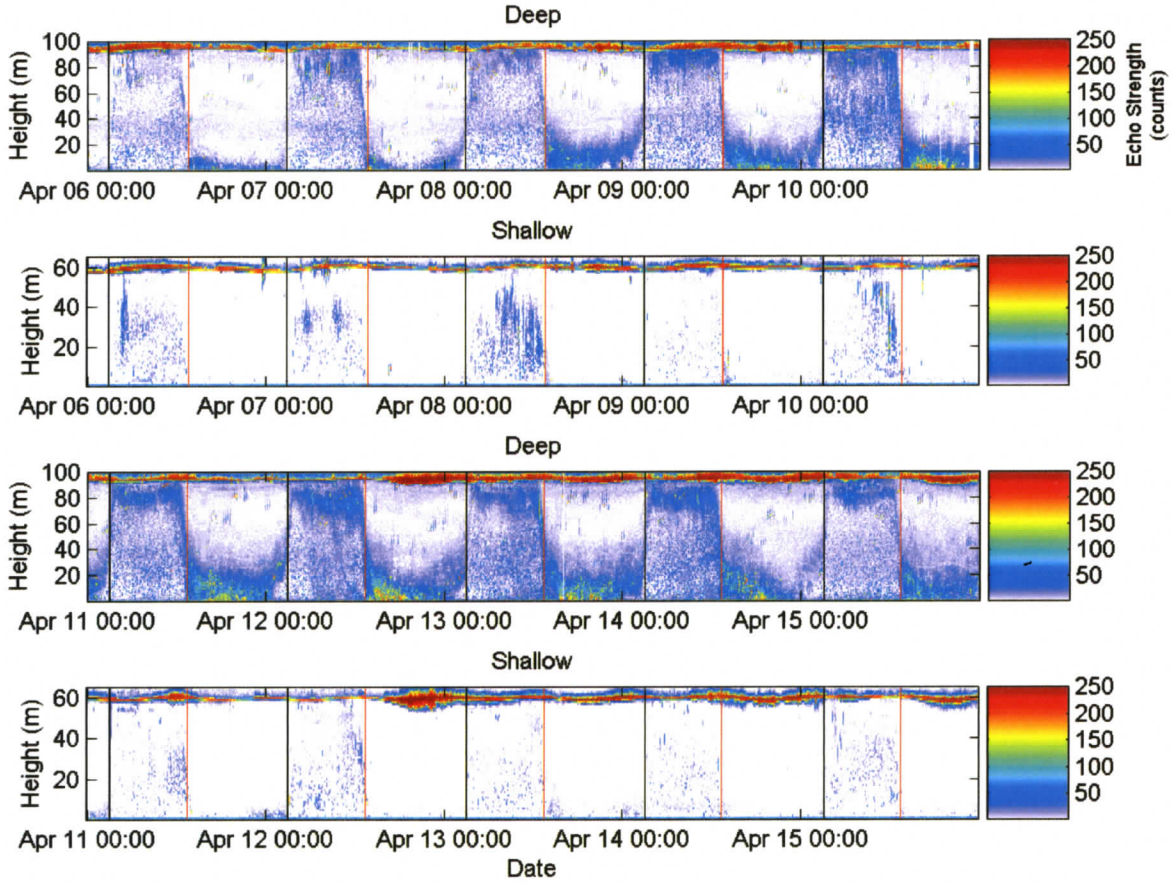

Figure 3.7 continued.

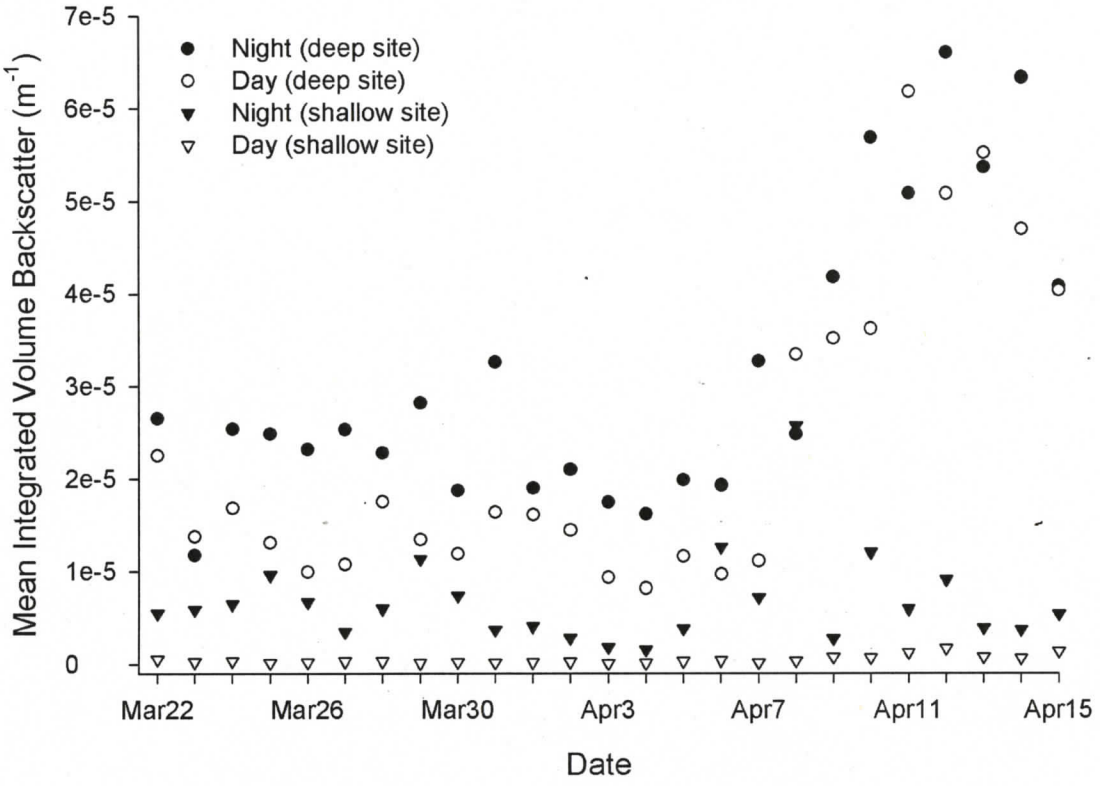

Figure 3.8. Mean day and night integrated volume backscatter for the deep (96m) and shallow (62m) sites between March 22 and April 15, 2006. Volume backscatter was integrated between the surface and one meter above the transducer at each site.

3.3.2 Vertical Migration Depth

Zooplankton from the deep scattering layer at the deep site migrated into near-surface waters each night and were concentrated within 20 meters of the surface until descending near sunrise (Figures 3.7, 3.9). In contrast, migrants at the shallow site remained deeper in the water column, rarely ascending to less than 20m depth (Figures 3.6, 3.7, 3.9). Mean ascent depth at the deep site varied between 3-18m depth. Ascent depth at the shallow site was more variable, ranging between 22-45m in February and 17-38m depth in March-April. Mean ascent depth was significantly different between sites (t-test, $p<0.001$). I found no significant correlation between zooplankton night depth and day of observation at the shallow site (Pearson product-moment correlation, $n=25$, $r=-0.272$, $p=0.189$), but a significant correlation did exist at the deep site ($n=25$, $r=-0.531$, $p=0.006$).

3.3.3 Near-surface Zooplankton

I observed near-surface backscatter on 30% of days at the shallow site (Table 3.1). Near-surface zooplankton appeared at the shallow site between 1.2 and 8.6 hours after sunset (mean = 5.8 hours after sunset; Figure 3.10). On seven nights, near-surface zooplankton remained at the shallow site until descending near sunrise. On two nights, near-surface zooplankton appeared for about 0.5 hours near the mid-point of the night, disappearing 4.5 hours before sunrise. On the last night of observation (April 15), near-surface plankton were present between 1.2 and 1.9 hours after sunset.

The arrival of near-surface zooplankton at the shallow site coincided with flood tides on nine of 12 days. Winds on the nights when near-surface zooplankton appeared at the shallow site were weak with variable direction (Table 3.1).

3.3.4 Vertical Migration Timing

Ascent

At the shallow site, zooplankton ascent times for the February and March-April deployments were similar (Figure 3.11A). Ascent ranged from 29 minutes before sunset to 42 minutes after sunset. Mean (± standard deviation) ascent times were 20 ± 14 and

11 ± 17 minutes after sunset for the February and March-April deployments, respectively.

At the deep site, two separate vertical migrations occurred near sunset (Figure 3.11A). Following the first ascent, there were relatively few scatterers near the seabed before the second ascent started (Figure 3.5). The first migration was initiated between 11 and 115 minutes before sunset (mean = 45 ± 29 minutes before sunset) whereas the second migration occurred after sunset on 80% of days (mean = 9 ± 17 minutes after sunset). The difference between these two ascent times was statistically significant (paired t-test, $p<0.001$). During the first ascent, the scatterers moved as a group towards the surface. The second ascent was characterized by the arrival of targets at the level of the transducer following the first ascent (Figure 3.5). The average timing of the second deep ascent differed by only two minutes from the shallow site ascent in March-April (Figure 3.11A) and the difference between these two ascents was not statistically significant (paired t-test, $p=0.566$).

For each of the three ascents, ascent timing changed relative to sunset. At the shallow site, between February 7 and April 15, ascent timing moved closer to sunset. I observed similar trends for the two ascents at the deep site (Figure 3.11A). These changes in ascent timing were significantly correlated with the day of observation (Pearson product-moment correlation, $p<0.01$ for each ascent) and the correlation coefficients were -0.628, -0.552, and -0.650 for the first deep ascent, second deep ascent, and the shallow site ascent, respectively. The slopes of these trends were -2.46, -1.27, and -0.70 for the first deep ascent, second deep ascent, and the shallow site ascent, respectively. I found no statistically significant difference between the slopes of these trends (ANCOVA, $df=2$, $F=1.66$, $p=0.198$). Relative to sunset, the first ascent was initiated earlier in April than in March. Variability in ascent timing also increased in April.

Descent

Descent at the two locations always occurred before sunrise and was most variable in March-April (Figure 3.11B). At the deep site, the descent of near-surface scatterers

Table 3.1. Zooplankton arrival and departure times for the zooplankton layer, defined as scattering within 20m of the surface, at the shallow site in Patricia Bay. Surface zooplankton at this site are assumed to originate from the mid-inlet scattering layer. Italicized dates indicate nights where surface zooplankton descended at the shallow site.

Date	**Surface Zooplankton**		**[1]Wind**		**Tide**	**[2]Fish**
	***Arrival**	****Departure**	**Direction**	**Speed (km h^{-1})**		**Schools**
February 17	3.3	3.0	NE (54°)	36	Ebb	Y
February 20	5.1	0.9	SE (247°)	10	Flood	Y
March 22	8.7	0.9	SW (163°)	8	Flood	Y
March 23	8.4	1.3	No data	-	Flood	N
March 24	5.8	0.8	SE (249°)	20	Flood	Y
March 25	5.0	4.4	No data	-	Flood	N
March 29	5.2	1.2	NE (293°)	10	Ebb	N
April 6	5.0	4.3	E (278°)	25	Flood	Y
April 8	3.8	0.6	SE (204°)	8	Flood	Y
April 12	0.9	0.5	NE (65°)	1	Ebb	Y
April 13	7.8	0.5	No data	-	Flood	Y
April 15	1.1	8.7	No data	-	Flood	Y
Mean ± std	5.0 ± 2.5	[§]1.7 ± 1.5				

* Hours after sunset

** Hours before sunrise

[1]Averaged between sunset and approximately 5 hours after sunset.

[2]Indicates fish school presence at the shallow site.

[§]Does not include April 15.

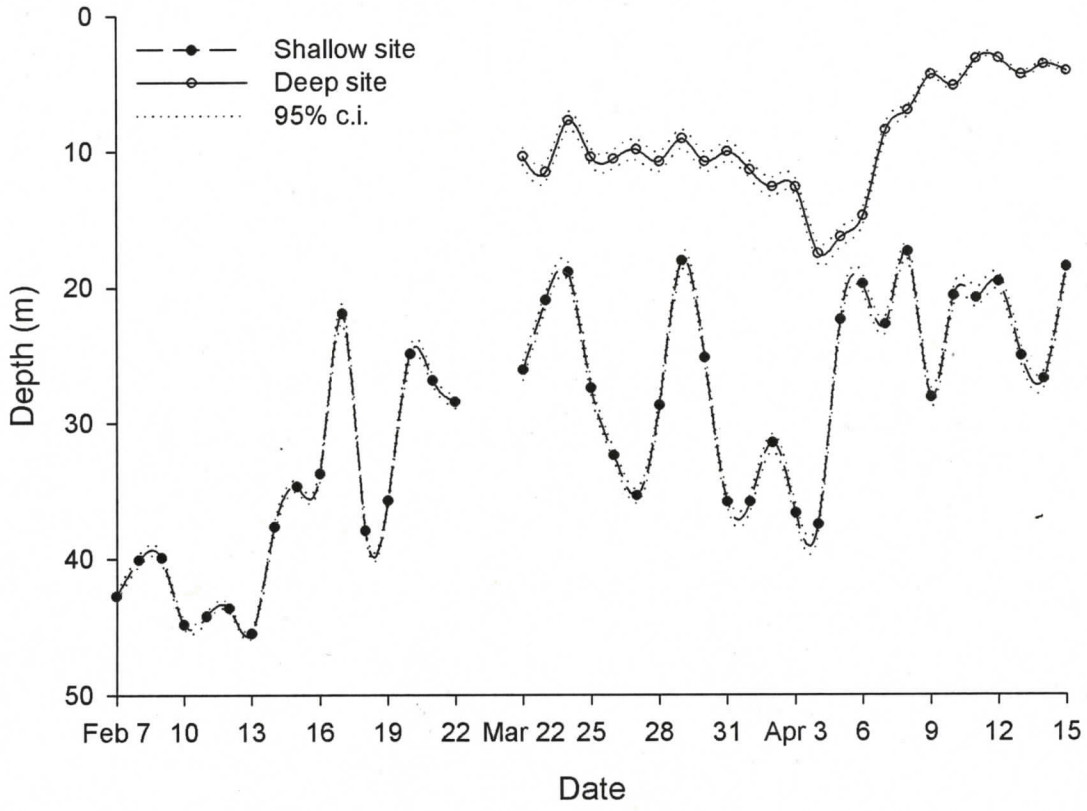

Figure 3.9. Mean night ascent depth at the deep and shallow sites in Patricia Bay between February 7 and April 15, 2006. Zooplankton migrated significantly shallower at the deep site. Zooplankton within 20 meters of the surface occurred each night at the deep site but near-surface zooplankton were infrequent at the shallow site.

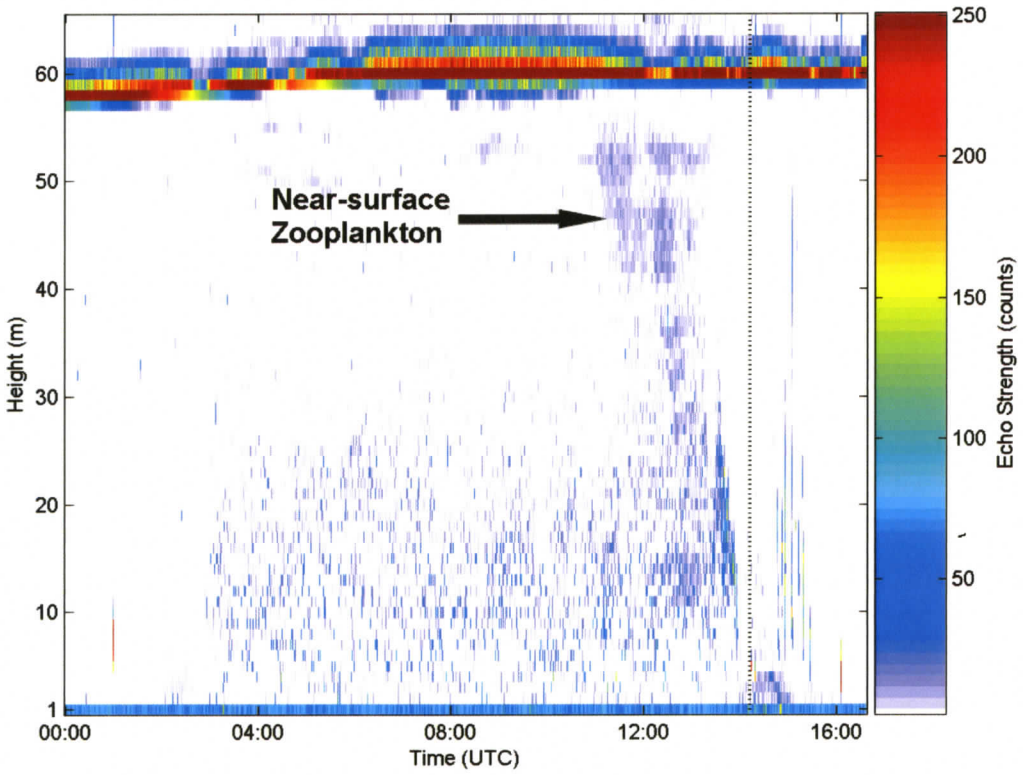

Figure 3.10. Example of near surface zooplankton at the shallow site on March 22, 2006. The dashed line represents sunrise. Ascending zooplankton at the shallow site typically remained within 30 meters of the bottom. On this date, near-surface zooplankton arrived at the shallow site approximately two hours before sunrise.

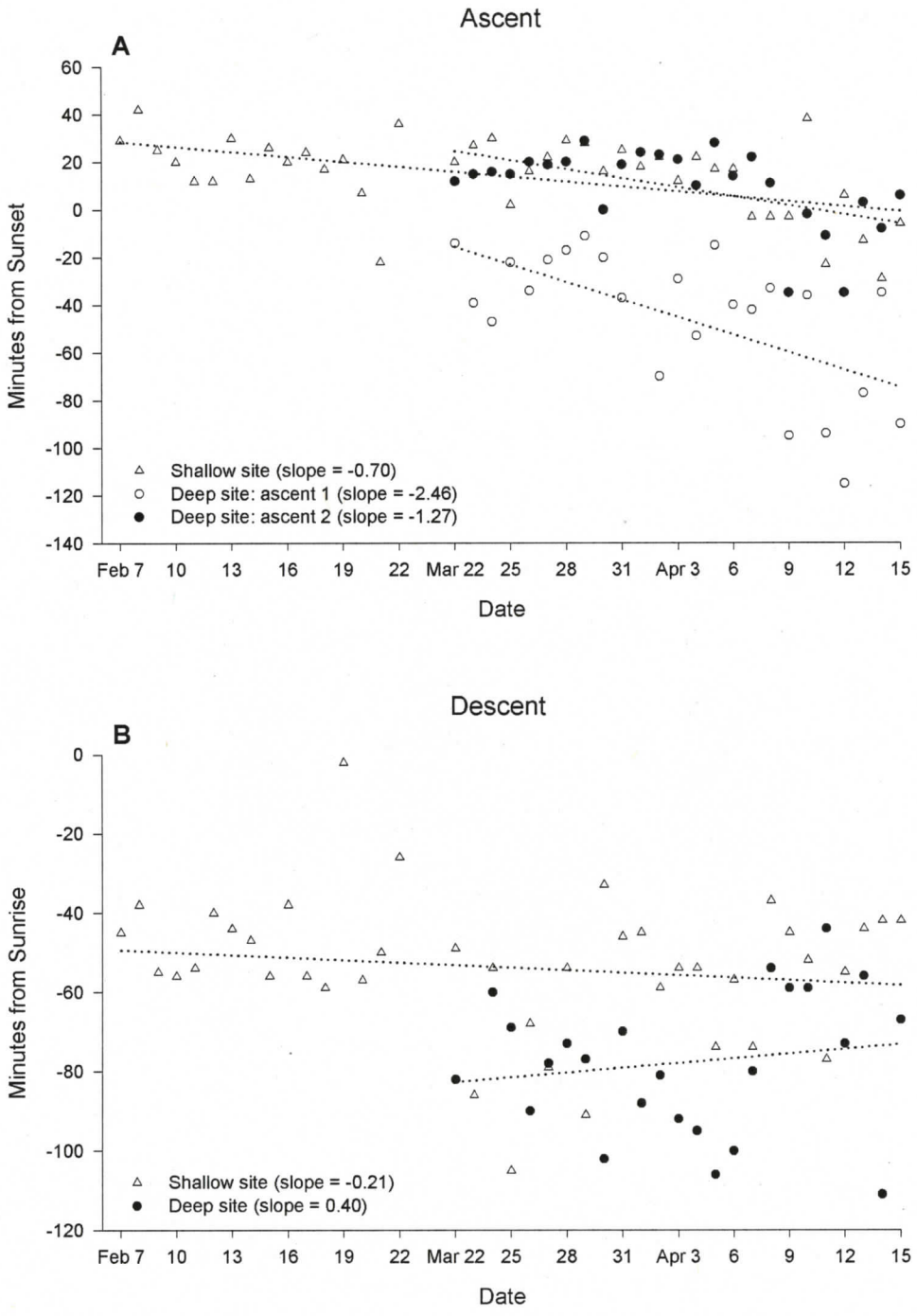

Figure 3.11. Zooplankton vertical migration timing relative to A) sunset and B) sunrise for zooplankton at the deep and shallow sites in Patricia Bay. Negative and positive values indicate times before and after sunset/sunrise, respectively. Two ascending migrations occurred at the deep site (A) but the descent of first group masked the second descent (B). The first deep ascent occurred before sunset whereas the second deep ascent and the shallow ascent both occurred after sunset. Descent always started before sunrise at both locations. The dashed lines show the trends in ascent and descent timing.

masks the descent of the second group of migrants. I was unable to distinguish between the two ascent groups during descent (Figure 3.7). Descent at the deep site was initiated sooner than at the shallow site on 83% of days and there was a significant difference in descent timing between the two sites (paired t-test, $p<0.001$). Mean (± standard deviation) descent at the deep and shallow sites occurred 78 ± 18 and 54 ± 18 minutes before sunrise, respectively. At the deep site, zooplankton descent started between 44 and 111 minutes before sunrise and at the shallow site, descent started between 2 and 105 minutes before sunrise. There were no statistically significant trends in descent time (Figure 3.11B).

3.3.5 Planktivore Distribution

Based on my ROV observations near the deep site, the fish schools I observed acoustically consisted of either Pacific herring or walleye pollock. Fish schools were most abundant at the deep site (n = 177) and I observed schools on 96% of days at this location. I observed far fewer schools at the shallow site ($n_{Feb} = 45$, $n_{Mar} = 58$) and these schools were present on fewer days: 64% and 69% of days for the February and March-April deployments, respectively (Table 3.2). On 75% of days when I observed near-surface zooplankton at the shallow site, I also observed fish schools (Table 3.1). However, the frequency of schools did not increase at the shallow site when near-surface zooplankton were present. The average number of schools I observed per day at the shallow site with and without near-surface zooplankton was 2.5 and 2.4, respectively. The maximum number of schools at the shallow site on a single day was 19 on April 10, a day without near-surface zooplankton (this value was excluded as an outlier from the calculation of mean number of schools per day). The maximum number of schools at the deep site was 21, also on April 10.

At both sites, schools occurred most often near sunrise (Figure 3.12). At the shallow site in February, I observed 56% of schools within two hours of sunrise (Table 3.2). In contrast, relatively few schools were present near sunset at either site. The deep site had the most schools near sunset (13%). At the shallow site, I observed no schools near sunset in February and only 7% of total schools during March-April.

Table 3.2. Spatial and temporal distribution of fish schools at the deep and shallow sample sites in Patricia Bay. Schools occurred more often at the deep site and were observed on most days. At the shallow site, schools were observed most often near sunrise. The duration of the February and March-April deployments were 16 and 25 days, respectively.

Location	Fish Schools		[1]Sunrise	[1]Sunset	20 [2]mab (%)		Mean Depth (m)	
	n	% days	(%)	(%)	Day	Night	Day	Night
$Shallow_{Feb}$	45	69	56	0	86	35	53	45
$Shallow_{Mar}$	58	64	38	7	77	19	42	[§]**25**
Deep	177	96	24	13	91	0	83	[§]**15**

[1]Schools observed within ± 2 hours of sunrise or sunset.
[2]Percentage of schools within 20 meters of the seafloor (mab=meters above bottom).
[§]Significantly different (t-test, $p<0.001$)

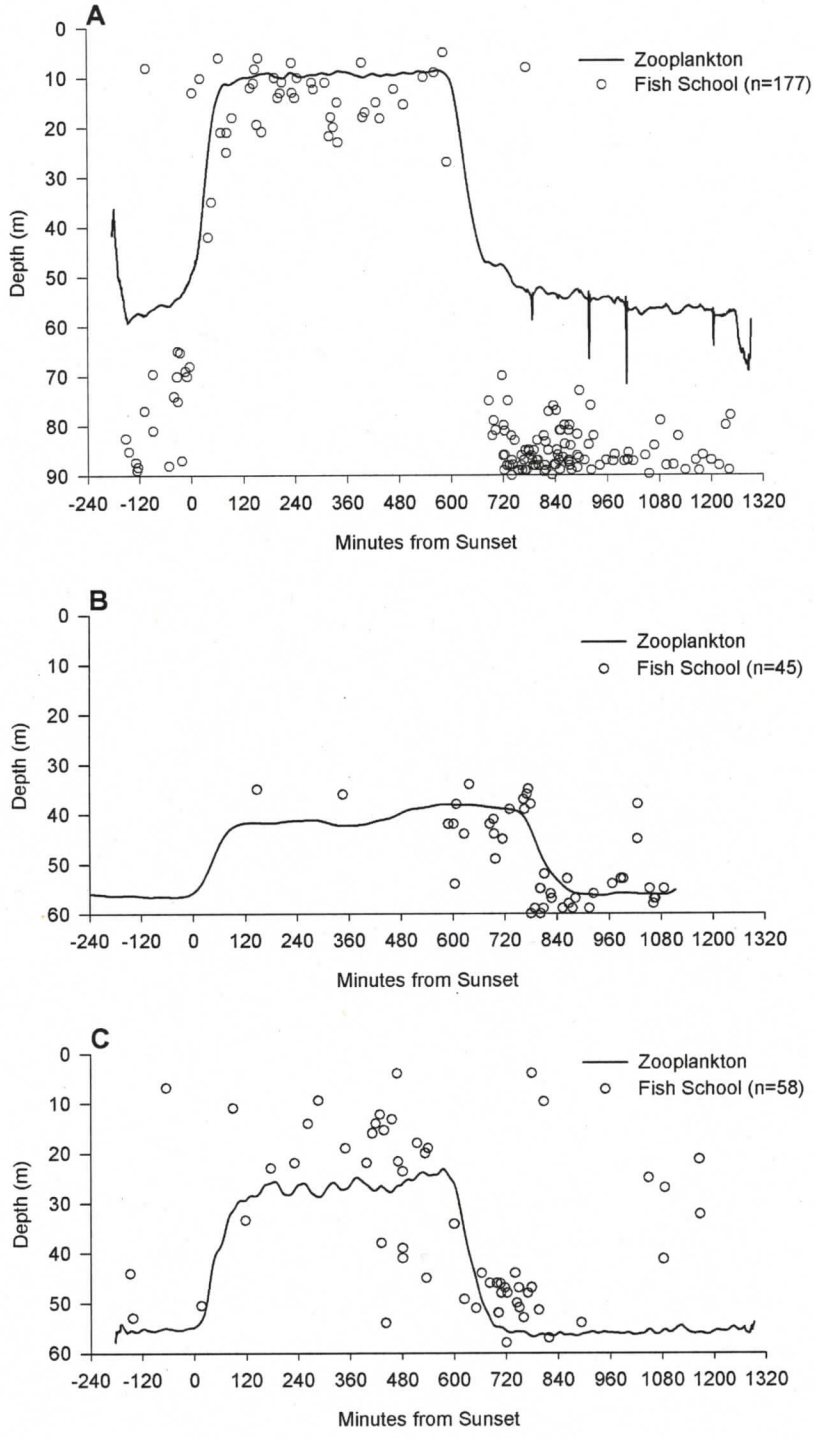

Figure 3.12. Location of fish schools and mean zooplankton depth (shallowest depth averaged over the days of deployment) in relation to sunset in Patricia Bay at the deep (A) and shallow sites (B = February; C = March-April). Day depths for zooplankton at the deep site represent the shallow boundary for zooplankton. Zooplankton were present from this boundary to the bottom at the deep site. Daytime plankton were rare at the shallow site. Fish schools followed a similar diel vertical migration pattern as zooplankton and were most abundant at each site near sunrise (~720 minutes from sunset in March-April).

Fish school distribution showed a diel vertical migration pattern, with most schools near the bottom during the day and above the bottom at night. The mean depth of schools decreased at both locations between day and night. At the deep site, mean depth decreased from 83m during the day to 15m during the night (Table 3.2). Night depth was significantly shallower at the deep site than at the shallow site (t-test, $p<0.001$). In March-April, I observed 77% and 91% of daytime schools within 20 meters of the seabed at the shallow and deep sites, respectively (Figure 3.12). At night, fish schools were closer to the surface and at the deep site, I observed 79% of night schools at less than 20 meters depth (Figure 3.12).

Due to the limited number of school observations at sunset/sunrise, I was not able to determine if fish schools were ascending/descending before or after zooplankton. The few observations near sunset at the deep site indicate that school ascent timing is similar to the first zooplankton ascent (Figure 3.12A).

The presence of fish schools at the deep site in the hour prior to ascent did not alter zooplankton ascent timing (Figure 3.13). I observed schools within one hour of sunset on eight days, with the number of schools ranging from one to six. Mean (± standard deviation) zooplankton first ascent times were 42 ± 33 and 47 ± 29 minutes before sunset for days with and without fish schools, respectively. Mean second ascent times were 5 ± 20 and 12 ± 15 minutes after sunset for days with and without fish schools, respectively. There were too few schools at the shallow site for this assessment.

3.4 Discussion

3.4.1 Zooplankton Distribution

At both the deep and shallow sites, the vertical distribution of scatterers changed between day and night as zooplankton undertook diel vertical migrations. Zooplankton DVM caused a significant increase in volume backscatter at night relative to day values. At the deep site, the increase in volume backscatter was caused by the ascent of the deep scattering layer from depths greater than the transducer and by benthic zooplankton

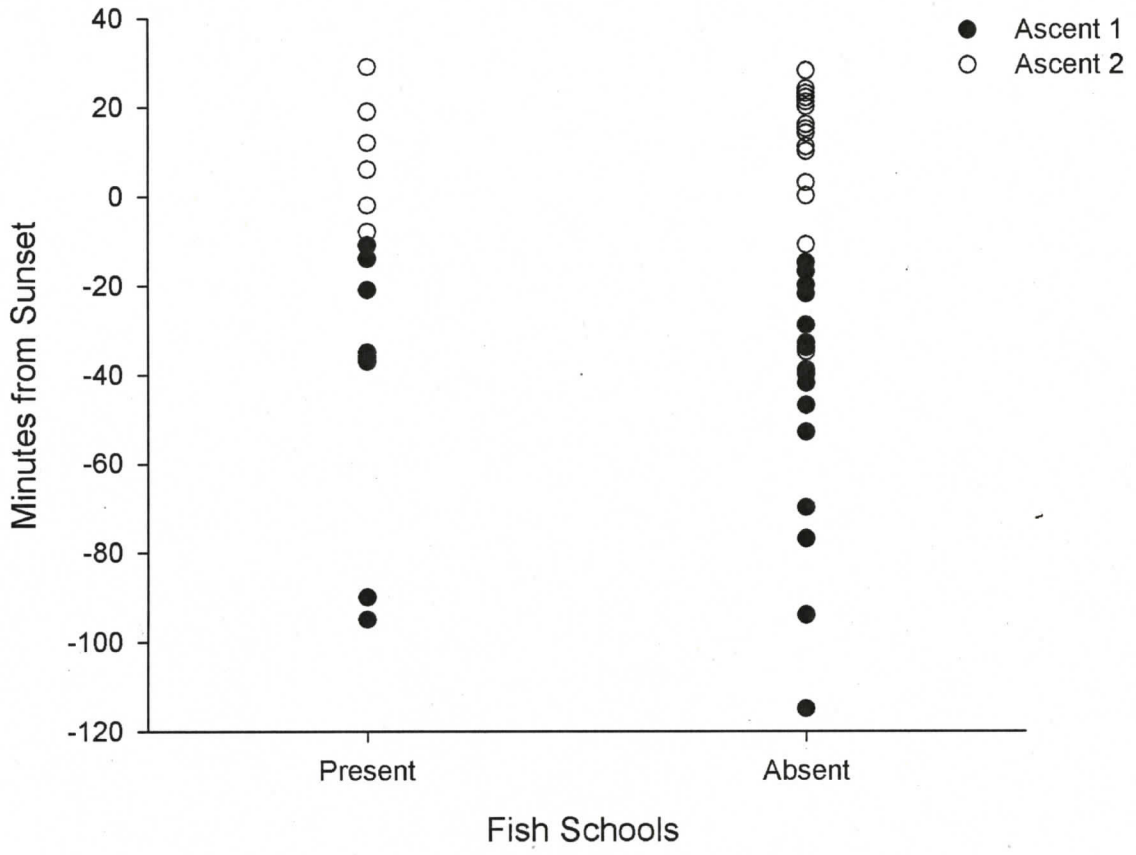

Figure 3.13. Influence of fish schools within one hour of sunset on zooplankton ascent timing at the deep site. Fish school presence did not alter ascent timing for the two vertical migrations.

emerging from the bottom. At the shallow site, the increase was due to emergence of benthic zooplankton.

The dense daytime zooplankton concentration I observed at the deep site represents the eastern limit of the deep scattering layer. In the mid-inlet, between April 2005 and March 2006, the mean depth of the base of the scattering layer ranged between 90 and 115 meters (Chapter 2, Figure 2.19A). At 96 meters depth, the deep site is within the day-depth range of deep scatterers seeking depth refuge from visual predators. The presence of the dense daytime zooplankton layer at the deep site indicates that this site provided sufficient refuge for some zooplankton species. In February 2007, I observed dense aggregations of euphausiids near the VENUS site during ROV surveys in Patricia Bay, supporting my interpretation that daytime scattering at this site was caused, in part, by deep scattering layer zooplankton (Table 2.3).

At night at the deep site, the entire water column was filled with scatterers, with the highest concentrations near the surface. The deep scatterers concentrated near the bottom ascended to the surface near sunset each day. This is characteristic behaviour of *Euphausia pacifica*, a strong vertical migrator and the dominant macrozooplankton species within the deep scattering layer of Saanich Inlet (Bary et al. 1962; De Robertis 2002). Euphausiids in Saanich Inlet are known to migrate into surface waters (Bary and Pieper 1970; Mackie and Mills 1983). On the night of January 31, 2007, I captured euphausiids in the upper 20 meters of the water column with a Tucker trawl in the mid-inlet. Similar euphausiid migrations were observed by Bollens et al. (1992) in Dabob Bay, a fjord in Washington State. Scatterers associated with the second ascent that I observed at the deep site also contributed to the significant increase in night-time volume backscatter.

In contrast to the deep site, daytime scatterers were absent at the shallow site. East-west acoustic transects I conducted during the day through Patricia Bay indicate that the deep scattering layer does not extend eastward to the shallow site (e.g. Figure 3.1). At 62

meters depth, this site was too shallow to provide sufficient depth refuge from visual predators for euphausiids or other pelagic zooplankton. Each day near sunset, scatterers appeared near the level of the transducer, causing the significant increase in volume backscatter at night compared to day values. These scatterers descended each morning near sunrise and the absence of scattering during the day suggests a vertically migrating benthic species that spends the day either within bottom sediments or near the bottom below the level of the transducer. It is possible that the absence of daytime scattering at the shallow site is due to zooplankton migrating away from the shallow site during the day. However, the appearance of scatterers at the shallow site each day near sunset suggests a local population.

The origin of the band of weak scattering at the deep site I observed between March 29 and April 15 is unknown. The absence of the band at the shallow site suggests that the higher gain setting used at the deep site allowed detection of small targets. The vertical extent of the band varied temporally, suggesting that it was a real phenomenon and not an artifact of noise generated by the higher gain setting. The band did not show DVM behaviour, suggesting that it was non-biological in origin. The ZAP is capable of detecting suspended sediment (personal observation), so the band may have been caused by tidal intrusions of turbid water related to runoff caused by the 11.1mm of rain in the seven days before March 29 (Environment Canada 2007).

3.4.2 Zooplankton Vertical Migration Timing and Depth

The two ascent reflectors I observed at the deep site indicate that there were two different zooplankton groups migrating. The first ascent group migrated to the surface each night between March 22 and April 15, 2006. From my ROV observations and net tows, I conclude that this group of scatterers was primarily *Euphausia pacifica* (Table 2.3). Previous observations in Saanich Inlet also found that this migrating layer was dominated by *Euphausia pacifica* (Bary et al. 1962; Bary and Pieper 1970; Mackie and Mills 1983; De Robertis 2002).

The second ascent at the deep site was initiated 54 minutes after the first migration, on average, and usually started after sunset. Acoustic targets of this second migration first appear near the level of the transducer, suggesting that they have emerged from the seabed at or near the VENUS instrument platform. The timing of this second migration was not significantly different from the single ascent I observed at the shallow site. Acoustic targets at the shallow site also first appeared at or near the transducer, indicating emergence of zooplankton from the seabed. The similarity in ascent timing at both the deep and shallow sites suggests that the same species is responsible for the emergence. This regular vertical migration of demersal zooplankton from the seabed in Patricia Bay is a previously unrecognized and potentially important component of benthopelagic coupling in Saanich Inlet.

Zooplankton ascent is initiated by changes in relative light intensity (Lampert 1989). The eyes of *Euphausia pacifica* in Saanich Inlet are adapted to cope with greater daytime light levels than offshore conspecifics (Boden and Kampa 1965). Boden and Kampa (1965) speculated that the greater light level they observed within the deep scattering layer in Saanich Inlet was due to the anoxic boundary limiting zooplankton descent to darker waters. The difference in ascent timing between the deep scattering layer and benthic zooplankton could be due to differences in sensitivity to changes in relative light intensity. The significantly later ascent of the benthic species suggests that it is less sensitive to light changes and requires a greater relative change in light intensity to initiate migration. This hypothesis is supported by the observation that ascent of benthic zooplankton was almost always initiated after sunset.

The trends I observed in ascent timing at both sites suggest a change in relative light intensity that altered ascent timing. At the shallow site, and the second ascent at the deep site, ascent timing moved closer to sunset from March to April. This change suggests relatively darker conditions that initiated ascent earlier in April than in March (Figure 3.11). This interpretation would also explain the change in ascent timing of the deep scattering layer. Ascent of the deep scattering layer started earlier relative to sunset in the latter half of the deployment, suggesting lower light levels prior to sunset relative to the

first half of the deployment. Perhaps a contributor to lower light levels in the latter part of the deployment was the band of scattering that appeared between March 29 and April 15. Ascent timing at the deep site became more variable once this band appeared and ascents started earlier in the day. A band of suspended sediment or increased turbidity would reduce the intensity of light reaching the deep site, potentially causing the observed change in ascent timing. Another possible cause of lower light levels is the spring phytoplankton bloom. The spring bloom occurred in April (D. Grundle, pers. comm.) and abundant phytoplankton in the surface waters would reduce the intensity of light reaching the deeper waters.

In contrast to the deep scattering layer, emergent zooplankton in Patricia Bay did not migrate all the way to the surface. Instead they remained at intermediate depths. This observation suggests that feeding on phytoplankton within the photic zone was not the primary driver of this vertical migration. It is possible that food availability was low as most observations were made prior to the April phytoplankton bloom (D. Grundle, pers. comm.). However, the presence of the deep scattering layer in surface waters at the deep site suggests that food was available. An alternative explanation is dispersal. Alldredge and King (1985) observed that large demersal zooplankton migrated to shallow depths and they suggested that these vertical migrants used stronger currents above the bottom as a dispersal mechanism. Vertically migrating animals would also escape sessile suspension feeders and benthic planktivorous fish by migrating into intermediate depths. In Patricia Bay, despite the weak currents, vertical migrants could potentially be dispersed by 10s to 100s of meters from their emergence site. The presence of these migrants at both the deep and shallow sites suggests a wide-spread distribution within Patricia Bay.

On the night of January 31, 2007, I acoustically observed a scattering layer near the bottom at my shallow site in Patricia Bay from *CCGS John P. Tully*. I assumed that this bottom scattering layer consisted of the same scatterers that I acoustically observed between February and April 2006 at this site. The January 31 layer extended to approximately 10 meters above the bottom. I attempted to capture these scatterers using

a Tucker trawl. From net tows within the layer, I captured immature squat lobsters (*Munida quadraspina*), copepods, euphausiids, and mysids. The deepest depth fished during this tow was approximately 10 meters above the bottom. In West Sound, Orcas Island, Kringel et al. (2003) acoustically observed emergence of the mysid *Neomysis kadiakensis*. They confirmed, using a combination of emergence traps and night net tows, that this mysid was emerging from the seabed and migrating to surface waters. *Neomysis kadiakensis* has not been documented in Saanich Inlet, but the mysid *Xenacanthomysis pseudomacropsis* has been recorded (Murie 1995). Based on my net tow, mysids do contribute to near-bottom scattering at night in Patricia Bay.

Other possibilities include benthic copepods (Teasdale et al. 2004) and amphipods (Ingram and Hessler 1983). Teasdale et al. (2004) observed that peak emergence of benthic copepods in shallow water in the Gulf of Mexico occurred at local darkness. Emergence timing at the shallow Patricia Bay site was usually after sunset, following a similar pattern. The other possibility is benthic amphipods. Ingram and Hessler (1983) observed that some species of benthic amphipods were regularly present at more than 20 meters above the seabed at night and I observed a similar pattern at the shallow Patricia Bay site. However, the amphipod *Orchomene obtusus,* abundant in the deep scattering layer in Saanich Inlet, is likely not the cause of scattering. This species prefers deep dark waters and forages on bottom sediments within the anoxic zone (De Robertis et al. 2001). Although *O. obtusus* does vertically migrate to intermediate depths (50m) in the mid-inlet (Liu 1989), it is not known from shallow waters in Patricia Bay.

3.4.3 Horizontal Migration/Advection

At the shallow site, near-surface zooplankton were present during 30% of nights but were only present during 20% of descents. Based on a sustained swimming speed of 5 cm s^{-1} (De Robertis et al. 2003), euphausiids could potentially swim the kilometer distance between sites in 5.5 hours. On eight nights, near-surface zooplankton arrived at the shallow site after 5.0-8.7 hours, suggesting they could have actively migrated between the two sites. However, the infrequent appearance of surface zooplankton at the shallow

site indicates that deep scattering layer zooplankton do not make regular horizontal migrations into Patricia Bay.

In freshwater lakes, horizontal migrations by crustacean zooplankton are usually attributed to predator avoidance (Van de Meutter et al. 2005, White 1998, Wojtal et al. 2003). In laboratory experiments, Van de Meutter et al. (2005) observed that *Daphnia* avoided vegetated habitats with high predator densities. White (1998) found that the copepod *Mesocyclops* made diel horizontal migrations. During the day, this copepod avoided vegetated littoral habitats when planktivores were abundant. My data do not support this hypothesis for zooplankton in Patricia Bay. The average number of fish schools I observed at night at the deep site was actually slightly higher (mean 8.3 fish schools) on nights where I did not observe near-surface zooplankton at the shallow site compared with nights where I did observe near-surface zooplankton (mean 5.2 fish schools). If zooplankton were migrating horizontally to avoid predators, I would expect to observe more schools at the deep site on nights where I observed near-surface zooplankton at the shallow site.

Another potential cause of horizontal zooplankton migration is increased food availability. Hamner et al. (1982) suggested that horizontal migrations of a scyphomedusae were related to nutrient requirements of a symbiont. Webb and Wooldridge (1990) determined that diel onshore horizontal migrations of a mysid were related to high near-shore phytoplankton concentrations at night. However, it is unlikely that food availability over shallower waters in Patricia Bay was higher than in the mid-inlet. Several studies have demonstrated that nutrient concentrations and phytoplankton abundance is highest near the inlet mouth (e.g. Parsons et al. 1983) and that these variables decrease with headward distance (Timothy and Soon 2001; Gargett et al. 2003). Although east-west horizontal distribution of phytoplankton abundance has not been studied in Saanich Inlet, I would expect food availability to be higher near the mid-inlet where phytoplankton are advected over the sill.

In Patricia Bay, horizontal movement of mid-inlet zooplankton seems to be related to flood tides or tidal advection and not a behavioural response to predation or increased food availability. Of the 12 nights when near-surface zooplankton appeared at the shallow site, nine occurred on a flood tide. This observation supports my interpretation that currents associated with flood tides affect the horizontal distribution of mid-inlet zooplankton by advecting pelagic animals over shallow depths in Patricia Bay.

Although infrequent, horizontal movement of surface zooplankton does occur and these descending zooplankton, most likely *Euphausia pacifica* (personal observation; De Robertis et al. 2000), will become trapped on the bottom at depths shallower than their preferred day-depth in the mid-inlet. The absence of surface zooplankton soon after sunset at the shallow site suggests that euphausiids trapped on the bottom were either consumed or were successful at migrating along the bottom to preferred depths. The abundance of fish schools at both the deep and shallow locations at sunrise indicates high zooplankton predation. Genin (2004) observed that topographic blockage, the prevention of descent by the seafloor, results in high zooplankton mortality at seamounts. In Patricia Bay, bottom trapping of pelagic zooplankton likely occurred on 20% of observed days during the late winter/early spring. However, only 41 days of observation were made prior to the spring growing and reproductive season of euphausiids (Bollens et al. 1992). Horizontal advection or migration may occur more frequently during summer months when zooplankton densities are higher. Descent of pelagic zooplankton was an infrequent contributor to benthopelagic coupling at the shallow site.

3.4.4 Planktivore Distribution

At the deep site, I observed three times the number of fish schools than at the shallow site. This difference can be attributed to predator avoidance behaviour by the fish and to greater prey availability at the deep site. As with pelagic zooplankton, planktivores such as Pacific herring seek dark waters during the day to avoid visual predators (Blaxter and Holliday 1963). At 96 meters, the deep site provides sufficient depth refuge. Deeper migrations are not be possible for these fish because of the variable and hypoxic oxygen concentrations below approximately 100 meters depth (Chapter 2). During ROV

transects into deep (>120m), severely hypoxic waters, I observed only individual Pacific hake (i.e. not in schools) and slender sole. This low-oxygen barrier may further concentrate schools of herring and pollock at depths near 100 meters. The high number of schools at the deep site can also be attributed to the dense concentration of daytime zooplankton. During ROV surveys in February 2007, I observed dense aggregations of euphausiids near the deep site. De Robertis et al. (2003) observed that euphausiids in the deep scattering layer of Saanich Inlet were quiescent during the day and they did not respond to planktivores, even when fish were within 20-300cm. The predator avoidance behaviour of other scattering layer species is unknown, but such an exploitable and concentrated resource would attract planktivores. Conversely, the lack of daytime zooplankton at the shallow site would make that location less attractive for foraging planktivores, explaining the low number of schools I observed during the day. Further, the shallow site likely does not provide sufficient depth refuge for pelagic planktivorous fish.

The highest frequency of schools occurred near sunrise at both sites, indicating that planktivores were preying on descending zooplankton as light levels increased. I had insufficient data to determine whether the fish were descending with the zooplankton or whether the schools were waiting near the bottom.

Diel vertical migration behaviour is well known in herring (Blaxter and Holliday 1963) and walleye pollock (Swartzman et al. 2002), the most common schooling planktivores in Saanich Inlet (De Robertis 2002). As with zooplankton, planktivore DVM behaviour is initiated by a change in relative light intensity (Blaxter and Holliday 1963). The extent of fish DVM in Patricia Bay was related to the ascent depth of their prey, indicating that fish were responding to zooplankton distribution. At the shallow site, where zooplankton did not ascend into surface waters at night, night schools were found at significantly greater depths than at the deep site where zooplankton ascended to the surface. This relationship was especially apparent in February at the shallow site when both zooplankton and fish schools remained within 30 meters of the bottom at night (Figure 3.12B).

In the presence of fish schools, zooplankton vertical migration ascent timing was not altered. Using acoustic and optical techniques, De Robertis (2002) and De Robertis et al. (2003) observed that *Euphausia pacifica* did not respond to the presence of planktivorous fish at horizontal scales less than 100 meters. Swartzman et al. (2002) observed that euphausiids limited their vertical migration depth when walleye pollock were abundant. Tjossem (1990) observed that *Chaoborus* larvae increased their rate of ascent when planktivorous fish chemical cues were present. I observed too few schools at the shallow site to determine if there was an effect of fish presence on zooplankton behaviour. At the deep site, fish school presence did not affect ascent timing (Figure 3.13). One explanation for this lack of a response is the frequent presence of fish schools throughout the day (Figure 3.12). Chemical cues from these fish would be a common occurrence and zooplankton may cease to respond to the presence of these fish, as observed by De Robertis (2002). However, the number of schools I observed in the hour before sunset was low, ranging from one to six and only 25 days of observation were considered. Analysis of vertical migration timing and fish school presence over a longer time period may reveal behavioural responses not observed during this study.

3.4.5 Conclusions

Daytime scattering at the deep site represents the eastern extent of the deep scattering layer. This scattering layer migrates to the surface each night but seldom moves horizontally into Patricia Bay. My data do not support the hypothesis that mid-inlet zooplankton make horizontal migrations. Horizontal movements of the deep scattering layer into shallow waters typically occurred during flood tides. Although these events were infrequent, the input of pelagic zooplankton to shallow bottoms may represent an important component of benthopelagic coupling. However, in shallow waters, the vertical migration of local zooplankton represents a more regular coupling between the benthic and pelagic environments.

I observed zooplankton vertical migration in shallow waters and I conclude that the increased zooplankton density at the shallow site at night was due to emergence of benthic zooplankton. I observed this regular pattern of emergence on 41 consecutive

days of observation over two deployments. This nightly migration represents a significant increase in water column biomass relative to daytime. At the shallow site, vertical migration of zooplankton resulted in a 14-fold increase in zooplankton density at night relative to daytime. I also observed this migration pattern of emergence at the deep site where emergent zooplankton increased night-time zooplankton density.

I observed a significant difference between the migration timing and ascent depth of the deep scattering layer and benthic zooplankton. The deep scattering layer initiated ascent and descent earlier than the emergent zooplankton. The difference in vertical migration timing between pelagic and benthic zooplankton is probably due to differences in sensitivity to changes in relative light intensity. Pelagic migrators ascended into surface waters each night whereas benthic zooplankton usually remained within 30 meters of the seafloor and did not ascend into the upper 20 meters of the water column

The distribution of zooplankton in the water column influenced pelagic planktivore distribution. Specifically, the increase in zooplankton at night attracts planktivorous fish to shallow waters. Fish schools were nearly absent during daylight hours but increased in frequency during the night when vertical migrants were in the water column. Further, the distribution of zooplankton and fish schools was closely related. Both groups were near the bottom or in deep waters during the day and the ascent depth of fish schools at night was similar to the ascent depth of zooplankton. However, despite this relationship, the presence of planktivorous fish did not influence the vertical migration behaviour of zooplankton.

Chapter 4

Summary

Zooplankton distribution patterns in Saanich Inlet showed marked differences between day and night and between deep and shallow habitats (Figure 4.1). During the day, I found that inlet position was related to dissolved oxygen concentration (Chapter 2), food resources (Chapter 2), and depth (Chapters 2 & 3). Zooplankton in the mid-inlet form a deep scattering layer during the day, but are absent from shallow (62m) bottoms and from deep areas with shallow (<60m) hypoxic boundaries. Differences in night-time distribution between deep and shallow habitats were related to the vertical migration behaviour of pelagic and benthic zooplankton (Chapter 3). Pelagic zooplankton in the deep scattering layer migrated into surface waters at night whereas emergent benthic zooplankton remained at intermediate depths (Figure 4.1). At my shallow site, the movement of benthic zooplankton into the water column at night resulted in a 14-fold increase in volume backscatter over daytime values (Chapter 3).

4.1 Pelagic Zooplankton Distribution

My *a priori* expectation was that zooplankton density would be higher near the mouth than at the head of Saanich Inlet based on higher primary productivity (Timothy and Soon 2001) and phytoplankton biomass (Parsons et al. 1983; Hobson and McQuoid 2001) at the mouth. Between April 2005 and March 2006, I found that zooplankton density followed a significant headward gradient, with the highest densities near the inlet mouth (Chapter 2). With the exception of June and September, I observed the highest densities near the mouth between April and November. Although the gradient was significant over the 12 months of observation, I did not observe a persistent distribution pattern in the winter months.

The headward zooplankton density gradient was related to oxygen concentration and was also likely influenced by a summer headward primary productivity gradient (Grundle in prep). Grundle (in prep) found that primary productivity was higher near the inlet mouth relative to the head between May and August 2005. Further, in July and August, I found that integrated chlorophyll fluorescence, a proxy for phytoplankton abundance, was

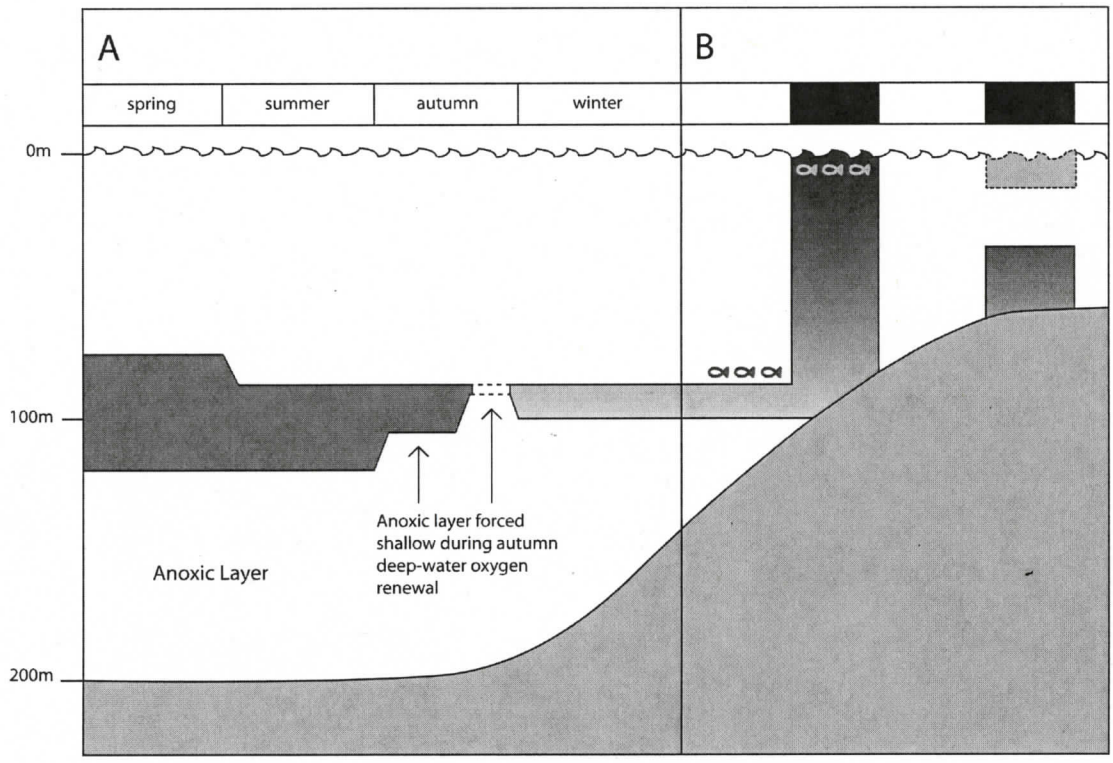

Figure 4.1. Summary of trends in the vertical distribution and density of the deep scattering layer (A) and the differences in zooplankton distribution between deep and shallow sites (B). Darker shading indicates greater zooplankton density. I observed the highest zooplankton densities in the spring and lowest in the winter (A). As the anoxic layer moved upward, the deep scattering layer became more compressed (A). The dashed line indicates the absence of zooplankton when the anoxic boundary was shallower than 90 meters depth in Squally Reach. In (B), the alternating light and dark bands at the top of the figure indicate day and night. Zooplankton migrated to the surface each night at the deep site whereas zooplankton at the shallow site remained within 30-40 meters of the seafloor and did not migrate into surface waters. The dashed surface scattering over the shallow site indicates the infrequent nighttime movement of the deep scattering layer to the shallow site. The fish symbols show the diel migration pattern of fish schools.

higher at the mouth than at the head (Chapter 2). During the summer, phytoplankton from Satellite Channel advect into the inlet (Hobson and McQuoid 2001), providing a food source for zooplankton not available at the inlet head. Advection of zooplankton over the sill from Satellite Channel also likely contributes to the higher densities I observed near the mouth. Krill are attracted to areas of high phytoplankton abundance (Price 1989) and in the Gulf of St. Lawrence, Sameoto (1976) observed that the density of euphausiid scattering layers was positively correlated with chlorophyll fluorescence. Sameoto (1976) suggested that this correlation was due to euphausiids seeking out and remaining in areas of high food concentration. These observations support my interpretation of higher food availability as a contributor to the higher zooplankton densities I observed at the mouth. This spring-summer pattern in a physically weak environment indicates a behavioural response by zooplankton to remain in an area of higher food availability. The absence of a persistent distribution pattern in winter is likely related to the absence of a primary productivity gradient (Grundle in prep), low winter primary productivity (Grundle in prep; Timothy and Soon 2001), and decreased zooplankton feeding. Between September 2005 and March 2006, within month differences between the mouth and head were low for primary productivity (Grundle in prep) and integrated chlorophyll fluorescence (Chapter 2).

In addition to food resources, inlet position was influenced by dissolved oxygen concentration. Saanich Inlet is seasonally anoxic with the depth of anoxia ranging from 83 to 167 meters between April 2005 and March 2006. In Chapter 2, I showed that the depth of the anoxic and hypoxic boundaries changed over time and that the depth of the hypoxic boundary was significantly shallower at head of the inlet compared to the mouth. The depth of these boundaries influenced zooplankton vertical migration behaviour, which affected horizontal zooplankton distribution between the mouth and head of the inlet. The lowest zooplankton densities I recorded were in Squally Reach during deep-water renewal in September and October. During these months, the anoxic boundary was shallower than 90 meters depth and the hypoxic boundary was shallower than 40 meters. The near absence of zooplankton during these months suggests that zooplankton may

actively avoid areas of shallow low oxygen. This absence from the inlet head contributed to the significant zooplankton density gradient between the mouth and head.

Zooplankton responded to shallow hypoxia by avoiding areas with limited depth refuge. In Patricia Bay, I observed very few scatterers during the day at my shallow site (62m). The depth of this shallow site is similar to the hypoxic depth in Squally Reach when zooplankton were absent. Shallow seafloor depth and 'false bottoms' caused by low oxygen seem to have the same effect on zooplankton distribution when shallower than about 60m depth.

As the areal extent and duration of hypoxia and anoxia increases in coastal areas (Diaz and Rosenberg 1995), changes in zooplankton distribution patterns will occur. Changing distributions of zooplankton caused by low oxygen will influence predator-prey interactions and can potentially change zooplankton community composition and energy flow in marine food-webs. In Gullsmarfjorden (Sweden), Spicer et al. (1999) observed that descent depth of northern krill was limited by hypoxia to about 80 meters depth. Although they did not look at interactions with predators, these krill would likely be more susceptible to predation by planktivorous fish. Limited depth refuge can increase daytime predation by planktivorous fish as the spatial overlap between predators and prey increases through compression of available habitat (Eby and Crowder 2002). In Chapter 3, I found that fish schools were most abundant during the day at depths similar to the deep scattering layer. However, the extent of foraging by planktivorous fish in the deep scattering layer is unknown. Foraging in the layer will likely be limited by the low oxygen concentrations and will be species specific.

Trophic interactions between predator and prey are also affected in hypoxic environments by the different low-oxygen tolerances of groups within the food web (Breitburg et al. 1997). For example, Decker et al. (2004) found that predation pressure by the ctenophore *Mnemiopsis leidyi* increased in hypoxic conditions. This increase was due to low oxygen-related changes in predator avoidance behaviour in its copepod prey and to reduced competition by planktivorous fish. Access to prey in hypoxic waters by

planktivorous fish is limited by their much higher oxygen demand (Breitburg et al. 2003). Pelagic communities could become dominated by invertebrate predators as the duration of low oxygen increases, altering energy pathways within low oxygen systems (Decker et al. 2004).

Although bottom waters in Saanich Inlet are anoxic for much of the year, only the amphipod *Orchomene obtusus*, has developed the ability to survive for extended periods in anoxia (Liu 1989; De Robertis et al. 2001). Heath (1977) speculated that euphausiids in Saanich Inlet were resident, but they have not developed low oxygen tolerance (Hoos 1970). In contrast, Childress and Seibel (1998) found that zooplankton living in oxygen minimum zones in the open ocean have evolved efficient adaptations (e.g. larger gill surfaces) to extract oxygen from water, allowing them to live within the oxygen minimum zone. The lack of low oxygen tolerance in Saanich Inlet euphausiids indicates that there is sufficient mixing with outside populations from well-oxygenated environments to limit development of low oxygen tolerance. In other hypoxic environments, krill can rely on anaerobic metabolism to survive temporary day-depth exposure to hypoxia (Spicer et al. 1999), but the anaerobic capability of *Euphausia pacifica* is unknown.

In Chapter 3, I found that night-time movements of the deep scattering layer into the shallower waters of Patricia Bay were infrequent. These horizontal movements were likely not the result of horizontal migrations as 75% were associated with flood tides, indicating advection of the zooplankton layer in the bay. The absence of zooplankton in surface waters over shallow depths suggests that phytoplankton biomass could be lower than in the mid-inlet. This relationship has not been tested, but I assume that food levels in the mid-inlet adjacent to Patricia Bay are higher than in the bay due to tidal advection of phytoplankton into the inlet (Hobson and McQuoid 2001) and high mid-inlet primary productivity near the mouth (Timothy and Soon 2001). Phytoplankton biomass in the mid-inlet could be sufficiently high that intraspecific competition for food is low, reducing the pressure for regular horizontal migrations.

4.2 Benthic Zooplankton

This study represents the first documented observation of benthic zooplankton behaviour in Saanich Inlet and highlights the continuous zooplankton monitoring capabilities of acoustic instruments and the VENUS observatory. Acoustic observations in the San Juan Islands of mysid emergence and vertical migration (Kringel et al. 2003) suggest that benthic emergence is a potentially widespread phenomenon in shallow coastal waters. Daily emergence of benthic zooplankton into the water column provides an important link between the benthic and pelagic environments and emerging zooplankton likely provide food for the abundant benthic planktivores I observed in Patricia Bay.

Emergence of benthic zooplankton can be initiated when oxygen concentrations within sediments reach critical levels (Thistle 2003) and animals are forced upwards to oxygenated depths in the water column. During oxygen renewal events in Saanich Inlet, the anoxic layer can move upwards as shallow as 83 meters (Chapter 2). The intrusion of anoxic or severely hypoxic water into shallow depths can have a negative impact on benthic zooplankton. Under these conditions, benthic zooplankton would likely experience high mortality through either suffocation or increased predation as they are forced to spend more time in the water column. The VENUS observatory is ideally positioned to study the response of benthic zooplankton to changing oxygen concentrations. Over the long term, it should be possible to observe how changing oxygen conditions influence zooplankton migration patterns and to correlate migration timing and depth with changes in oxygen concentration.

At the deep site in Patricia Bay, zooplankton were distributed throughout the water column with both pelagic and emergent benthic zooplankton contributing to night biomass. The highest concentrations were typically near the surface following the migration of the dense euphausiid layer. In contrast to the deep scattering layer, zooplankton at a shallow site remained within 30-40 meters of the seafloor at night and did not migrate into surface waters (Chapter 3). The vertical migration of zooplankton at the shallow site resulted in a 14-fold increase in volume backscattering at night.

The significant difference I observed in migration timing between pelagic and benthic zooplankton indicates that each group has different sensitivities to changes in relative light intensity. The deep scattering layer always initiated vertical migration earlier than the benthic zooplankton. During the first two weeks of April, ascent timing became earlier and more variable for both pelagic and benthic zooplankton and this change coincided with an unidentified band of scattering at the deep site in Patricia Bay. I interpreted this band as increased turbidity that affected zooplankton migration behaviour. How zooplankton respond to episodic events could have implications for modeling biological mixing in the aphotic zone (Dewar et al. 2006) and for understanding the magnitude of biologically mediated nutrient transport into the euphotic zone (Huntley and Zhou 2004).

4.3 Future Research

My observations of pelagic zooplankton response to changing oxygen levels and benthic emergence in shallow waters raise several new questions. The deep scattering layer at the inlet head was consistently in lower oxygen concentrations during the day than at the mouth. Zooplankton within the deep scattering layer have different tolerances for low oxygen (Hoos 1970). Does the deep scattering layer zooplankton community have a different species composition at the inlet head compared to the mouth? The same question can also apply to planktivores. Gelatinous planktivores have a greater low oxygen tolerance than many pelagic planktivorous fish. Are there more gelatinous planktivores near the head of the inlet where oxygen concentrations are typically lower? Hamner et al. (1994) observed that the density of the scyphomedusa *Aurelia aurita* increased at the head of the inlet in September.

In Squally Reach, the base of the deep scattering layer was almost always in severely hypoxic water. If euphausiids are abundant at the inlet head, this would indicate that euphausiids are either more tolerant of low oxygen than suggested by Hoos (1970) or that they have some capacity for anaerobic respiration while in hypoxic waters. Laboratory and field experiments similar to those conducted by Spicer et al. (1999) could be conducted to determine if Saanich Inlet euphausiids are capable of anaerobic metabolism.

Lastly, sampling should be conducted to determine the identity of the emergent scatterers at the shallow site. Seasonal night acoustic transects would determine whether this pattern of emergence occurs year-round and concurrent net sampling of the scatterers should be conducted to determine if there is a seasonal shift in emergent benthic zooplankton community composition.

Appendix 1
Acoustic Theory

A1.1 Introduction

Following the sinking of the Titanic and during World War I, echo-ranging instruments were designed to detect objects such as icebergs and submarines located within the water column (Beamish 1971). The first experiment to demonstrate that fish could alter acoustic beams was conducted by Kimura (1929). Using a 200 kHz frequency sound source, modulated at 1 kHz so that it was audible, and a separate receiver, Kimura observed that received sound was noticeably disturbed when fish were in the acoustic beam. Sund (1935) made the first recordings of echoes from schools of spawning cod in a Norwegian fjord using a 16 kHz transducer. Through his observations on the distribution of schools and their characteristics, Sund recognized the potential for echosounders as useful tools in fisheries research.

Echosounders were first used to detect zooplankton during early investigations into the origin of deep scattering layers. The first documented observation of a deep scattering layer was in 1942 off the coast of California. Eyring et al. (1948) observed a sound scattering layer at a depth much shallower (300 yards) than the known depth of the ocean bottom (1300 yards) using echo ranging instruments. The origins of this 'phantom bottom' (Lyman 1948) were unknown but observations in 1945 of diel vertical migration (DVM) of the deep scattering layer towards surface waters at sunset followed by a return to deep waters at sunrise suggested a biological origin (Johnson 1948). Based on the known DVM behaviour of marine zooplankton (Russell 1928) and the capture of various planktonic organisms during net tows through deep scattering layers, Johnson (1948) speculated that the deep scattering layer was created by plankton and associated nekton.

Following World War II, echosounders became an essential tool for commercial fishers and fisheries scientists (Misund 1997) to locate fish schools and zooplankton. Coupled with environmental observations, acoustic methods allow for direct observation of predator-prey interactions, spatial and temporal distribution patterns, and other ecosystem

processes (Bertrand et al. 2003). Recent applications of acoustics include scanning sonar observations of fin whales feeding on herring schools (Nøttestad et al. 2002), multi-frequency detection and analysis of planktivore and zooplankton distributions (Swartzman et al. 2002), and three-dimensional visualization of zooplankton patches (Greene et al. 1998).

The following sections provide background on how acoustic sampling is used to study the distribution and abundance of biological organisms in a body of water using a single-beam echosounder.

A1.2 Sound

Sound is a result of mechanical vibrations that set up periodic oscillations in pressure, particle displacement, and particle velocity in an elastic medium (Albers 1965; Johannesson and Mitson 1983). Sound is transmitted through water as sinusoidal pressure waves caused by the periodic compression and rarefaction of water molecules that create areas of high and low pressure, respectively (MacLennan and Simmonds 1992; Figure A1.1). In a plane wave, typical of sound waves in water (Tucker and Gazey 1966), the instantaneous pressure, p, changes in the direction of wave propagation and varies as $\sin(\omega t)$, where ω is the angular frequency in radians per unit time. Planes where p is maximal are wavefronts, and the distance between successive wavefronts is the acoustic wavelength, λ (Figure A1.1). Wavelength is related to frequency, f, by:

$$\lambda = c/f$$

where c is the speed of sound in water (m s^{-1}), and frequency is cycles (or λ) per second or Hertz (Hz). For example, assuming c = 1480 m s^{-1}, the wavelengths for 38kHz and 200kHz sound are 38.9mm and 7.4mm, respectively. The acoustic wavelength has implications for target detection. The smaller the wavelength, the smaller the object that can be effectively detected. Typical frequencies used for bioacoustics are 38, 50, 120, and 200kHz (Misund 1997).

Another component of sound waves is the particle displacement and particle velocity that occurs as a pressure wave passes through the medium. Individual particles move only a short distance with the changing pressure of a propagating wave. The movement of individual particles or water molecules also follows a sine wave pattern for plane waves. The particle movement and the pressure wave are in phase and are related by:

$$p_{max} = \rho c v$$

where p_{max} is the maximum pressure of the propagating wave or the pressure of the wavefront, ρ is the density of sea water, and v is the particle velocity. The pressure of a travelling wave is dependent on the water density, speed of sound, and particle velocity; pressure is independent of the acoustic frequency (MacLennan and Simmonds 1992).

As the wave propagates, energy is transferred in the direction of travel. This energy flux is defined as the energy of the waves passing through a unit area normal to the direction of propagation. The acoustic intensity, I, is the energy flux per unit time and is related to pressure by:

$$I = p^2/\rho c.$$

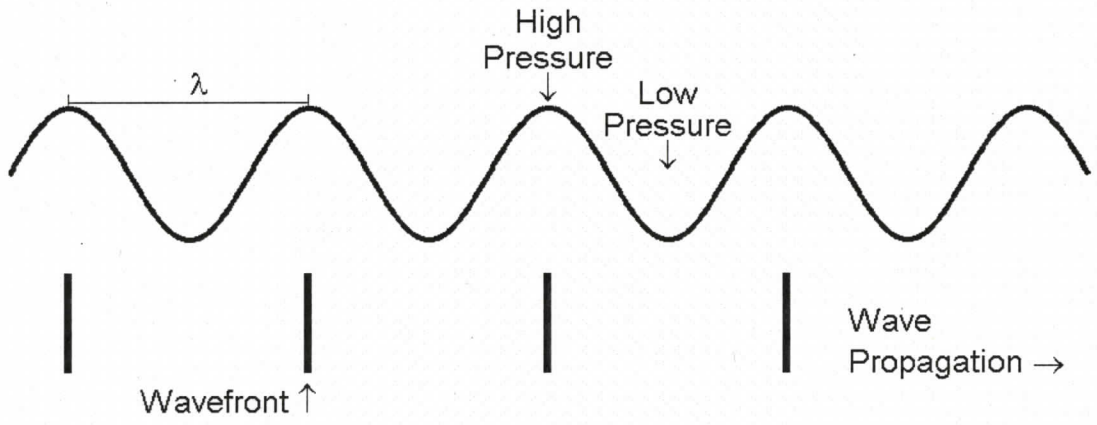

Figure A1.1. Schematic representation of an acoustic sine wave, showing regions of high and low pressure, position of wavefronts, and the direction of wave propagation.

A1.3 Sound Measurement

Sound measurements typically span several orders of magnitude, and because of this large dynamic range, sound levels are usually described by decibels (dB) rather than the SI units for intensity (watt m^{-2}) or pressure (Newton m^{-2}; Pascal). Through continuous use, the decibel has been adopted as the standard measure in fisheries acoustics (MacLennan and Simmonds 1992). The decibel is a logarithmic ratio of two intensities, expressed as:

$$IL_{dB} = 10 \log (I_{obs}/I_{ref})$$

where IL_{dB} is the intensity level or strength of the measured sound in decibels, I_{obs} is the observed or measured intensity, and I_{ref} is a reference intensity (Johannesson and Mitson 1983). Large differences between I_{obs} and I_{ref} can be described by a small range of decibels. For example, a change of 30 dB indicates a 1000 times difference between the two intensities.

Another measure of sound level is the sound pressure level (SPL). SPL is the common measure in underwater acoustics as the instruments detecting echoes measure pressure changes. When a transducer receives an echo or pressure wave, the pressure is converted into a proportional voltage *(V)*. Acoustic intensity is proportional to the square of the voltage or pressure, such that:

$$p \propto V;\ I \propto V^2;\ \text{and}\ I \propto p^2$$

It follows that:

$$\begin{aligned} SPL_{dB} &= 10 \log (V_{obs}/V_{ref})^2 \\ &= 20 \log (V_{obs}/V_{ref}) \\ &= 20 \log (p_{obs}/p_{ref}). \end{aligned}$$

The same relationship applies to echosounders where analogue voltages are converted into digital counts (*C;* ASL Environmental Sciences 2004). The acoustic counts are proportional to the voltage, and:

$$SPL_{dB} = 20 \log (C_{obs}/C_{ref}).$$

A reference pressure of 1 μPa is typically used for sound measurements in water. Without mention of the reference pressure, a dB value for an absolute quantity (e.g. source level) is a meaningless value. SPLs are described relative to this reference pressure, such that a signal of 20 dB would be shown as 20 dB relative to 1 μPa.

A1.4 Sound Transmission

Sound waves are generated by mechanical displacement of a portion of the medium about an equilibrium position. In most modern active acoustic systems, sound waves are generated, transmitted, and received by a single transducer. Most transducers used in bioacoustics are made with piezo-electric ceramics. When a voltage is applied to a piezo-electric ceramic, the ceramic expands and contracts at the transducer frequency, radiating sound waves. This process is reversible such that returning pressure waves (echoes) vibrate the ceramic generating an oscillating voltage that is amplified and recorded by the echosounder (MacLennan and Simmonds 1992).

Sound generated by echosounders is generated as discrete pulses or pings rather than as continuous waves. A sound pulse is generated at the operating frequency, and the number of cycles (λ) within the pulse is dependent on the pulse duration (τ):

$$\text{cycles} = \tau f.$$

For example, a 300μs pulse at 38kHz and 200kHz would consist of 11 and 60 cycles, respectively. Because each pulse consists of a number of wavelengths or cycles of a specific length, the physical length (L) of a pulse is determined by:

$$L = \tau c.$$

Assuming τ = 300μs and c = 1480 m s^{-1}, the length of this pulse would be 0.44 meters. The pulse length (L) determines the vertical resolution of an echosounder, where the minimum distance to resolve two objects as separate targets is $L/2$ (Johannesson and Mitson 1983). Short pulses have the greatest vertical resolution but the power or ability

to detect targets with a short pulse is limited. Longer pulses have reduced vertical resolution but will have a greater chance of detecting targets. Pulse durations used for this project were 300μs and 600μs at 200kHz.

A1.4.1 Far-Field

Parallel wave fronts from successive acoustic pulses are not fully formed for a distance from the transducer that is dependent on the acoustic frequency. Where acoustic waves are fully formed is referred to as the far-field. The distance of the far-field from a transducer can be estimated as:

$$R_f = a^2/\lambda$$

where R_f is the distance (m) of the far-field from the transducer, a is the transducer diameter (m), and λ is the acoustic wavelength (m). The estimated far-field for a 200kHz transducer with a 7.5cm diameter is $R_f = 0.075^2/0.0074 = 0.76$m. When far-field conditions are assumed, echoes received from the near-field, that is, from $R < 2R_f$ are ignored.

A1.5 Beam Pattern and Width

The beam or directivity pattern of a transducer represents the sensitivity of a transducer as a function of spatial angle and is the same for both transmission and reception of sound (Figure A1.2; MacLennan and Simmonds 1992). The beam pattern is also a function of transducer shape and operating frequency. Transducers can be designed to radiate sound in many different patterns, from omni-directional point-sources to narrow focused beams. The beam pattern results from the constructive and destructive interference effects of overlapping sine waves.

Transducers typically consist of several piezo-electric elements arranged to maximize the acoustic energy along a main acoustic axis (Figure A1.2). For circular transducers, elements are usually arranged in a concentric circle around a central element to focus the waves into a narrow conical beam. The acoustic axis ($\theta = 0°$) is the region of maximum

intensity (and sensitivity) and is perpendicular to the transducer face. The acoustic intensity decreases as the angle from this axis increases until the first null (zero intensity) is reached. This first null defines the boundary of the main lobe (Figure A1.2). As the angle from the acoustic axis continues to increase, side-lobes of decreasing intensity, separated by nulls, appear. Echoes are interpreted as coming from the main lobe of the beam pattern so the inclusion of side-lobe echoes can result in errors during analysis of the acoustic signals. Transducers are designed to minimize the number and intensity of side lobes, and for most transducers, more than 99% of transmitted energy is in the main lobe (MacLennan and Simmonds 1992).

The beam width of a transducer is defined as the angle from the acoustic axis where the acoustic intensity is half the intensity of the main axis. The 'half-power' point is ±3 dB of the intensity of the main axis (Figure A1.2). Beam width also depends on the size of the transducer, with larger transducers generating narrower beam widths (MacLennan and Simmonds 1992). The circular transducer used in this thesis had a nominal beam width of 8°.

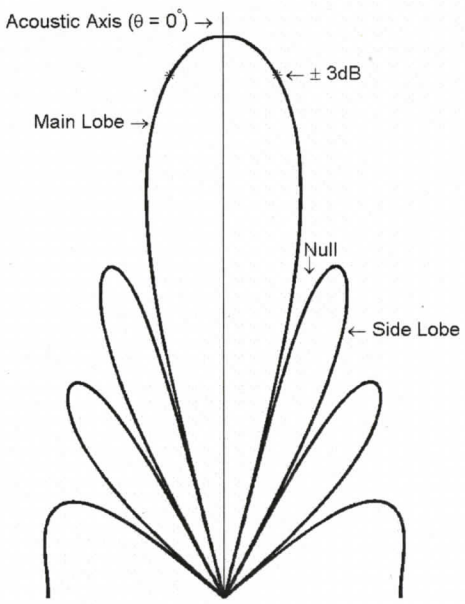

Figure A1.2. Typical beam pattern for a circular transducer.

A1.6 Propagation Losses

A1.6.1 Beam Spreading

An acoustic wavé in a conical beam radiating away from a transducer spreads over an increasing spherical area as the distance from the transducer increases. The total energy in an acoustic wave is finite, so as the wave front spreads over a greater unit area, the intensity of the wave per unit area decreases (MacLennan and Simmonds 1992). When the distance from the transducer, R, is large relative to the diameter of the transducer (i.e. far-field), the intensity decreases as a function of the inverse square of the distance, such that:

$$I_R = I_0/R^2$$

where I_R is the intensity of the acoustic wave at a distance from the transducer and I_0 is the initial intensity of the acoustic wave at one meter from the transducer.

A1.6.2 Absorption

Particle displacement caused by propagating sound waves generates heat as molecules are oscillated, and this energy is lost by the travelling wave to the fluid medium (Albers 1965). The rate (dB m^{-1}) of absorption is determined primarily by the acoustic frequency, with high frequencies (e.g. 200kHz) losing energy more rapidly than low frequencies (e.g. 38kHz). Depth, temperature, and salinity also contribute to absorption losses (MacLennan and Simmonds 1992). In seawater, the most significant chemical contributions to sound absorption come from magnesium sulphate ($MgSO_4$) and boric acid (Francois and Garrison 1982). The calculation of total absorption (α) is summarized by Francois and Garrison (1982) as:

α = boric acid contribution + $MgSO_4$ contribution + pure water contribution.

Average absorption loss between 10 and 130 meters for each transect was calculated using the Francois and Garrison equation for each transect (Table A1.1).

Table A1.1. Mean absorption loss (α) and sound speed (c) values between 10 and 130 meters for each mid-inlet acoustic transect between April 2005 and March 2006.

Month	**α (dB m^{-1})**	**c (m s^{-1})**
April 2005	0.047	1481
May	0.047	1482
June	0.048	1484
July	0.049	1486
August	0.049	1486
September	0.050	1487
October	0.050	1486
November	0.049	1485
December	0.048	1484
January	0.047	1482
February	0.046	1480
March 2006	0.046	1480

A1.7 Sound Speed

Depth or range measurements from an echosounder are based on the time interval, t, for an initial sound pulse to return as an echo, where range = $t/2$. The time interval is directly dependent on the speed of sound. Sound speed in seawater is affected by temperature, salinity, and depth, and typically varies between 1450 to 1550 m s^{-1} (MacLennan and Simmonds 1992). A typical value for British Columbia coastal water is 1480 m s^{-1}. Sound speed can be accurately calculated using the equation of Mackenzie (1981):

$$c = 1448.96 + 4.591T - 0.05304T^2 + 2.374\text{x}10^{-4}T^3 + 1.34(S-35) + 0.0163D$$
$$+ 1.675\text{x}10^{-7}D^2 - 0.01025T(S-35) - 7.139\text{x}10^{-13}TD^3$$

where T is temperature (°C), S is salinity (ppt), and D is depth (m). Sound speed averaged between 10 and 130 meters was calculated using the Mackenzie equation for each transect in this thesis (Table A1.1).

A1.8 Acoustic Scattering

Acoustic scattering occurs when a sound wave encounters an object with a different acoustic impedance (Z) than the surrounding water, where $Z = \rho c$ (Medwin 2005). When an acoustic wave encounters a small target, some of the incident energy is scattered in all directions as secondary waves that propagate away from the object. The proportion of the incident energy that is scattered is determined by the reflection coefficient (r) (Tucker and Gazey 1966):

$$r = (Z_t - Z_w)/(Z_t + Z_w)$$

where Z_t and Z_w are the acoustic impedances of the target and water, respectively. Large differences in Z across a boundary will result in stronger scattering. The portion of the scattered energy that is detected as an echo by a transducer is referred to as backscatter (MacLennan and Simmonds 1992).

The ability of a target to backscatter sound can be described by the backscattering cross-section, σ_{bs} (Clay and Medwin 1977). The backscatter cross-section has units of area per volume ($m^2\ m^{-3}$) and can be calculated in terms of intensity or pressure as:

$$\sigma_{bs} = R^2(I_{bs}/I_i), \text{ or}$$
$$\sigma_{bs} = R^2(p_{bs}/p_i)^2$$

where R is the range from the transducer (m), I_{bs} and p_{bs} are the backscattered intensity and pressure, and I_i and p_i are the incident intensity and pressure at the target.

The logarithmic (dB) measure of backscattered energy is the target strength (MacLennan et al. 2002):

$$TS = 10 \log (\sigma_{bs}).$$

When multiple targets are insonified by a sound pulse, the volume scattering strength (S_v) and the volume scattering coefficient (s_v) are used to describe the level of the received echo (Medwin 2005). If many different targets (e.g. zooplankton) contribute to the received energy (E) from a pulse, and the targets are randomly distributed within the

beam cross-section, then E is proportional to the density of targets, in numbers per unit area (MacLennan and Simmonds 1992). The acoustic echo from an aggregation or volume of acoustic scatterers is the sum of their individual echoes (Foote 1983). The volume backscattering coefficient is calculated as:

$$s_v = \Sigma\sigma_{bs}/V, \text{ or}$$

$$s_v = N_t \cdot \sigma_{bs}$$

where V is the volume (m^3) insonified, and N_t is the number of targets in the volume. S_v is the logarithmic equivalent of s_v and is calculated as:

$$S_v = 10 \log (s_v)$$

where the units of S_v are dB m^{-3}. If the average backscatter cross-section and S_v are known for a volume of targets (e.g. euphausiids), then the density of targets (N m^{-3}) can be calculated:

$$N = 10^{Sv/10}/\sigma_{bs}.$$

If different species contribute to S_v and the relative abundance of each species is known from net tows, then the proportion of the acoustic signal from each species can be determined and the density of each species can be calculated.

A1.9 SONAR Equation

The SONAR equation can be used to convert the voltage or counts output from the echosounder into S_v (Clay and Medwin 1977). This equation corrects echosounder output for acoustic calibration, transmission losses, time-varied gain, and the directional sensitivity of the transducer (Greenlaw 1979).

For S_v, the SONAR equation takes the form:

$$S_v = 20 \log (C) - G_{TVG} - RS - SL + 20 \log R + 2\alpha R - 10 \log (c\tau\psi/2) - 20 \log K$$

where,

C = acoustic count
G_{TVG} = time varied gain (dB)
RS = receive sensitivity (dB re 1 μPa at 1m)

SL = source level (dB re 1 μPa at 1m)
R = range from the transducer (m)
α = absorption coefficient (dB m^{-1})
c = speed of sound in seawater (m s^{-1})
τ = pulse length (s)
ψ = equivalent beam angle (steradians)
K = calibration constant (dB).

Acoustic counts are the digital output (after 8-bit A/D conversion) from the echosounder. The source level, received sensitivity, calibration constant, and equivalent beam angle are specific and constant for each transducer (Table A1.2). The equivalent beam angle or integrated beam pattern, ψ, is the solid angle of an ideal conical beam equivalent to the integral of the actual beam pattern (Medwin 2005) and is used to describe the volume effectively insonified by the transducer (MacLennan and Simmonds 1992). The pulse length is set by the user (either 300μs or 600μs for this project) and c and α are determined by environmental conditions. The 20 log R term is the signal loss due to beam spreading from the transducer to the target and $2\alpha R$ is the combined absorption loss of the incident and reflected waves.

Table A1.2. Transducer constants for ASL Water Column Profiler®, s/n 1006.

Parameter	**Value**
Source Level	213.5 dB re 1 μPa at 1m
Receive Sensitivity	-191 dB re 1 μPa at 1m
Equivalent Beam Angle (ψ)	0.01531 steradians
Calibration Constant	144.25

References

Abraham, C.L. and W.J. Sydeman. 2006. Prey-switching by Cassin's auklet *Ptychoramphus aleuticus* reveals seasonal climate-related cycles of *Euphausia pacifica* and *Thysanoessa spinifera*. Marine Ecology Progress Series, 313: 271-283.

Albers, V.M. 1965. Underwater Acoustics Handbook II. Pennsylvania State University Press, University Park, Pennsylvania, 356p.

Alldredge, A.L. and J.M. King. 1985. The distance demersal zooplankton migrate above the benthos: implications for predation. Marine Biology, 84: 253-260.

Anderson, J.J. and A.H. Devol. 1973. Deep water renewal in Saanich Inlet, an intermittently anoxic basin. Estuarine and Coastal Marine Science, 1: 1-10.

ASL Environmental Sciences. 2004. Water Column Profiler: Operators Manual for Model VENUS Version. Sidney, BC, 38p.

Bary, B.M., W.E. Barraclough, and R. Herlinveaux. 1962. Scattering of underwater sound in Saanich Inlet, British Columbia. Nature, 194: 36-37.

Bary, B.M. 1966. Qualitative observations of scattering of 12 kc/s sound in Saanich Inlet, British Columbia. Deep Sea Research, 13: 667-677.

Bary, B.M. and R.E. Pieper. 1970. Sonic-scattering studies in Saanich Inlet, British Columbia: a preliminary report. In: *Proceedings of an International Symposium on Biological Sound Scattering in the Ocean,* G. B. Farquhar (Ed.). US Naval Oceanographic Office, Warrenton, Virginia, pg 601-609.

Batty, R.S., J.H.S. Blaxter, and J.M. Richard. 1990. Light intensity and the feeding behaviour of herring, Clupea harengus. Marine Biology, 107: 383-388.

BC Environment. 1996. Saanich Inlet Study, Synthesis Report: Technical Version. Ministry of Environment, Lands, and Parks, Victoria, BC.

Beamish, P.C. 1971. Quantitative measurements of acoustic scattering from zooplanktonic organisms. Deep Sea Research, 18: 811-822.

Benoit-Bird, K.J. and W.W.L. Au. 2004. Diel migration dynamics of an island-associated sound-scattering layer. Deep Sea Research I, 51: 707-719.

Bertrand, A., E. Josse, P. Bach, and L. Dagorn. 2003. Acoustics for ecosystem research: lessons and perspectives from a scientific programme focusing on tuna-environment relationships. Aquatic Living Resources, 16: 197-203.

Blaxter, J.H.S. and F.G.T. Holliday. 1963. The behaviour and physiology of herring and other clupeids. Advances in Marine Biology, 1: 262-393.

Boden, B.P. and E.M. Kampa. 1965. An aspect of euphausiid ecology revealed by echo-sounding in a fjord. Crustaceana, 9: 155-173.

Bollens, S.M. and B.W. Frost. 1989. Zooplanktivorous fish and variable diel vertical migration in the marine planktonic copepod *Calanus pacificus*. Limnology and Oceanography, 34(6): 1072-1083.

Bollens, S.M., B.W. Frost, and T.S. Lin. 1992. Recruitment, growth, and diel vertical migration of *Euphausia pacifica* in a temperate fjord. Marine Biology, 114: 219-228.

Breitburg, D.L., T. Loher, C.A. Pacey, and A. Gerstein. 1997. Varying effects of low dissolved oxygen on trophic interactions in an estuarine food web. Ecological Monographs, 67(4): 489-507.

Breitburg, D.L., A Adamack, K.A. Rose, S.E. Kolesar, M.B. Decker, J.E. Purcell, J.E. Keister, and J.H. Cowan Jr. 2003. The pattern and influence of low dissolved oxygen in the Patuxent River, a seasonally hypoxic estuary. Estuaries, 26: 280-297.

Brodeur, R.D. and M.T. Wilson. 1996. Mesoscale acoustic patterns of juvenile walleye pollock (*Theragra chalcogramma*) in the western Gulf of Alaska. Canadian Journal of Fisheries and Aquatic Sciences, 53: 1951-1963.

Childress, J.J. and B.A. Seibel. 1998. Life at stable low oxygen levels: adaptations of animals to oceanic oxygen minimum layers. Journal of Experimental Biology, 201: 1223-1232.

Clay, C.S. and H. Medwin. 1977. Acoustical Oceanography: principles and applications. John Wiley and Sons, New York, 544p.

Croll, D.A., B.R. Tershy, R.P. Hewitt, D.A. Demer, P.C. Fiedler, S.E. Smith, W. Armstrong, J.M. Popp, T. Kiekhefer, V.R. Lopez, J. Urban, and D. Gendron. 1998. An integrated approach to the foraging ecology of marine birds and mammals. Deep Sea Research II, 45: 1353-1371.

Decker, M.B., D.L. Breitburg, and N.H. Marcus. 2003. Geographical differences in behavioral responses to hypoxia: local adaptation to an anthropogenic stressor? Ecological Applications, 13(4): 1104-1109.

Decker, M.B., D.L Breitburg, and J.E. Purcell. 2004. Effects of low dissolved oxygen on zooplankton predation by the ctenophore *Mnemiopsis leidyi*. Marine Ecology Progress Series, 280: 163-172.

De Robertis, A., J.S. Jaffe, and M.D. Ohman. 2000. Size-dependent visual predation risk and the timing of vertical migration in zooplankton. Limnology and Oceanography, 45(8): 1838-1844.

De Robertis, A. 2001. Validation of echo counting for studies of zooplankton behavior. ICES Journal of Marine Science, 58: 543-561.

De Robertis, A., K. Eiane, and G.H. Rau. 2001. Eat and run: anoxic feeding and subsequent aerobic recovery by Orchomene obtusus in Saanich Inlet, British Columbia, Canada. Marine Ecology Progress Series, 219: 221-227.

De Robertis, A. 2002. Small-scale spatial distribution of the euphausiid *Euphausia pacifica* and overlap with planktivorous fishes. Journal of Plankton Research, 24(11): 1207-1220.

De Robertis, A., C. Schell, and J.S. Jaffe. 2003. Acoustic observations of the swimming behavior of the euphausiid *Euphausia pacifica* Hansen. ICES Journal of Marine Science, 60: 885-898.

Devol, A.H. 1981. Vertical distribution of zooplankton respiration in relation to the intense oxygen minimum zones in two British Columbia fjords. Journal of Plankton Research, 3(4): 593-602.

Dewar, W.K., R.J. Bingham, R.L. Iverson, D.P. Nowacek, L.C. St. Laurent, and P.H. Wiebe. 2006. Does the marine biosphere mix the ocean? Journal of Marine Research, 64: 541-561.

Diaz, R.J. and R. Rosenberg. 1995. Marine benthic hypoxia: a review of its ecological effects and the behavioural responses of benthic macrofauna. Oceanography and Marine Biology: An Annual Review, 33: 245-303.

Eby, L.A. and L.B Crowder. 2002. Hypoxia-based habitat compression in the Neuse River estuary: context-dependent shifts in behavioral avoidance thresholds. Canadian Journal of Fisheries and Aquatic Sciences, 59: 952-965.

Environment Canada. [cited 2007 Jan 15]. Daily Data [Internet]. Available from: http://www.climate.weatheroffice.ec.gc.ca/climateData/dailydata_e.html?timeframe=1&Prov=XX&StationID=118&Year=2006&Month=3&Day=1

Eyring, C.F., R.J. Christensen, and R.W. Raitt. 1948. Reverberation in the sea. Journal of the Acoustical Society of America, 20(4): 462-475.

Foote, K.G. 1983. Linearity of fisheries acoustics, with additional theorems. Journal of the Acoustical Society of America, 73(6): 1932-1940.

Francois, R.E. and G.R. Garrison. 1982. Sound absorption based on ocean measurements. Part II: Boric acid contribution and equation for total absorption. Journal of the Acoustical Society of America, 72(6): 1879-1890.

Gargett, A.E., D. Stucchi, and F. Whitney. 2003. Physical processes associated with high primary production in Saanich Inlet, British Columbia. Estuarine, Coastal, and Shelf Science, 56: 1141-1156.

Gauthier, S. and J.K. Horne. 2004. Acoustic characteristics of forage fish species in the Gulf of Alaska and Bering Sea based on Kirchhoff-approximation models. Canadian Journal of Fisheries and Aquatic Sciences, 61: 1839-1850.

Genin, A. 2004. Bio-physical coupling in the formation of zooplankton and fish aggregations over abrupt topographies. Journal of Marine Systems, 50: 3-20.

Greene, C.H., P.H. Wiebe, C. Pelkie, M.C. Benfield, and J.M. Popp. 1998. Three-dimensional acoustic visualization of zooplankton patchiness. Deep Sea Research II, 45: 1201-1217.

Greenlaw, C.F. 1979. Acoustical estimation of zooplankton populations. Limnology and Oceanography, 24(2): 226-242.

Grundle, D.S. In Prep. Temporal variations in primary productivity, phytoplankton assemblages, and nutrient dynamics in Saanich Inlet, a British Columbia fjord. MSc Thesis, University of Victoria.

Hamner, W.H. and I.R. Hauri. 1981. Long-distance horizontal migrations of zooplankton (Scyphomedusae: *Mastigias*). Limnology and Oceanography, 26(3): 414-423.

Hamner, W.H., R.W. Gilmer, and P.P. Hamner. 1982. The physical, chemical, and biological characteristics of a stratified, saline, sulfide lake in Palau. Limnology and Oceanography, 27(5): 896-909.

Hamner, W.M., P.P. Hamner, and S.W. Strand. 1994. Sun-compass migration by *Aurelia aurita* (Scyphozoa): population retention and reproduction in Saanich Inlet, British Columbia. Marine Biology, 119: 347-356.

Haury, L.R., J.A. McGowan, and P.H. Wiebe. 1978. Patterns and processes in the time-space scales of plankton distribution. In: J.H. Steele (ed.), Spatial Patterns in Plankton Communities, Plenum Press, New York, pg 277-327.

Hay, D.E., J.R. Brett, E. Bilinski, D.T. Smith, E.M. Donaldson, G.A. Hunter, and A.V. Solmie. 1988. Experimental impoundments of prespawning Pacific herring (*Clupea harengus pallasi*): effect of feeding and density on maturation, growth, and proximate analysis. Canadian Journal of Fisheries and Aquatic Sciences, 45: 388-398.

Hay, D.E. and S.M. McKinnell. 2002. Tagging along: association among individual Pacific herring (*Clupea pallasi*) revealed by tagging. Canadian Journal of Fisheries and Aquatic Sciences, 59: 1960-1968.

Heath, W.A. 1977. The ecology and harvesting of euphausiids in the Strait of Georgia. PhD Thesis, University of British Columbia.

Herlinveaux, R.H. 1962. Oceanography of Saanich Inlet in Vancouver Island, British Columbia. Journal of the Fisheries Research Board of Canada, 19: 1-37.

Hobson, L.A. 1983. Phytoplankton crops, bacterial metabolism and oxygen in Saanich inlet, a fjord in Vancouver Island, British Columbia. Sedimentary Geology, 36: 117-130.

Hobson, L.A. and M.R. McQuoid. 2001. Pelagic diatom assemblages are good indicators of mixed water intrusions into Saanich Inlet, a stratified fjord in Vancouver Island. Marine Geology, 174: 125-138.

Hollander, M. and D.A. Wolfe. 1999. Nonparametric Statistical Methods, 2nd edition. John Wiley and Sons, New York. 787p.

Holohan, B.A., E.G. Klos, and C.A. Oviatt. 1998. Population density, prey selection, and predator avoidance of the burrowing anemone (*Ceriantheopsis americanus*) in Narragansett Bay, Rhode Island. Estuaries, 21(3): 466-469.

Hoos, R. 1970. Distribution and physiology of zooplankton in an oxygen minimum layer. MSc Thesis, University of Victoria.

Horne, J.K. and C.S. Clay. 1998. Sonar systems and aquatic organisms: matching equipment and model parameters. Canadian Journal of Fisheries and Aquatic Sciences, 55: 1296-1306.

Huntley, M.E. and M. Zhou. 2004. Influence of animals on turbulence in the sea. Marine Ecology Progress Series, 273: 65-79.

Ingram, C.L. and R.R. Hessler. 1983. Distribution and behavior of scavenging amphipods. Deep Sea Research, 30: 243-249.

Jaffe, J.S., M.D. Ohman, and A. De Robertis. 1999. Sonar estimates of daytime activity levels of *Euphausia pacifica* in Saanich Inlet. Canadian Journal of Fisheries and Aquatic Sciences, 56: 2000-2010.

Johannesson, K.A. and R. B. Mitson. 1983. Fisheries Acoustics. A practical manual for aquatic biomass estimation. FAO Fisheries Technical Paper (240), 249p.

Johnson, M.W. 1948. Sound as a tool in marine ecology, from data on biological noises and the deep scattering layer. Journal of Marine Research. 7: 443-458.

Keister, J.E., E.D. Houde, and D.L. Breitburg. 2000. Effects of bottom-water hypoxia on abundances and depth distributions of organisms in Patuxent River, Chesapeake Bay. Marine Ecology Progress Series, 205: 43-59.

Kern, J.W. and K.O. Coyle. 2000. Global block kriging to estimate biomass from acoustic surveys for zooplankton in the western Aleutian Islands. Canadian Journal of Fisheries and Aquatic Sciences, 57: 2112-2121.

Kimura, K. 1929. On the detection of fish-groups by an acoustic method. Journal of the Imperial Fisheries Institute, Tokyo, 24: 41-45.

Kringel, K., P.A. Jumars, and D.V. Holliday. 2003. A shallow scattering layer: high-resolution acoustic analysis of nocturnal vertical migration from the seabed. Limnology and Oceanography, 48(3): 1223-1234.

Kunze, E., J.F. Dower, I. Beveridge, R. Dewey, and K.P. Bartlett. 2006. Observations of biologically generated turbulence in a coastal inlet. Science, 313: 1768-1770.

Lampert, W. 1989. The adaptive significance of diel vertical migration of zooplankton. Functional Ecology, 3: 21-27.

Largier, J.L. 1993. Estuarine fronts: how important are they? Estuaries, 16(1): 1-11.

Lasker, R. 1966. Feeding, growth, respiration and carbon utilization of an Euphausiid crustacean. Journal of the Fisheries Board of Canada, 23: 1291-1317.

Liu, Q. 1989. Ecophysiological studies of *Orchomenopsis affinis* (Holmes) (Lysianassidae Amphipoda) in an intermittently anoxic fjord. MSc Thesis, University of Victoria.

Lyman, J. 1948. The sea's phantom bottom. Scientific Monthly, 66: 87-88.

Macaulay, M.C. 1994. A generalized target strength model for euphausiids, with applications to other zooplankton. Journal of the Acoustical Society of America, 95(5): 2452-2466.

Mackas, D.L., K.L. Denman, and M.R. Abbott. 1985. Plankton patchiness: biology in the physical vernacular. Bulletin of Marine Science, 37: 652-674.

Mackas, D.L., R. Kieser, M. Saunders, D.R. Yelland, R.M. Brown, and D.F. Moore. 1997. Aggregation of euphausiids and Pacific hake (*Merluccius productus*) along the outer continental shelf off Vancouver Island. Canadian Journal of Fisheries and Aquatic Sciences, 54: 2080-2096.

Mackenzie, K.V. 1981. Nine-term equation for sound speed in the oceans. Journal of the Acoustical Society of America, 70(3): 807-812.

Mackie, G.O. and C.E. Mills. 1983. Use of the *Pisces IV* submersible for zooplankton studies in coastal waters of British Columbia. Canadian Journal of Fisheries and Aquatic Sciences, 40: 763-776.

MacLennan, D.N. and E.J. Simmonds. 1992. Fisheries Acoustics. Chapman and Hall, London, 325p.

MacLennan, D.N., P.G. Fernandez, and J. Dalen. 2002. A consistent approach to definitions and symbols in fisheries acoustics. ICES Journal of Marine Science, 59: 365-369.

Marcus, N.H. and F. Boero. 1998. The importance of benthic-pelagic coupling and the forgotten role of life cycles in coastal aquatic systems. Limnology and Oceanography, 43(5): 763-768.

Medwin, H. 2005. Sounds in the Sea: From Ocean Acoustics to Acoustical Oceanography. Cambridge University Press, Cambridge, 643p.

Misund, O.A. 1997. Underwater acoustics in marine fisheries and fisheries research. Reviews in Fish Biology and Fisheries, 7: 1-34.

Misund, O.A. 1993. Dynamics of moving masses: variability in packing density, shape, and size among herring, sprat, and saithe schools. ICES Journal of Marine Science, 50:145-160.

Miyashita, K., K. Tetsumura, S. Honda, T. Oshima, R. Kawabe, and K. Sasaki. 2004. Diel changes in vertical distribution patterns of zooplankton and walleye pollock (*Theragra chalcogramma*) off the Pacific coast of eastern Hokkaido, Japan, estimated by volume back scattering strength (Sv) difference method. Fisheries Oceanography, 13 (Suppl. 1): 99-110.

Murie, D.J. 1995. Comparative feeding ecology of two sympatric rockfish congeners, *Sebastes caurinus* (copper rockfish) and *S. maliger* (quillback rockfish). Marine Biology, 124: 341-353.

Nøttestad, L., A. Fernö, S. Mackinson, T. Pitcher, and O.A. Misund. 2002. How whales influence herring school dynamics in a cold-front area of the Norwegian Sea. ICES Journal of Marine Science, 59: 393-400.

Ohman, M.D. 1984. Omnivory in *Euphausia pacifica*: the role of copepod prey. Marine Ecology Progress Series, 19: 125-131.

Ohman, M.D. 1988. Behavioural responses of zooplankton to predation. Bulletin of Marine Science, 43(3): 530-550.

Outram, D.N. and C. Haegele. 1972. Food of Pacific hake (*Merluccius productus*) on an offshore bank southwest of Vancouver Island, British Columbia. Journal of the Fisheries Research Board of Canada, 29(12): 1792-1795.

Page, E.B. 1963. Ordered hypotheses for multiple treatments: a significance test for linear ranks. Journal of the American Statistical Association, 58: 216-230.

Parsons, T.R., R.I. Perry, E.D. Nutbrown, W. Hsieh, and C.M. Lalli. 1983. Frontal zone analysis at the mouth of Saanich Inlet, British Columbia, Canada. Marine Biology, 73: 1-5.

Pickard, G.L. 1963. Oceanographic characteristics of inlets of Vancouver Island, British Columbia. Journal of the Fisheries Research Board of Canada, 20: 1109-1144.

Pickard, G.L. and B.R. Stanton. 1980. Pacific fjords - a review of their water characteristics. In: H.J. Freeland, D.M. Farmer, and C.D. Levings (eds.), Fjord Oceanography, Plenum Press, New York.

Pihl, L., S.P. Baden, and R.J. Diaz. 1991. Effects of periodic hypoxia on distribution of demersal fish and crustaceans. Marine Biology, 108: 349-360.

Pinel-Alloul, B. 1995. Spatial heterogeneity as a multiscale characteristic of zooplankton community. Hydrobiologia, 300/301: 17-42.

Potvin, C. and D.A. Roff. 1993. Distribution-free and robust statistical methods: viable alternatives to parametric statistics? Ecology, 74(6): 1617-1628.

Price, H.J. 1989. Swimming behaviour of krill in response to algal patches: a mesocosm study. Limnology and Oceanography, 34(4): 649-659.

Rabalais, N.N., R.E. Turner, and W.J. Wiseman Jr. 2002. Gulf of Mexico hypoxia, aka "the dead zone". Annual Review of Ecological Systematics, 33: 235-263.

Raffaelli, D., E. Bell, G. Weithoff, A. Matsumoto, J.J. Cruz-Motta, P. Kershaw, R. Parker, D. Parry, and M. Jones. 2003. The ups and downs of benthic ecology: considerations of scale, heterogeneity and surveillance for benthic-pelagic coupling. Journal of Experimental Marine Biology and Ecology, 285-286: 191-203.

Richmond, C., N.H. Marcus, C. Sedlacek, G.A. Miller, and C. Oppert. 2006. Hypoxia and seasonal temperature: short-term effects and long-term implications for *Acartia tonsa* dana. Journal of Experimental Marine Biology and Ecology, 328: 177-196.

Russell, F.S. 1928. The vertical distribution of marine macroplankton. VII. Observations on the behaviour of *Calanus finmarchicus*. Journal of the Marine Biological Association of the United Kingdom, 15: 429-449.

Sameoto, D.D. 1976. Distribution of sound scattering layers caused by euphausiids and their relationship to chlorophyll *a* concentration in the Gulf of St. Lawrence estuary. Journal of the Fisheries Research Board of Canada, 33: 681-687.

Siegel, V. 2000. Krill (Euphausiacea) life history and aspects of population dynamics. Canadian Journal of Fisheries and Aquatic Sciences, 57(Suppl. 3): 130-150.

Simard, Y. and D.L. Mackas. 1989. Mesoscale aggregations of euphausiid sound scattering layers on the continental shelf of Vancouver Island. Canadian Journal of Fisheries and Aquatic Science, 46: 1238-1249.

Spicer, J.I., M.A. Thomasson, and J-O Stromberg. 1999. Possessing a poor anaerobic capacity does not prevent the diel vertical migration of Nordic krill *Meganyctiphanes norvegica* into hypoxic waters. Marine Ecology Progress Series, 185: 181-187.

Stadler, L.C. and N.H. Marcus. 1997. Zooplankton responses to hypoxia: behavioral patterns and survival of three species of calanoid copepods. Marine Biology, 127: 599-607.

Sund, O. 1935. Echo sounding in fishery research. Nature. 135: 953.

Swartzman, G., J. Napp, R. Brodeur, A. Winter, and L. Ciannelli. 2002. Spatial patterns of pollock and zooplankton distribution in the Pribilof Islands, Alaska nursery area and their relationship to pollock recruitment. ICES Journal of Marine Science, 59: 1167-1186.

Takahashi, M., D.L. Seibert, and W.H. Thomas. 1977. Occasional blooms of phytoplankton during summer in Saanich Inlet, B.C., Canada. Deep Sea Research, 24: 775-780.

Tanasichuk, R.W. 1998. Interannual variations in the population biology and productivity of *Euphausia pacifica* in Barkley Sound, Canada, with special reference to the 1992 and 1993 warm ocean years. Marine Ecology Progress Series, 173: 163-180.

Tarling, G.A., J.B.L. Matthews, R. Saborowski, and F. Buchholz. 1998. Vertical migratory behaviour of the euphausiid, *Meganyctiphanes norvegica*, and its dispersion in the Kattegat Channel. Hydrobiologia, 376: 331-341.

Teasdale, M., K. Vopel, and D. Thistle. 2004. The timing of benthic copepod emergence. Limnology and Oceanography, 49(3): 884-889.

Thistle, D. 2003. Harpacticoid copepod emergence at a shelf site in summer and winter: implications for hydrodynamic and mating hypotheses. Marine Ecology Progress Series, 248: 177-185.

Thomson R.E., T.A. Curran, M.C. Hamilton, and R. McFarlane. 1988. Time series measurements from a moored fluorescence-based dissolved oxygen sensor. Journal of Atmospheric and Oceanic Technology, 5: 614-624.

Thomson, R.E., and S.E. Allen. 2000. Time series acoustic observations of macrozooplankton diel migration and associated pelagic fish abundance. Canadian Journal of Fisheries and Aquatic Sciences, 57: 1919-1931.

Timothy, D.A. and M.Y.S. Soon. 2001. Primary production and deep-water oxygen content in two British Columbia fjords. Marine Chemistry, 73: 37-51.

Tjossem, S.F. 1990. Effects of chemical cues on vertical migration behavior of *Chaoborus*. Limnology and Oceanography, 35(7): 1456-1468.

Trevorrow, M.V. 2005. The use of moored inverted echo sounders for monitoring meso-zooplankton and fish near the ocean surface. Canadian Journal of Fisheries and Aquatic Sciences, 62: 1004-1018.

Tucker, D.G. and B.K. Gazey. 1966. Applied Underwater Acoustics. Pergamon Press, Oxford, 244p.

Tunnicliffe, V. 1981. High species diversity and abundance of the epibenthic community in an oxygen-deficient basin. Nature, 294: 354-356.

Van de Meutter, F., R. Stoks, and L. De Meester. 2005. Spatial avoidance of littoral and pelagic invertebrate predators by *Daphnia*. Oecologia, 142: 489-499.

VENUS. [cited 2006 Sep 1]. University of Victoria – VENUS Victoria Experimental Network Under the Sea [Internet]. Available from: http://www.venus.uvic.ca/index.html

Webb, P and T.H. Wooldridge. 1990. Diel horizontal migration of *Mesopodopsis slabberi* (Crustacea, Mysidacea) in Algoa Bay, Southern Africa. Marine Ecology Progress Series, 62: 73-77.

White, M.D. 1998. Horizontal distribution of pelagic zooplankton in relation to predation gradients. Ecography, 21: 44-62.

Wilson, S.G., T. Pauly, and M.G. Meekan. 2002. Distribution of zooplankton inferred from hydroacoustic backscatter data in coastal waters off Ningaloo Reef, Western Australia. Marine and Freshwater Research, 53: 1005-1015.

Wojtal, A., P. Frankiewicz, K. Izydorczyk, and M. Zalewski. 2003. Horizontal migration of zooplankton in a littoral zone of the lowland Sulejow Reservoir (Central Poland). Hydrobiologia, 506-509: 339-346.

Yahel, R., G. Yahel, and A. Genin. 2005. Near-bottom depletion of zooplankton over coral reefs: 1: diurnal dynamics and size distribution. Coral Reefs, 24: 75-85.